

# More about Diatomic Molecules

Our study of  $\text{H}_2^+$  and  $\text{H}_2$  has given us some idea of the basic principles of chemical bonding and the electronic properties associated with the simple chemical bond. There is much more to learn about molecular structure, even for the relatively simple case of diatomic molecules. In this chapter we consider the general properties of diatomic molecules.

In Chapter 6 we were concerned only with the distribution and energy of the electrons; we only mentioned the motion of the atomic nuclei. Nuclei are never fixed in space. In a molecule, they oscillate around their equilibrium positions as if the bond were a spring; they can revolve about the molecule's center of mass; and the molecule as a whole can move in space. There are energy levels associated with all these motions, and we must find out what they are. Fortunately, we have already done most of the work to accomplish this, in terms of simple models. As we develop a description of these energy levels, we shall be able to analyze the full richness of molecular spectroscopy.

We are by no means through with electrons either. Although  $\text{H}_2$  does illustrate the nature of the chemical bond, there are many phenomena that appear only in more complicated molecules. We shall discuss the general properties of diatomic molecules, mainly in terms of the molecular orbital approach, and go on to study several interesting classes of molecules in some detail. These include homonuclear molecules such as  $\text{N}_2$ , which have the same symmetry properties as  $\text{H}_2$ ; first-row hydrides such as OH, the simplest heteronuclear molecules; and several series of related molecules in which trends can be discerned. We shall also look in a little more detail at how one may carry out calculations of electronic structure.

Let us examine more carefully a molecule of  $\text{H}_2$  in its ground electronic state. We know the  $E(R)$  curve, but just what does this curve mean? According to our interpretation in Chapter 6,  $E(R)$  is the electronic energy of the molecule at internuclear distance  $R$ , calculated with the nuclei fixed. But the uncertainty principle ensures that no real molecule can have fixed nuclei. The more precisely we know the positions of the nuclei, the more uncertain become their

momenta. Thus the best we can say (in classical language) is that the nuclei oscillate or vibrate within a certain range about their equilibrium positions. This language still assumes the molecule as a whole (i.e., its center of mass) to be fixed in space, but this cannot be generally true either: The molecule almost certainly has some translational momentum. Finally, the orientation of the molecule cannot be fixed in space, or the uncertainty in its angular momentum would be infinite. Thus we must also consider the molecule's rotation about its center of mass. We wish to describe all these types of motion.

## 7.1 Vibrations of Diatomic Molecules

Our starting point is again the Born–Oppenheimer approximation, which says that the nuclear and electronic motions are separable. We rationalized this on the basis that electrons move much faster than nuclei, and indeed Born and Oppenheimer derived the approximation from the full Schrödinger equation, cf. footnote 2 of Chapter 6. Just as we could consider the nuclei at rest when treating the electronic motion, we can consider the electrons as a smoothly averaged distribution that adjusts at once to the nuclear motion. The Born–Oppenheimer approximation is expressed by Eqs. 6.2 and 6.3; for the nuclear motion it yields Eq. 6.4, which we can rewrite as

$$\left( \frac{\mathbf{p}_A^2}{2m_A} + \frac{\mathbf{p}_B^2}{2m_B} \right) \psi_{\text{nuc}}(R_n) = [E - E(R)] \psi_{\text{nuc}}(R_n). \quad (7.1)$$

Here  $R_n$  is shorthand for all the nuclear coordinates,  $E$  is the molecule's total energy, and  $E(R)$  is its electronic energy—which is also the *effective* potential energy field in which the nuclei move.

Now we make another assumption, that the translational, vibrational, and rotational motions of the nuclei are also separable from one another. (This is not quite accurate, and

later we shall mention some corrections to this approximation.) We thus have

$$H_{\text{nucl}} \equiv \frac{\mathbf{P}_A^2}{2m_A} + \frac{\mathbf{P}_B^2}{2m_B} = H_{\text{trans}} + H_{\text{vib}} + H_{\text{rot}}, \quad (7.2)$$

$$E - E(R) = E_{\text{trans}} + E_{\text{vib}} + E_{\text{rot}}, \quad (7.3)$$

and

$$\psi_{\text{nucl}}(R_n) = \psi_{\text{trans}}\psi_{\text{vib}}\psi_{\text{rot}}; \quad (7.4)$$

$H_{\text{trans}}$  and  $\psi_{\text{trans}}$  depend only on the center-of-mass coordinates,  $H_{\text{vib}}$  and  $\psi_{\text{vib}}$  only on the internuclear distance  $R$ , and  $H_{\text{rot}}$  and  $\psi_{\text{rot}}$  only on the angles giving the molecule's orientation in space. For each type of motion we obtain a wave equation in the form  $H_j\psi_j = E_j\psi_j$ . In a gas, the translational wave equation is simply that for a free particle in three dimensions, the solution of which we already know. The rotational motion will be considered in the next section; let us now analyze the vibrational motion.

Classically, the total energy of the nuclei can be written as

$$E - E(R) = \left[ \frac{p_X^2 + p_Y^2 + p_Z^2}{2M} \right] + \left[ \frac{p_R^2}{2\mu} + V(R) \right] + \left[ \frac{1}{2\mu R^2} \left( p_\theta^2 + \frac{p_\phi^2}{R^2 \sin^2 \theta} \right) \right], \quad (7.5)$$

where  $X, Y, Z$  are the coordinates of the center of mass,  $M$  is the total molecular mass,  $\mu$  is the reduced mass  $m_A m_B / (m_A + m_B)$ , and  $p_R, p_\theta, p_\phi$  have the same meaning as in Eq. 3.147. When the  $p$ 's are converted to the corresponding operators, the three expressions in square brackets become  $H_{\text{trans}}$ ,  $H_{\text{vib}}$ , and  $H_{\text{rot}}$ , respectively. According to the Hellmann–Feynman theorem, the potential energy  $V(R)$  for vibration (motion along the internuclear axis) must be the same as our  $E(R)$ . Separating the variables in Eq. 7.1 in the usual way, we find that the wave equation for vibrational motion is simply

$$H_{\text{vib}}\psi_{\text{vib}}(R) = \left[ \frac{p_R^2}{2\mu} + E(R) \right] \psi_{\text{vib}}(R) = E_{\text{vib}}\psi_{\text{vib}}(R), \quad (7.6)$$

where  $p_R \equiv -i\hbar(\partial/\partial R)$ , the operator for the relative momentum of the nuclei. Given the  $E(R)$  curve for a molecule, one can solve Eq. 7.6 to obtain the vibrational eigenfunctions  $\psi_{\text{vib}}(R)$  and eigenvalues  $E_{\text{vib}}$ . But the function  $E(R)$  is in general quite complicated and known only in numerical form. Although Eq. 7.6 can be solved by numerical methods, it is useful to obtain a simpler function that will give a good approximate solution.

As we have indicated before, one of the scientist's most powerful tools for understanding a system is to find a parallel to it in a system already understood. By "parallel" we mean "similar in mathematical structure." If the parallelism is exact, then one has solved the new problem. Even if the

parallelism is only approximate, one can generally learn a great deal about the new system by asking just how it deviates from the old one. The point of all this, of course, is that such a parallel model exists for molecular vibrations; not surprisingly, the model is our old friend the harmonic oscillator. Let us see why this is a good model.

The most significant characteristic of a molecule like  $H_2$  is the existence of a stable minimum in the potential energy curve. Remember that the bonding force is  $dE(R)/dR$ ; thus at the minimum  $R_e$ , where the slope of the  $E(R)$  curve is zero, there is no net bonding force on the nuclei. If we squeeze or stretch the molecule, there will be a force tending to restore the internuclear distance to  $R_e$ . This restoring force is what gives rise to molecular vibrations, with the distance oscillating back and forth around the value  $R_e$ . This motion is mathematically equivalent to that of a single particle of mass  $\mu$  in a one-dimensional potential well defined by  $E(R)$ . We have described the properties of such potential wells in Chapter 4. Bound states (those with  $E < 0$ , in terms of Fig. 6.2) have quantized energies; their wave functions are oscillatory where  $E > V$ , but decay rapidly toward zero in the classically forbidden region where  $E < V$ . The actual number of bound states and the energies at which they fall depend very specifically on the form of the potential energy curve. A molecule in a given electronic state may exist in any one of the vibrational states associated with the potential curve for that state. For the  $H_2$  molecule in its ground electronic state, for example, spectroscopy reveals the existence of 14 bound vibrational states,<sup>1</sup> shown in Fig. 7.1.

We still have not introduced our model. We know that there is a restoring force tending to bring  $R$  to its equilibrium value. The simplest assumption one can make about the restoring force is that it is proportional to the displacement from equilibrium,  $F(R) \propto |R - R_e|$ . This is just what we have defined as a harmonic oscillator, for which Eqs. 4.4 and 4.5 give us

$$F(R) = -k(R - R_e) \quad \text{and} \quad V(R) = \frac{1}{2}k(R - R_e)^2, \quad (7.7)$$

with  $R - R_e$  replacing the displacement  $x$ ; here  $F(R)$  is the magnitude of the force tending to increase  $R$ , and  $V(R)$  is zero at the bottom of the potential well. To the extent that the harmonic oscillator model is valid, we can apply all the results of Section 4.2 to molecular vibrations. Obviously it is not really valid for any molecule, because  $E(R)$  always levels off at large  $R$ , where the atoms dissociate and no longer interact. However, it is approximately valid for all stable molecular states near equilibrium. In other words, any  $E(R)$  curve with a stable minimum can be approximated by a parabola in the vicinity of that minimum; this is illustrated for the  $H_2$  molecule in Fig. 7.1.

<sup>1</sup> In the case of  $H_2$ , the complete (non-Born–Oppenheimer) wave equation can be solved with sufficient accuracy to confirm this experimental result.

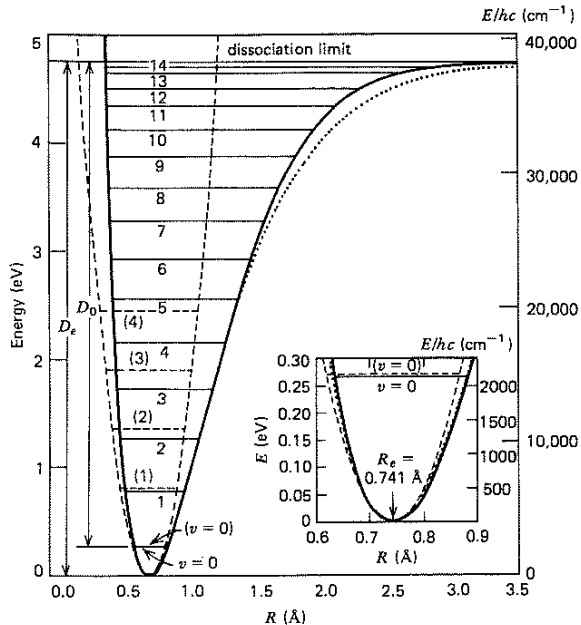


**Figure 7.1** Vibrational energy levels of the  $\text{H}_2$  molecule. Solid lines (—) represent the experimental  $E(R)$  curve and energy levels; dashed lines (---) give the parabolic approximation described in the text and the first few of the corresponding harmonic oscillator levels; and the dotted line (· · ·) is a Morse potential fit. The inset shows an enlargement of the region near the minimum. The two “dissociation energies” are indicated:  $D_e = 4.748 \text{ eV}$ ,  $D_0 = 4.477 \text{ eV}$ .

How good this approximation is depends on the spacing of the vibrational energy levels. For bound states at energies for which the true and parabolic curves nearly coincide, the harmonic oscillator model should give an excellent description. But how many states fall in this range of energies, and how likely is the molecule to be in these states? To find out, let us make an order-of-magnitude calculation.

For most stable diatomic molecules in their ground states, the potential well has a depth of about 5 eV, or  $8 \times 10^{-19} \text{ J}$ . To keep the numbers simple, let us say that the best parabola fitted to the minimum is 1 Å wide ( $R - R_e = 0.5 \text{ Å}$ ) when  $V(R) = 8 \times 10^{-19} \text{ J}$ ; this is approximately correct for  $\text{H}_2$ . Solving Eq. 7.7 for the force constant  $k$ , we obtain

$$k = \frac{2V(R)}{(R - R_e)^2} = \frac{2 \times 8 \times 10^{-19} \text{ J}}{(0.5 \times 10^{-10} \text{ m})^2} = 640 \text{ N/m.}$$

The force constant of a harmonic oscillator is related to the frequency by Eq. 2.38; here, for the mass  $m$  we must use the molecule's reduced mass  $\mu$ . For the  $\text{H}_2$  molecule  $\mu$  is just half the mass of a single hydrogen atom, or about  $8 \times 10^{-28} \text{ kg}$ . The oscillator frequency in our approximate model should thus be

$$\nu(\text{H}_2) = \frac{1}{2\pi} \left( \frac{k}{\mu} \right)^{1/2} = \frac{1}{2\pi} \left( \frac{640 \text{ N/m}}{8 \times 10^{-28} \text{ kg}} \right)^{1/2} = \frac{(80 \times 10^{28} \text{ s}^{-2})^{1/2}}{2\pi} \approx 1.5 \times 10^{14} \text{ s}^{-1},$$

equivalent to a wavenumber  $\nu/c \equiv \tilde{\nu} \approx 5000 \text{ cm}^{-1}$ . Since the spacing of harmonic oscillator energy levels is  $\hbar\nu$ , this corresponds to

$$\Delta E(\text{H}_2) = \hbar\nu(\text{H}_2) \approx (6.6 \times 10^{-34} \text{ J s})(1.5 \times 10^{14} \text{ s}^{-1}) \approx 10^{-19} \text{ J},$$

which is one-eighth of our assumed well depth. The lowest energy level is  $\frac{1}{2}\hbar\nu$  above the bottom of the well (the zero-point energy), the next level is  $\hbar\nu$  higher, and so on. Looking at Fig. 7.1, we can see that the harmonic oscillator model should be reasonably good for at least the first level or two. For many processes at room temperature it is only these levels that will be significantly occupied, as we shall see in Part II.<sup>2</sup> All other molecules have greater reduced masses than  $\text{H}_2$ , and none have significantly larger force constants. Thus the harmonic oscillator model gives a fairly good description of the energy-level spacing in nearly all stable diatomic molecules. (There are a few exceptions—molecules with very shallow or highly nonparabolic potential wells, such as  $\text{HgH}$  or  $\text{Ar}_2$ .)

To check the accuracy of our calculations, let us now look at some data. The vibrational energy levels of a diatomic molecule can be fitted (see below) to a power series in the quantum number  $\nu$ , beginning with a harmonic oscillator term  $(\nu + \frac{1}{2})\hbar\nu_e$ . For  ${}^1\text{H}_2$  the frequency  $\nu_e$  is found to be  $1.3192 \times 10^{14} \text{ s}^{-1}$ , which is quite close to our crude estimate.<sup>3</sup> The various isotopic forms of the  $\text{H}_2$  molecule presumably have the same electronic structure and thus the same potential curve.<sup>4</sup> Then the best parabolic fits to  $E(R)$

<sup>2</sup> The relative population of two energy levels in thermal equilibrium is given by

$$N_2/N_1 = e^{-(E_2 - E_1)/k_B T},$$

where  $k_B = 1.38 \times 10^{-23} \text{ J/K}$  and  $T$  is the absolute temperature. At room temperature (300 K) we have, for two levels  $10^{-19} \text{ J}$  apart,

$$\frac{N_2}{N_1} = e^{-10^{-19} \text{ J}/(1.38 \times 10^{-23} \text{ J/K}(300 \text{ K}))} \approx e^{-24} \approx 4 \times 10^{-11};$$

in other words, each level will contain only  $4 \times 10^{-11}$  as many molecules as the one below it. Since there are about  $3 \times 10^{22}$  gas molecules/liter under ordinary conditions, only about 50 molecules/liter will be in the third vibrational level.

<sup>3</sup> Working backward from this frequency gives a force constant

$$k = 4\pi^2 \mu \nu_e^2 = 4\pi^2 (8.3676 \times 10^{-28} \text{ kg})(1.3192 \times 10^{14} \text{ s}^{-1})^2 = 574.9 \text{ N/m},$$

the value used to draw the parabolic curve in Fig. 7.1.

<sup>4</sup> This is not quite true. As in atoms (see footnote 24 on page 208), there is a very small isotopic shift in the electronic energy, but this effect can be ignored here.

**Table 7.1** Test of Harmonic Oscillator Model with Vibrational Constants of H<sub>2</sub> Isotopes

(Atomic masses: <sup>1</sup> H, 1.00782 amu; D, 2.01410 amu)			
Molecule	Reduced Mass, $\mu$ (amu)	Vibrational Frequency, $\nu_e \times 10^{-14}(\text{s}^{-1})$	$\mu^{1/2}\nu_e$ $10^{14}\text{amu}^{1/2}\text{s}^{-1}$
<sup>1</sup> H <sub>2</sub>	0.50391	1.3192	0.9365
<sup>1</sup> HD	0.67171	1.1429	0.9367
D <sub>2</sub>	1.00705	0.9345	0.9378

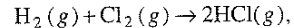
should all have the same  $k$ , and Eq. 2.38 shows the harmonic oscillator frequency should be proportional to  $\mu^{-1/2}$ . We can thus test the validity of the harmonic oscillator model with the measured values of the vibrational constant  $\nu_e$ . If the model were valid,  $\nu_e$  would be the oscillator frequency and all the isotopes would have the same value of  $\mu^{-1/2}\nu_e$ . The data are given in Table 7.1. The deviations from exact correspondence to  $\nu_e \propto \mu^{-1/2}$  are largely due to the deviation of the real curve from its parabolic approximation.

Since the harmonic oscillator model does work rather well for most diatomic molecules, we can apply the results of Section 4.2. The vibrational energy levels should thus be given by

$$E_{\text{vib}}(\nu) + \left(\nu + \frac{1}{2}\right)\hbar\nu_0 \quad (\nu = 0, 1, 2, \dots), \quad (7.8)$$

where  $\nu_0$  is the oscillator frequency and  $\nu$  is the conventional symbol for the vibrational quantum number in a diatomic molecule. The vibrational wave functions in this model are  $\psi_\nu(z)$ , as listed in Table 4.1, in terms of the dimensionless displacement variable  $z \equiv (4\pi^2\mu\nu_0/\hbar)^{1/2}(R - R_e)$ . For example, the ground vibrational state is described by a wave function with a single maximum at  $R_e$ ; the first excited state, by a wave function with two maxima and a node at  $R_e$ , and so on. The vibration is not strictly harmonic, so these are only approximations to the true wave functions (for which the ground state's maximum and the next state's node will not lie exactly at  $R_e$ ); but the qualitative behavior is given correctly. As  $\nu$  increases, the harmonic model becomes less accurate. But as  $\nu$  increases, the molecule behaves more and more like a classical oscillator, in that the difference between adjacent energy levels becomes a small fraction of the total vibrational energy.

Note in Fig. 7.1 the distinction between the two “dissociation energies,”  $D_e$  and  $D_0$ . The well depth  $D_e$  is fundamentally more interesting to the theoretician. However, a measurement of the minimum energy required to dissociate a molecule in its ground state yields  $D_0$ , since no molecule can have less than the zero-point vibrational energy. For the same reason, when one calculates the energy change of a chemical reaction in which a given bond is formed or broken, it is  $D_0$  that must be taken into account. For example, the energy required to bring about the reaction



with reactants and product in their ground states, is

$$\Delta E_{\text{reac}} = D_0(\text{H}_2) + D_0(\text{Cl}_2) - 2D_0(\text{HCl}).$$

Thus, only  $D_0$  is properly called the dissociation energy, and, to be strict, we should but will not always refer to it by that name. When a distinction must be made,  $D_e$  can be called the well depth. In the harmonic oscillator model, the two quantities are related by the equation  $D_e = D_0 + \frac{1}{2}\hbar\nu_0$ .

Suppose that we want to describe molecular vibrations with more accuracy than the harmonic oscillator model can yield, but without going all the way to a numerical solution. How can we do this? The harmonic model approximates the potential curve by a parabola. The actual curve, however, rises more steeply at small  $R$  and falls off more slowly at large  $R$ . We can thus improve the fit by adding to  $V(R)$  a correction that is positive for  $R < R_e$  and negative for  $R > R_e$ . An obvious choice is a term proportional to  $(R - R_e)^3$ , which changes sign at  $R = R_e$ . We can thus replace Eqs. 7.7 by

$$F(R) = -kx + k'x^2 \quad \text{and} \quad V(R) = \frac{1}{2}kx^2 - \frac{1}{3}k'x^3, \quad (7.9)$$

with  $x \equiv R - R_e$ . This is an *anharmonic oscillator* model, with the added term called the *anharmonicity*. Equations 7.9, of course, fit the experimental data appreciably better near  $R_e$  than does the harmonic model. For most vibrational levels observed at room temperature the anharmonicity effect simply shifts  $E_{\text{vib}}$  by a small amount, generally less than 1%. However, this model is clearly unsuitable for describing the vibrational levels high in the potential well (which might be occupied in a very hot gas), since the predicted  $V(R)$  diverges at large  $R$  instead of leveling off. One can obtain a still better fit by adding a term in  $x^4$ , a term in  $x^5$ , and as many terms as the data can justify; given enough terms, one can approximate the potential curve to any desired accuracy. In general, the energy eigenvalues can be written in the form

$$E_{\text{vib}}(\nu) = \hbar\nu_e \left[ \left( \nu + \frac{1}{2} \right) - x_e \left( \nu + \frac{1}{2} \right)^2 + y_e \left( \nu + \frac{1}{2} \right)^3 + \dots \right] \quad (\nu = 0, 1, 2, \dots), \quad (7.10)$$

where  $\nu_e, x_e, y_e, \dots$  are constants that can be fitted to the spectroscopic data;<sup>5</sup> this equation defines the  $\nu_e$  we introduced in Table 7.1.

<sup>5</sup> Since most spectroscopists express their data in wavenumbers, one usually finds tabulated the values of  $\tilde{\nu}_e \equiv \nu_e/c$ ,  $\tilde{\nu}_e x_e$ ,  $\tilde{\nu}_e y_e, \dots$ . The wavenumber corresponding to  $E_{\text{vib}}(\nu)$  is called  $G(\nu) \equiv E_{\text{vib}}(\nu)/hc$ . A general expansion of the energy of nuclear motion in powers of the quantum numbers is called a Dunham expansion.

The experimental  $E(R)$  curve can be obtained by numerical calculation from the observed  $E(v)$  values, but this is difficult. However, there are a number of empirical functions in closed form that can be used to give potential energy curves that offer adequate approximations for many purposes. The best known of these is the *Morse potential*,<sup>6</sup>

$$V(R) = D_e [1 - e^{-a(R-R_e)}]^2, \quad (7.11)$$

where  $D_e$  is the well depth and  $a$  is a constant; to a good approximation one has  $a = \pi\nu_e(2\mu/D_e)^{1/2}$ . Note that this function correctly rises steeply at small  $R$  and levels off at large  $R$ , giving  $V(0) = \infty$  and  $V(\infty) = D_e$ . In fact the Schrödinger equation can be solved with  $V(R)$  given by Eq. 7.11. The energy eigenvalues of the Morse potential are given by the first two terms of Eq. 7.10 with  $x_e = \hbar\nu_e/4D_e$ , and can be used to approximate the true energy levels all the way to the dissociation limit. A Morse potential curve for  $H_2$  is included in Fig. 7.1; note that the agreement is rather poor at large  $R$ .

One can learn much about the vibrational energy levels of molecules by observing transitions between these levels. Such transitions can be induced by radiation, giving rise to discrete spectral lines in the usual manner (Section 4.5). Molecular vibrations are most commonly studied by observing the vibrational absorption spectra, which for diatomic molecules are found primarily in the near-infrared region. Most observed values of  $\nu_e$  lie in the range  $(0.6-12) \times 10^{13} \text{ s}^{-1}$ , corresponding to wavenumbers of  $200-4000 \text{ cm}^{-1}$  or wavelengths of  $2.5-50 \mu\text{m}$  (cf. Table 7.2). The molecules observed can be in gas, pure liquid, solution, or solid form; the effects of the surrounding medium on  $\nu_e$  are usually small but observable and not negligible. But not all molecules display such spectra. In fact, isolated homonuclear molecules such as  $H_2$  or  $O_2$  have no pure vibrational spectra at all. To see the reasons for this and other features of vibrational spectra, let us examine the excitation process in greater detail.

We consider excitation in terms of a classical model, essentially the same as that we applied to the hydrogen atom in Section 4.5. Any heteronuclear diatomic molecule has a dipole moment, since no two elements have exactly the same electronegativity. Thus such a molecule can be considered as an oscillating dipole, as illustrated in Fig. 7.2a (where  $+q$  and  $-q$  indicate the positive and negative ends of the dipole, respectively). Suppose that the molecule is bathed in infrared radiation, the wavelength of which is far greater than any dimension of the molecule. We can thus assume the electric field of the radiation to be uniform in space near the molecule, but oscillatory in time. At a given time, the component of this field parallel to the bond axis<sup>7</sup>

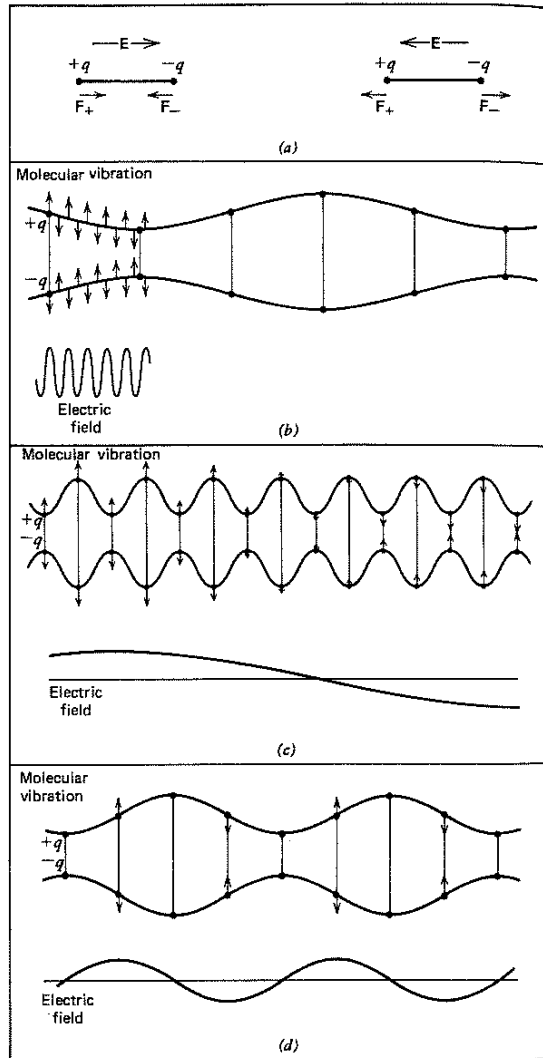


**Figure 7.2** Interaction between an electric field and an oscillating (molecular) dipole. (a) The forces exerted on the dipole by the field, which alternately tend to compress or stretch the dipole as the field direction changes. (b) Field varies much faster than the molecular vibration ( $\nu \gg \nu_e$ ); here and in the subsequent diagrams, the instantaneous forces on the dipole are indicated by arrows. (c) Field varies much slower than the molecular vibration ( $\nu \ll \nu_e$ ). (d) Field and dipole oscillate at the same frequency ( $\nu = \nu_e$ ), but  $90^\circ$  out of phase. As shown here, the dipole absorbs energy from the field; for a field phase  $180^\circ$  different, the forces are reversed and the dipole gives up energy to the field.

exerts an instantaneous force on the dipole that tends to either stretch or compress the bond (Fig. 7.2a).

The effect of this oscillating force on the molecular vibration is the same as in our earlier analysis. Let the field frequency be  $\nu$  and the molecule's natural vibration frequency be  $\nu_e$ . If  $\nu \gg \nu_e$  (Fig. 7.2b), the field reverses itself

<sup>6</sup> P. M. Morse, *Phys. Rev.* 34, 57 (1929).

<sup>7</sup> Since the force exerted by an electric field acts in the same direction as the field itself ( $\mathbf{F} = q\mathbf{E}$ ), the field components perpendicular to the bond axis do not affect the bond length and can be neglected here.

many times during a single vibration period, and can only impose a slight quivering onto the normal vibration. If  $\nu \ll \nu_e$  (Fig. 7.2c), the field varies slowly compared to the vibration rate, and can only slightly increase or decrease the average value of  $R$  for some number of cycles. In either of these extremes, the field cannot easily transfer energy to the molecule. But when  $\nu = \nu_e$ , and the phase relationship is right (Fig. 7.2d), the field stretches the bond when it is expanding and compresses it when it is contracting, or vice versa. These are just the conditions that maximize energy exchange between the field and the dipole, which absorbs energy in the first case and gives it up in the second. Such an exchange of energy is an *electric dipole* transition.

Thus far we have been considering a heteronuclear molecule, which is necessarily an oscillating dipole. But what if the two ends of the molecule are identical, as in H<sub>2</sub> or any other homonuclear diatomic? Can such a molecule, with no dipole moment, absorb electromagnetic radiation? Our model says no, provided that the electric field is uniform over the length of the molecule; for then the forces on the two ends of the molecule are equal at all times, and the oscillations of the field can have no effect on the bond length. In our simple model, this is the explanation for the absence of vibrational spectra of homonuclear molecules.

This classical model is inadequate for a full explanation of vibrational spectra. For one thing, a classical dipole can absorb energy in any amount from an oscillating electric field, with its own vibration amplitude varying continuously; we know that this is not true of a quantized oscillator. To go beyond the simple model, we refer to Eq. 4.33, which gives the probability of a transition between any two quantum states. Here we are interested only in the vibrational part of the wave function, for which Eq. 4.33 reduces to

$$\mu_{\nu' \nu} = \int_0^{\infty} \psi_{\nu'}^*(R) \mu(R) \psi_{\nu}(R) dR, \quad (7.12)$$

where  $\mu(R)$  is the molecule's instantaneous dipole moment and  $\psi_{\nu}$  and  $\psi'_{\nu}$  are the vibrational wave functions in states  $\nu$  and  $\nu'$ . The probability of a transition between these two states is proportional to  $|\mu_{\nu' \nu}|^2$ . It is immediately clear what happens in a homonuclear molecule: The dipole moment is zero for all values of  $R$ , the integral  $\mu_{\nu' \nu}$  vanishes for all  $\nu, \nu'$ , and there is thus zero probability of any vibrational electric dipole transition.

We have thus shown (on two levels) why homonuclear diatomic molecules have no pure vibrational spectra. But if that is the case, then how does one obtain vibrational energy levels like those in Fig. 7.1? One way is to look at the vibrational "structure" of *electronic* spectra. Transitions between different bound electronic states can be associated with specific initial and final vibrational states. In particular, transitions from a single vibrational level in an upper electronic state to a set of vibrational levels in a lower electronic state involve a series of quanta (a *band* of spectral

lines) whose energies differ by the vibrational energy interval in the lower state. We shall consider spectra of this type in Section 7.3. One can also observe vibrational transitions in homonuclear diatomics directly by bombarding the molecules with electrons of precisely known energy and measuring the characteristic energy losses of the scattered electrons; this is essentially a variation of the Franck–Hertz experiment. In such a collision, of course, the electric field due to the electron does vary over molecular dimensions, and our previous arguments prohibiting vibrational transitions no longer apply.

Now let us return to Eq. 7.12 and see what transitions are allowed in heteronuclear molecules. For the integral to be nonzero it is not enough that  $\mu \neq 0$ ; the dipole moment of the molecule must vary<sup>8</sup> with  $R$ . But this is no problem, because the dipole moments of all polar molecules do vary with the internuclear distance  $R$ . An especially simple result is obtained with the harmonic oscillator model, the vibrational wave functions of which are defined by Eq. 4.8. Setting  $|\mu| = qR$  (with  $q$  constant), one can show without much difficulty that the integral of Eq. 7.12 is nonzero only when  $\nu$  and  $\nu'$  differ by 1. In other words, for the harmonic oscillator we have the *selection rule* for electric dipole transitions

$$\Delta\nu = \pm 1; \quad (7.13)$$

all other transitions are forbidden. This means that the quantum mechanical harmonic oscillator can absorb or give up only one quantum at a time.

The mathematical basis for the selection rule 7.13 can be seen easily if we consider the situation of small-amplitude oscillations, which are the only ones for which the harmonic approximation and the  $\Delta\nu = \pm 1$  rule apply. If we so restrict our model, then we can write our wave functions  $\psi_{\nu}(R)$  as functions of the displacement of  $R$  from the equilibrium distance  $R_e$  ( $\mu$  is the reduced mass, not to be confused with the dipole moment  $\mu$ ):

$$z = (\mu\omega/\hbar)^{1/2} (R - R_e), \quad (7.14)$$

and the vibrational wave function is given by Eq. 4.8. Moreover,  $\mu(R)$  can also be expanded about  $R_e$  in a Taylor series—i.e., in powers of the displacement and successively higher derivatives of  $\mu$ :

$$\begin{aligned} \mu(R) &= \mu(R_e) \frac{d\mu(R)}{dR} \Big|_{R_e} z + \frac{1}{2} \frac{d^2\mu(R)}{dR^2} \Big|_{R_e} z^2 + \dots \end{aligned} \quad (7.15)$$

<sup>8</sup> If  $\mu$  is constant, it can be taken out of the integral, which then becomes  $\int_0^{\infty} \psi_{\nu'}^* \psi_{\nu} dR = 0$ , vanishing because the vibrational eigenfunctions are orthogonal (see Appendix 6A).

Note that  $\mu(R_e)$  and all the derivatives of  $\mu(R)$  evaluated at  $R = R_e$  are constants. Hence the *transition dipole*, Eq. 7.12, becomes

$$\begin{aligned}\mu_{v'v} &= \mu(R_e) \int \psi_{v'}(z) \psi_v(z) dz \\ &+ \frac{d\mu(R)}{dr} \Big|_{R_e} \int \psi_{v'}(z) z \psi_v(z) dz \\ &+ \frac{1}{2} \frac{d^2\mu(R)}{dR^2} \Big|_{R_e} \int \psi_{v'}(z) z^2 \psi_v(z) dz + \dots \quad (7.16)\end{aligned}$$

The limits of integration can be taken as  $\pm\infty$  so long as we make the harmonic approximation. Because  $\psi_{v'}(z)$  and  $\psi_v(z)$  are eigenfunctions of the same Hermitian operator and have different eigenvalues (if we are considering a transition), they are orthogonal. Hence  $\int \psi_{v'}(z) \psi_v(z) dz$  vanishes. The next term does not vanish. First, note that neither  $\int \psi_{v'}^* \psi_v dz$  nor  $\int e^{-z^2} H_v^2(z) dz$  vanishes. Next, from the definition of the Hermite polynomials, we find by direct substitution that

$$2zH_v(z) = 2vH_{v-1}(z) + H_{v+1}(z). \quad (7.17)$$

In words, multiplication of  $H_v(z)$  by  $z$  transforms  $H_v(z)$  into a sum of one higher and one lower  $H_{v'}(z)$ , on the scale of eigenvalues. This in turn means that the integral multiplying  $d\mu/dR$  in Eq. 7.16 does not vanish provided that either  $v' = v + 1$  or  $v' = v - 1$ . Therefore the harmonic oscillator satisfies Eq. 7.13. We shall not show here why the harmonic oscillator does not exhibit transitions with  $|\Delta v| > 1$ . Real molecules, which are never strictly harmonic, do exhibit transitions with  $|\Delta v| > 1$ , but these are generally much less probable than those with  $\Delta v = \pm 1$  provided that the molecule has a nonvanishing dipole moment. The higher terms of Eq. 7.16 for general anharmonic oscillators are not zero but are small.

The form of the vibrational spectrum is governed by the spacing of the energy levels. Since the energy levels of the harmonic oscillator are equally spaced, the selection rule 7.13 limits its vibrational spectrum to a single line, with  $\Delta E = \pm h\nu_0$ ; this is illustrated in Fig. 7.3a. The spectrum of a real molecule is of course more complicated. First, as mentioned above, the selection rule (Eq. 7.13) does not hold rigorously for an anharmonic oscillator, although transitions with  $\Delta v = \pm 1$  do remain far more likely than those with  $\Delta v = \pm 2, \pm 3, \dots$ . Also, the spacing of the energy levels is no longer constant. According to our reasoning in Section 4.2, since the real potential is “flatter” (i.e., widens more rapidly) than that of the harmonic oscillator, the spacing should decrease with increasing energy; this is indeed what one observes (cf. Fig. 7.1) for almost all stretching vibrations. Thus the transition  $(v = 0) \rightarrow (v = 1)$  requires more energy than the transition  $(v = 1) \rightarrow (v = 2)$ , and so on upward. The vibrational spectrum therefore consists of many lines rather than one, as shown in Fig. 7.3b. If one takes an absorption spectrum of a gas sample, molecules in the ground state absorb light at one

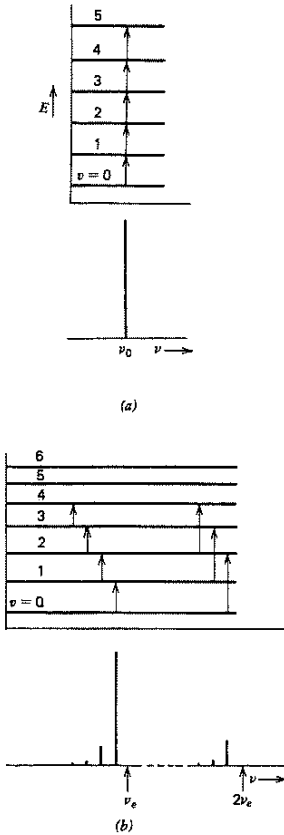


**Figure 7.3** Schematic representation of molecular vibrational absorption spectra (neglecting rotational effects). (a) Harmonic oscillator model:  $\Delta v = \pm 1$  only, all transitions at the same frequency  $\nu_0$ . (b) Real diatomic molecule: The energy levels are not evenly spaced, so one can observe a band of lines beginning near  $\nu_e$ , since the selection rule is not rigorous, there is a weaker band ( $\Delta v = \pm 2$ ) near  $2\nu_e$ , and still weaker bands at  $3\nu_e$ ,  $4\nu_e$ , . . . . Within each band, the intensity of a given line is proportional to the population of the initial state; the intensities as drawn here correspond to a gas with  $\hbar\nu_e/k_B T \approx 1.8$  (cf. Chapter 21).

frequency (close to  $\nu_e$ ), molecules in the first excited state absorb at a slightly lower frequency, and so forth. The intensity of an absorption line is of course proportional to the number of molecules in the initial state. For light molecules at moderate temperatures virtually all the molecules are in the ground vibrational state (cf. Chapter 21 and footnote 2 on page 184), and only the line corresponding to  $(v = 0) \rightarrow (v = 1)$  is normally observed; at higher temperatures one can use the intensity ratios to determine the distribution of molecules among the vibrational states. (This, too, is discussed in Chapter 21.)

The above discussion and Fig. 7.3 refer to a pure vibrational spectrum. Real molecular spectra are complicated by the fact that a molecule's rotational energy may also change when the vibrational energy changes. As a result, each of the

Table 7.2 Vibrational and Rotational Constants of Some Diatomic Molecules

Molecule	$\mu$ (amu)	$R_e$ (Å)	$\tilde{\nu}_e$ ( $\text{cm}^{-1}$ )	$\tilde{\nu}_e x_e$	$\tilde{\nu}_e Y_e$	$D_0$	$B_e$	$\alpha_e$
			( $\tilde{\nu}_e \equiv \nu_e/c$ )	( $\text{cm}^{-1}$ )	( $\text{cm}^{-1}$ )	(eV)	( $\text{cm}^{-1}$ )	( $\text{cm}^{-1}$ )
${}^1\text{H}_2$	0.50391	1.7412	4400.39	120.815	0.7242	4.4773	60.864	3.0764
$\text{HD}$ ( ${}^1\text{H}{}^2\text{H}$ )	0.67171	0.7412	3812.29	90.908	0.504	4.5128	45.663	2.0034
$\text{D}_2$ ( ${}^3\text{H}_2$ )	1.00705	0.7412	311.70	61.82	0.562	4.5553	30.457	1.0786
<i>First-row homonuclear molecules</i>								
${}^7\text{Li}_2$	3.50800	2.6725	351.44	2.592	-0.0058	1.12	0.6727	0.00704
${}^{11}\text{B}_2$	5.50465	1.590	1051.3	9.4		2.9	1.212	0.014
${}^{12}\text{C}_2$	6.00000	1.2425	1854.71	13.340	-1.172	6.24	1.8198	0.01765
${}^{14}\text{N}_2$	7.00154	1.094	2358.07	14.188	-0.0124	9.7598	1.9987	0.01781
${}^{16}\text{O}_2$	7.99745	1.2075	580.19	11.98	0.0475	5.1156	1.4456	0.01593
${}^{19}\text{F}_2$	9.49910	1.409	919.0	13.6		1.604	0.8901	0.0146
<i>Other homonuclear molecules</i>								
${}^{23}\text{Na}_2$	11.4949	3.0786	159.23	0.726	-0.0027	0.75	0.1547	0.00079
${}^{39}\text{K}_2$	19.48185	3.923	92.64	0.354		0.51	0.0562	0.00022
${}^{85}\text{Rb}_2$	42.4558	4.20	57.28	0.96	-0.0008	0.47	0.0127	0.0000264
${}^{133}\text{Cs}_2$	66.9525	4.58	41.99	0.080	-0.0002	0.45		
${}^{35}\text{Cl}_2$	17.48222	1.9878	559.71	2.70		2.484	0.2441	0.00153
${}^{79}\text{Br}{}^{81}\text{Br}$	39.9524	2.2809	323.33	1.081		1.9708	0.0811	0.00032
${}^{127}\text{I}_2$	63.4502	2.6666	214.52	0.607	-0.0013	1.5437	0.0374	0.00012
<i>Hydrides</i>								
${}^7\text{Li}{}^1\text{H}$	0.88123	1.5954	1405.65	23.200	0.1633	2.429	7.5131	0.2132
${}^{12}\text{C}{}^1\text{H}$	0.92974	1.124	2859.1	63.3		3.47	14.448	0.530
${}^{16}\text{O}{}^1\text{H}$	0.94808	0.9706	3735.21	82.81		4.392	18.871	0.714
${}^1\text{H}{}^{19}\text{F}$	0.95705	0.9168	4139.04	90.05	0.932	5.86	20.9560	0.7958
${}^1\text{H}{}^{35}\text{Cl}$	0.97959	1.2746	2991.09	52.82	0.2244	4.4361	10.5936	0.3072
${}^1\text{H}{}^{81}\text{Br}$	0.99511	1.4145	2649.21	45.22	-0.0029	3.755	8.4651	0.2333
${}^1\text{H}{}^{127}\text{I}$	0.99988	1.6090	2308.09	38.981	-0.1980	3.053	6.5108	0.1686
<i>Other heteronuclear molecules</i>								
${}^7\text{Li}{}^{19}\text{F}$	5.12381	1.5638	910.34	7.929		5.94	1.3454	0.02030
${}^9\text{Be}{}^{16}\text{O}$	5.76432	1.3310	1487.32	11.830	0.0224	4.60	1.6510	0.0190
${}^{11}\text{B}{}^{14}\text{N}$	6.16351	1.281	1514.6	12.3		3.99	1.666	0.025
${}^{12}\text{C}{}^{14}\text{N}$	6.46219	1.1720	2068.70	13.144		7.567	1.8991	0.01735
${}^{12}\text{C}{}^{16}\text{O}$	6.85621	1.1283	2169.82	13.294	0.0115	11.09	1.9313	0.01751
${}^{14}\text{N}{}^{16}\text{O}$	7.46676	1.1508	1904.03	13.97	-0.0012	6.50	1.7046	0.0178
${}^{23}\text{Na}{}^{35}\text{Cl}$	13.8707	2.3606	366	2.05		4.25	0.2181	0.00161
${}^{39}\text{K}{}^{79}\text{Br}$	26.0850	2.8207	213	0.80	0.0011	3.925	0.0812	0.00040

lines in the vibrational spectrum resolves into a band of closely spaced rotational-vibrational lines. We shall consider this and other complications in Section 7.3.

Let us now say a little about how the vibrational constants vary among diatomic molecules. In the harmonic oscillator model, as we have already noted, the oscillator frequency is proportional to  $\mu^{-1/2}$ , where  $\mu$  is the molecule's reduced mass. This is a fairly good approximation for real molecules. For homonuclear molecules  $\mu$  is one-fourth the molecular weight (half the atomic weight), so heavy molecules have relatively low vibrational frequencies. However, the reduced mass of a heteronuclear molecule cannot exceed

the mass of the lighter atom, which does most of the actual vibrating relative to the center of mass; all diatomic hydrides thus have  $\mu < 1$  amu, and high vibrational frequencies. The variation of force constants ( $k$ ) among molecules is not nearly so great as that of  $\mu$ . In spite of these variations, the actual magnitudes of molecular vibrational frequencies (or energies) fall within a rather short and well-defined range. This can be seen in Table 7.2, in which  $\tilde{\nu}_e$  ( $\equiv \nu_e/c$ ),  $x_e$ ,  $y_e$  are the constants in Eq. 7.10: The wavenumber  $\tilde{\nu}_e$  ranges from over  $4000 \text{ cm}^{-1}$  for  ${}^1\text{H}_2$  to below  $50 \text{ cm}^{-1}$  in some heavy molecules, but this covers only two decades of the whole electromagnetic spectrum.

Finally, as can also be seen in Table 7.2, there is at least a qualitative correlation between the length of a chemical bond ( $R_e$ ) and its fundamental vibration frequency  $\nu_e$ . This is not difficult to rationalize. Chemical bonds fall within a relatively narrow range of energies and lengths, so most ground-state  $E(R)$  curves are similar in shape. This is why they can almost all be approximated by a given function like a Morse potential. The bond length is the distance at which the short-range repulsive force balances the more slowly varying attractive force. The smaller the value of  $R_e$ , the more steeply both forces vary with  $R$ , and the narrower is the potential well near  $R_e$ . But a narrow well is one with a high force constant and thus a high vibration frequency. There we have our qualitative correlation.<sup>9</sup> Potential wells at small  $R$  tend to be not only steeper, but also deeper, because almost all the bonding forces fall off with distance. Thus, we also have a correlation between bond energy and vibration frequency. To sum up: Long bonds are weak and correspond to slow, low-frequency vibrations with large amplitudes; short bonds are strong, with deep potential wells, and correspond to high vibration frequencies with small amplitudes of motion.

## 7.2 Rotations of Diatomic Molecules

Next we consider the rotational behavior of diatomic molecules. We continue to assume that the translational, vibrational, and rotational motions of the nuclei are separable, Eqs. 7.2–7.4. Thus we begin by considering rotation in the absence of vibration, that is, with fixed internuclear distance. Just as vibration is well described by the harmonic oscillator model, the rotational motion of the molecule is well described by another model familiar to us, that of the rigid rotator (see Section 3.12).

<sup>9</sup> There are a number of empirical formulas correlating vibrational constants with bond lengths. These are accurate enough to be used in estimating bond lengths in new compounds from their infrared spectra. One of the most widely used is *Badger's rule*,

$$k = a(R_e - d_{ij})^{-3},$$

where  $k$  is the force constant,  $R_e$  is the usual equilibrium internuclear distance,  $a \approx 186 \text{ (N/m)}\text{\AA}^3$  (a universal "constant"), and  $d_{ij}$ , which is not universal, depends on the rows of the periodic table in which the atoms  $i$  and  $j$  fall. The following table gives  $d_{ij}$  in angstroms for various rows of the periodic table:

$i$	$H$	$j$		
		Row 1	Row 2	Row 3
H	0.025	0.335	0.585	0.650
Row 1	0.335	0.680	0.900	
Row 2	0.585	0.900	1.180	

More specifically, to a good approximation we can treat any diatomic molecule as a rigid symmetric top. This, it will be recalled, is a rigid body with two equal moments of inertia,  $I_0 \equiv I_x = I_y \neq I_z$ ; the  $z$  axis is as usual the bond axis. We have already analyzed this case in detail. The rotational Hamiltonian of the rigid symmetric top is

$$\left| H_{\text{rot}} = \frac{1}{2I_0} \mathbf{L}^2 + \frac{1}{2} \left( \frac{1}{I_z} - \frac{1}{I_0} \right) \mathbf{L}_z^2 \right|, \quad (7.18)$$

where  $\mathbf{L}^2$  and  $\mathbf{L}_z^2$  are angular momentum operators; the eigenvalues of  $H_{\text{rot}}$  are given by Eq. 3.177. Now, in a diatomic molecule the only contributions to  $I_z [\equiv \sum_i m_i (x_i^2 + y_i^2)]$  are those due to the electrons and the nonzero radii of the nuclei, both very small;  $I_0$ , on the other hand, is essentially  $\mu R^2$ , where  $\mu$  is the molecule's reduced mass and  $R$  is the internuclear distance. Thus we have  $I_z \ll I_0$ , and the coefficient of  $\mathbf{L}_z^2$  in Eq. 7.18 is much larger than that of  $\mathbf{L}^2$ . The energy term associated with  $\mathbf{L}_z^2$  is either very large (when  $L_z \neq 0$  for the electrons, i.e., in all except  ${}^1\Sigma$  states) or negligibly small (in  ${}^1\Sigma$  states). In either case it is a constant in any given electronic state, and can conveniently be included in the electronic energy.

Thus, we can disregard the second term in Eq. 3.177 and write the rotational energy of the molecule as simply

$$E_{\text{rot}} - \frac{J(J+1)\hbar^2}{2I_0} = \frac{J(J+1)\hbar^2}{2\mu R_e^2} \quad (J = 0, 1, 2, \dots), \quad (7.19)$$

where  $J$  (replacing the earlier  $l$ ) is the conventional symbol for the rotational quantum number of a molecule; we have evaluated  $I_0$  at the equilibrium internuclear distance,  $R_e$ . This equation is identical in form to Eq. 3.170, which gives the energy levels of the pure rigid rotator. Each energy level is thus  $(2J+1)$ -fold degenerate: The angular momentum about a given axis through the center of gravity is  $M_J \hbar$ , where for each  $J$  the quantum number  $M_J$  can assume the values  $J, J-1, \dots, -J+1, -J$ . And the rotational wave functions are simply the spherical harmonics  $Y_{J,M_J}(\theta, \phi)$ .

This is all quite straightforward, but how valid is the model? The assumption of fixed internuclear distance seems questionable, since the molecule is certainly vibrating (at least with the zero-point energy) at the same time as it rotates. But let us compare the rates of the two motions. If the molecule is rotating with angular velocity  $\omega$ , its angular momentum for fixed  $R$  is  $\mu R_e^2 \omega$ ; combining this with the eigenvalue equation  $L^2 = J(J+1)\hbar^2$ , we obtain

$$\omega = \frac{[J(J+1)]^{1/2} \hbar}{\mu R_e^2} = \left( \frac{2E_{\text{rot}}}{\mu R_e^2} \right)^{1/2} \quad (7.20)$$

for the angular velocity. We shall see in Chapter 21 that the average rotational energy of gaseous diatomic molecules is  $k_B T$ , where  $k_B = 1.381 \times 10^{-23} \text{ J/K}$  and  $T$  is the absolute tem-

perature. For  $^1\text{H}_2$  molecules at room temperature, the average period of a rotation is thus

$$\begin{aligned}\tau_{\text{rot}} &= \frac{2\pi}{\omega} \approx 2\pi \left( \frac{\mu R_e^2}{2k_B T} \right)^{1/2} \\ &= 2\pi \left[ \frac{(8.368 \times 10^{-28} \text{ kg})(0.7412 \times 10^{-10} \text{ m})^2}{2(1.381 \times 10^{-23} \text{ J/K})(300 \text{ K})} \right]^{1/2} \\ &= 2\pi (5.55 \times 10^{-28} \text{ s}^2)^{1/2} = 1.48 \times 10^{-13} \text{ s}.\end{aligned}$$

On the other hand, the period of a harmonic oscillator is simply  $\nu^{-1}$ , so for  $^1\text{H}_2$  we have (cf. Table 7.1)

$$\tau_{\text{vib}} \approx \nu_e^{-1} = (1.3192 \times 10^{14} \text{ s}^{-1})^{-1} = 7.58 \times 10^{-15} \text{ s}.$$

Thus, the  $^1\text{H}_2$  molecule at room temperature goes through about 20 vibrational periods in the course of a single rotation; for most molecules the ratio  $\tau_{\text{rot}}/\tau_{\text{vib}}$  is even greater.<sup>10</sup> As a first approximation, then, it seems reasonable to assume that the vibrational effects average out, justifying our calculation of rotational energy with fixed  $R$ . This is exactly the same reasoning as that leading to the Born–Oppenheimer assumption.<sup>11</sup>

Although the simple rigid-rotator model is adequate for qualitative purposes, more accurate expressions are needed to meet the demands of quantitative spectroscopy. One must allow for the effect of vibration on the rotational motion. Strictly, the  $R_e^{-2}$  in Eq. 7.19 should be replaced by the average value of  $R^{-2}$  over a vibration; because of the asymmetry of the  $E(R)$  curve, the average value of  $R$  must increase with  $\nu$ , so that we have  $\langle R \rangle_\nu > R_e$ ,  $\langle R^{-2} \rangle_\nu < R_e^{-2}$ . The actual rotational energies are thus somewhat less than those given by Eq. 7.19, and can be approximated by<sup>12</sup>

$$\begin{aligned}E_{\text{rot}} &= J(J+1)hcB_\nu \\ &= J(J+1)hc \left[ B_e - \alpha_e \left( \nu + \frac{1}{2} \right) + \dots \right], \\ &\quad \left( B_e \equiv \frac{\hbar}{4c\mu R_e^2} \right),\end{aligned}\quad (7.21)$$

<sup>10</sup> For example,

	$^1\text{H}^{35}\text{Cl}$	$^{35}\text{Cl}_2$	$^{127}\text{I}_2$
$\tau_{\text{rot}}(300 \text{ K})/\text{s}$	$4.05 \times 10^{-13}$	$2.34 \times 10^{-12}$	$5.98 \times 10^{-12}$
$\tau_{\text{vib}}/\text{s}$	$1.12 \times 10^{-14}$	$5.90 \times 10^{-14}$	$1.55 \times 10^{-13}$

<sup>11</sup> Note that both  $\tau_{\text{rot}}$  and  $\tau_{\text{vib}}$  are appreciably longer than the Bohr period of about  $10^{-16} \text{ s}$  (Table 2.2), which is typical of the time scale of electronic motions.

<sup>12</sup> There is also a smaller correction for centrifugal distortion, i.e., the stretching of the bond by centrifugal force. This appears in  $E_{\text{rot}}$  as a term  $D_\nu hcJ^2/(J+1)^2$ , where, typically,  $D_\nu < 10^{-4} B_\nu$ .

where  $\alpha_e$  is a constant,  $B_\nu$  is the rotational constant for vibrational state  $\nu$ , and  $B_e$  is the rigid-rotator value. The factor  $hc$  is inserted to give  $B_e$  and  $\alpha_e$  the units of wavenumbers. For  $^1\text{H}_2$  we readily obtain

$$\begin{aligned}B_e &= \frac{1.0546 \times 10^{-34} \text{ J s}}{4\pi(2.9979 \times 10^{-8} \text{ m/s})} \\ &\quad \times (8.3676 \times 10^{-28} \text{ kg})(0.7412 \times 10^{-10} \text{ m})^2 \\ &= 60.9 \text{ cm}^{-1},\end{aligned}$$

in agreement with experiment, whereas  $\alpha_e$  is found empirically to be about  $3.0 \text{ cm}^{-1}$ . (Actually, as we shall see, the value of  $R_e$  is obtained from the measured  $B_e$ .) Other molecules have larger moments of inertia ( $I = \mu R_e^2$ ) and thus smaller  $B_e$ 's; values of  $B_e$  and  $\alpha_e$  for a number of molecules are listed in Table 7.2.

In writing Eq. 7.19 for a diatomic molecule, we have effectively assumed the atoms to be point masses, so that we can neglect rotation about the internuclear axis. This is valid enough for a molecule in a  ${}^1\Sigma$  state, where the electrons have zero angular momentum relative to the nuclei, but suppose that this is not the case. Let us go back to the symmetric-top model. We can rewrite the eigenvalue equation (Eq. 3.177) as

$$\begin{aligned}E_{\text{rot}} &= J(J+1)hcB_\nu + M_J^2 hc(A - B_\nu), \\ (J = 0, 1, 2, \dots; M_J = J, J-1, \dots, -J+1, -J),\end{aligned}\quad (7.22)$$

where  $A \equiv \hbar/4\pi c I_z$  and  $B_\nu$  is the same as in Eq. 7.21. The quantum numbers  $J$  and  $M_J$  are defined by the equations

$$|\mathbf{J}|^2 = J(J+1)\hbar^2 \quad \text{and} \quad J_z = M_J \hbar,\quad (7.23)$$

which respectively give the square and the  $z$  component of the molecule's total angular momentum  $\mathbf{J}$ . Although both electronic and nuclear motions contribute to  $\mathbf{J}$ , its  $z$  component consists almost entirely of the angular momentum of the electrons about the bond axis. There are a number of ways in which the orbital and spin electronic angular momenta (which we call  $\mathbf{L}$  and  $\mathbf{S}$ , respectively) can couple with each other and with the nuclear rotation; we shall look at only the simplest case. In most electronic states the orbital electronic angular momentum is strongly coupled to the bond axis, and only its  $z$  component is quantized; thus we have  $|L_z| = \Lambda \hbar$ , as we assumed in the last chapter. In singlet states ( $S = 0$ ),  $L_z$  is the only contribution to  $J_z$ , so we also have  $|J_z| = \Lambda \hbar$ ,  $|M_J| = \Lambda$ . Thus for most singlet states Eq. 7.22 can be written in the form

$$\begin{aligned}E_{\text{rot}} &= J(J+1)hcB_\nu + \Lambda^2 hc(A - B_\nu), \\ (\Lambda = 0, 1, 2, \dots; J = \Lambda, \Lambda+1, \Lambda+2, \dots).\end{aligned}\quad (7.24)$$

Similar equations can be derived for other cases. Since the second term can be included in the electronic energy, what is the point of obtaining these equations? The answer is that

they reveal restrictions on the allowable energy levels. In an electronic state described by Eq. 7.24, for example, we can only have  $J \geq \Lambda$ , since the total angular momentum,  $[J(J+1)]^{1/2} \hbar$ , cannot be less than its  $z$  component  $\Lambda \hbar$ . Since  $A \gg B_\nu$ , electronic states with different  $\Lambda$ 's can have very different total rotational energies, often differing by several electron volts. Within a given electronic (and vibrational) state, however, adjacent rotational levels may differ by as little as  $10^{-5}$  eV.

This brings us to rotational spectra. In the next section we shall consider the complications that arise when a molecule simultaneously undergoes rotational and vibrational (or electronic) transitions; here we are concerned only with pure rotational spectra, which are found in the far infrared and microwave regions. As in the case of vibration (pages 186–188), rotational electric dipole spectra appear only for heteronuclear diatomic molecules, since a homonuclear molecule has a dipole moment  $\mu = 0$  in all orientations. For heteronuclear molecules the moment  $\mu$  varies in direction, though not magnitude, in the course of a rotation. The selection rule for electric dipole transitions of a heteronuclear rigid rotator is

$$\Delta J = \pm 1, \quad (7.25)$$

which also usually holds for a real molecule in a given electronic state. (The logic leading to this rule is very much like that following Eq. 7.13, with rotational wave functions replacing the Hermite polynomials and the permanent dipole operator, rather than its derivative, playing the role of the operator inducing the transition. Another way of interpreting Eq. 7.25 is as a consequence of the fact that the photon has an intrinsic angular momentum of one unit of  $\hbar$ .) Substituting in Eq. 7.21, we find that the only allowed pure rotational transitions are those with

$$\Delta E = 2J'hcB_\nu \quad \text{or} \quad \tilde{\nu} = 2J'B_\nu, \quad (7.26)$$

where  $J'$  is the quantum number of the *upper* state. We thus obtain a series of equally spaced spectral lines, beginning at  $\tilde{\nu} = 2B_\nu$  and proceeding to higher wavenumbers at intervals of  $2B_\nu$ . This is illustrated in Fig. 7.4. Since  $2B_e$  ranges from  $120 \text{ cm}^{-1}$  ( ${}^1\text{H}_2$ ) down to less than  $0.1 \text{ cm}^{-1}$ , corresponding to  $0.08 \times 10^{-10} \text{ cm}$  in wavelength, at least the beginning of this series may be in the microwave region. However, in experiments at room temperature, one frequently observes transitions in which the quantum number  $J'$  is quite large, giving rise to higher-frequency lines well into the infrared.<sup>13</sup>

The spacing of rotational lines is one of the best methods for determining internuclear distances (bond lengths). It is worth describing here how one carries out such a determi-

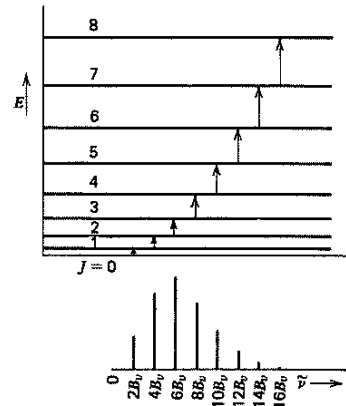


**Figure 7.4** Pure rotational absorption spectrum of a diatomic molecule. Given the selection rule  $\Delta J = \pm 1$ , there is a series of lines with the constant wavenumber spacing  $2B_\nu$ . The intensities of the lines are proportional to the populations of the initial states, and as drawn here correspond to a gas with  $B_\nu h c / k_B T \approx 0.1$  (cf. Chapter 21).

nation. The pure rotational spectrum, as we have said, lies in the far infrared or microwave region. To obtain such a spectrum, one can pass radiation through a rather rarefied gaseous sample of the molecule in question, vary the frequency of the applied radiation, and measure the fraction of energy transmitted from the power source to a detector.<sup>14</sup> The source may be electrons oscillating in a vacuum (a klystron tube), electrons accelerated in a nonmetallic solid by a sufficiently high voltage, or a variable-frequency laser operating in the microwave region of the spectrum; the detector is ordinarily a crystal-diode rectifier. One can carry out such measurements with exceedingly high accuracy—so high, in fact, as to outstrip the ability of existing theories to interpret all the details, which include interactions with vibration, electronic motion, and nuclear spins. In first approximation, however, the lines in a given band are equally spaced, and  $B_\nu$  is simply half the wavenumber spacing. Given such experimental values of  $B_\nu$  for several vibrational states, one simply uses Eq. 7.21 to calculate  $B_e$  and thus  $R_e$ .

We mention in passing the other principal method of determining bond lengths of gaseous molecules, which utilizes electron diffraction (see Sections 3.1 and 11.6). This method is less precise and often less accurate than

<sup>13</sup> As we mentioned earlier, in a gas the average value of  $E_{\text{rot}}$  is  $k_B T$ , which at 300 K is  $4.14 \times 10^{-21} \text{ J}$  (0.0258 eV), corresponding to a wavenumber of  $208 \text{ cm}^{-1}$ . Thus at room temperature the average value of  $J(J+1)$  for  ${}^1\text{H}_2$  is about 3.5 ( $J = 1 - 2$ ), for  $I_2$  about 5500 ( $J = 75$ ).

<sup>14</sup> In practice, rotational spectroscopy usually involves a technique somewhat more complicated than direct absorption. In a laboratory system, the amount of energy absorbed directly is always an extremely small fraction of the total incident radiation, so that the direct spectral signal would be very weak. Instead, one alternately applies and turns off an external electric or magnetic field, which splits and shifts the spectral lines (by the Stark or Zeeman effect), moving them on and off the frequency of the applied radiation. The observed signal is then the difference between the amounts of microwave power detected with the external field on and off. The effect of taking such a difference signal is a strong enhancement of the signal strength relative to the background "noise" reaching the detector.

microwave spectroscopy, but it does give a direct measure of  $R_e$ . A beam of electrons is allowed to impinge on a gas of diatomic molecules; because the electrons are deliberately given quite high energies, they are scattered primarily by the massive atomic nuclei. Since the molecules move randomly, one obtains a quite complex pattern of scattering intensity averaged over all possible molecular orientations. Nevertheless, this pattern contains information on the internuclear spacing. Each nucleus in a molecule produces a set of scattered wavelets, and the wavelets from each pair of nuclei interfere with each other. A single diatomic molecule thus scatters electrons much as two pinholes in a screen produce a diffraction pattern with light from a point source. Despite the random orientation, the net effect of all the molecules is to produce a diffraction pattern which depends on the scattering angle in a very specific way. One can compare this pattern with that corresponding to an assumed  $R_e$ , and adjust the latter until the two match. Similar calculations can be made for even very complex molecules, but for diatomic molecules the computation is simple and limited only by the accuracy with which one can measure the shapes of the diffraction peaks.

### 7.3 Spectra of Diatomic Molecules

Most of our knowledge of molecular structures derives from spectroscopic measurements of one kind or another. Suppose that one subjects a gas of diatomic molecules to electromagnetic radiation, varying the frequency  $\nu$  across the

spectrum. Whenever  $h\nu$  equals the difference between two molecular energy levels, a transition may be induced. What kinds of transitions are these? In the microwave and far infrared regions, as just described, one observes pure rotational transitions, in which only the quantum number  $J$  changes. In the near and middle infrared one sees vibrational transitions. In Section 7.1 we described the pure vibrational spectrum, in which only  $\nu$  changes; unfortunately, things are not really that simple, since rotational transitions of various kinds usually occur at the same time. Radiation in the visible and ultraviolet regions is associated with transitions between different electronic states, again complicated by simultaneous vibrational and rotational transitions. At still higher energies, x-rays produce transitions among the energy levels of the atomic cores (see Chapter 2). Figure 7.5, which illustrates some of the energy levels in a diatomic molecule, should give an idea of the energy differences involved in various kinds of transitions.

These transitions are observed by the standard techniques of experimental spectroscopy, which we shall review here briefly. In *emission spectroscopy*, the sample is subjected to thermal, electric, or other excitation, and the excited atoms or molecules emit energy as they drop to lower energy levels. The emitted radiation is collected at a detector and its intensity is measured as a function of wavelength. An emission spectrum of atomic iron was shown in Fig. 2.9. In *absorption spectroscopy*, a sample of the material under study is subjected to radiation in an appropriate part of the spectrum, and the molecules absorb energy, undergoing

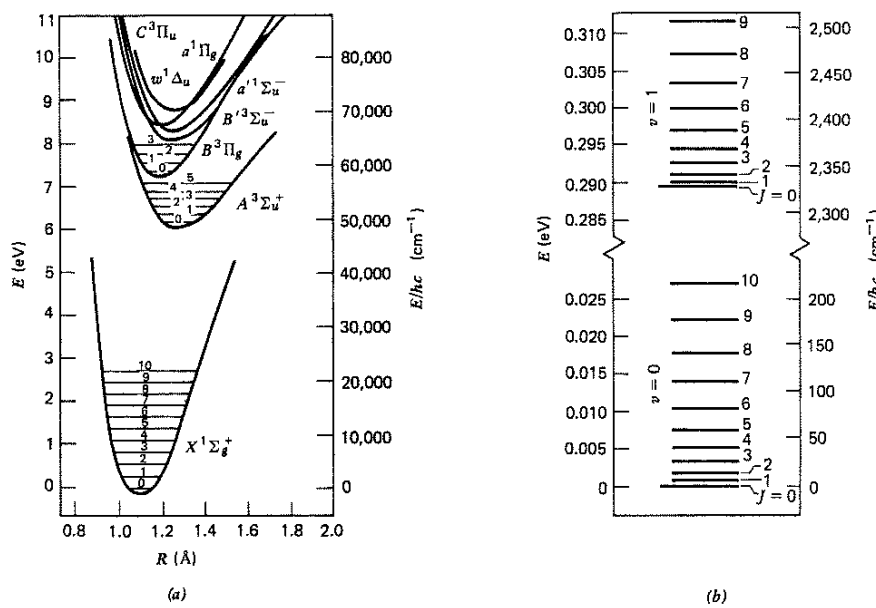


**Figure 7.5** Energy levels of the  $N_2$  molecule. (a) Electronic states, with vibrational levels ( $v = 0, 1, 2, \dots$ ) shown in the lowest three. [Not shown is the  $W^3\Delta_u$  state; this state has about the same minimum energy as the  $B^3\Pi_g$  (see Table 7.6), but its  $R_e$  is not known.] The energy zero is the ground electronic-vibrational state ( $X^1\Sigma_g^+$ ,  $v = 0$ ). After W. Benesch, J. T. Vanderslice, S. G. Tilford, and P. G. Wilkinson, *Apophys. J.* **142**, 1227 (1965). (b) Rotational structure of the two lowest vibrational levels of the ground state; the energy zero is the same as in (a).

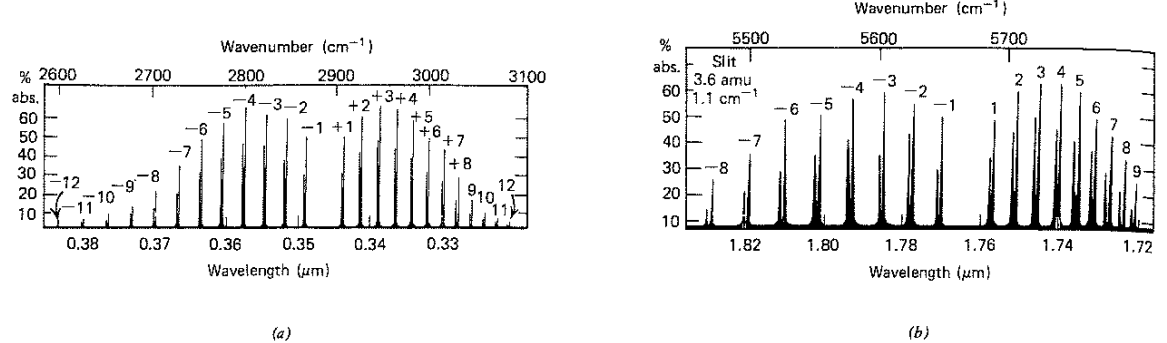


**Figure 7.6** The infrared spectrum of HCl vapor associated with transitions (a)  $\nu=0 \rightarrow \nu=1$  and (b)  $\nu=0 \rightarrow \nu=2$ . The individual rotation-vibration lines are all doublets because of the presence of the isotopic species  $\text{H}^{35}\text{Cl}$  and  $\text{H}^{37}\text{Cl}$ ; the former is the more intense. Numbers above spectral lines specify  $\Delta J$ . From C. F. Meyer and A. A. Levin, *Phys Rev* **34**, 44 (1929).

transitions to higher energy levels. This energy transfer depletes the incident radiation at specific wavelengths (one for each transition), giving rise to a set of spectral lines. The radiation passing through the sample is collected at a detector, where its intensity is measured. The signal of interest is the amount of radiation absorbed, that is, the difference between incident and transmitted intensities. What we usually call a "spectrum" is a representation of the amount of absorption as a function of wavelength or frequency; two regions of the infrared spectrum of HCl are shown in Fig. 7.6. *Fluorescence spectroscopy* is a process of exciting emission spectra, usually by excitation with radiation; in this process, one may measure the distribution of wavelengths of emitted radiation, as in any other kind of emission spectroscopy, or the dependence of the intensity of emission (at a selected wavelength or at all wavelengths simultaneously) on the frequency of the exciting radiation, to obtain an *excitation or action spectrum*.

All experimental spectrometers have the same basic components, but their details can vary greatly, especially with the region of the spectrum under study. These components include the following.

1. *Sample*. When the sample is gaseous or liquid, it must be placed in a holder of some kind; such a sample holder must be reasonably transparent to the radiation one is using. In the ultraviolet below 2000 Å even air becomes opaque, and the whole apparatus must be placed in (or be) a vacuum chamber.
2. *Radiation source*. For absorption spectra in the visible and ultraviolet regions older sources were the standard types of broad-band, continuous light sources: tungsten filament lamps, electric discharges and arcs, and so on. Usual infrared sources were heated rods of refractory material such as SiC. Klystron tubes are still used in the microwave region, and standard radiofrequency generators at longer wavelengths. In all regions of the spectrum, tunable (variable-wavelength) lasers are now the most commonly-used radiation sources. In emission spec-

troscopy the radiation source is the sample itself; it may be excited by simple heating, by electric discharge, by chemical reaction (as in a flame), or by laser-induced excitation.

3. *Optical system*. The optical system consists of whatever devices are used to select or disperse radiation of different wavelengths and collect it at detectors. In most spectral regions of interest, the separation of radiation of many wavelengths can be performed by *dispersing elements*, either prisms or diffraction gratings; the separated radiation can be focused with mirrors and lenses. Prisms and lenses can be used, of course, only where they are transparent. With variable-wavelength lasers, one can dispense with dispersing elements. In the long-wavelength microwave and radio regions, different wavelengths are also obtained by "tuning" the radiation source.
4. *Detector*. The simplest type of radiation detector used to be a photographic emulsion; the intensity is determined by measuring the extent of darkening. Now one typically uses photosensitive semiconductors, photoelectric cells (visible and ultraviolet), thermocouples and bolometers (infrared), and crystal diodes (microwave). The apparatus is usually so designed to record and display a record of the relation between intensity and wavelength or frequency.

We saw that any transition between bound states of a molecule has a definite energy and frequency ( $\Delta E = h\nu$ ), and should thus give rise to a sharply defined spectral line. Yet in practice one always observes "lines" of nonzero width (in wavelength or energy), at best resembling narrow spike-like curves. Sometimes this is an apparatus effect, due to the limited resolution of the optical system, but with sufficient resolving power one obtains line widths characteristic of the sample itself. This broadening of spectral lines has several causes, principally the following. (1) The *natural line width* is the consequence of the uncertainty principle, as stated in Eq. 3.87. Any measurement carried out in a finite time  $\Delta t$  has an energy uncertainty of the order of  $\hbar/\Delta t$ . But the natu-

ral line width is usually extremely small, about  $10^{-4}$  Å for spontaneous emission of visible light. (2) *Doppler broadening* results from the fact that the molecules of the sample are in motion in various directions, so that the frequency of the radiation absorbed or emitted is shifted up or down by the well-known Doppler effect. (3) *Pressure broadening* results from the perturbation of energy levels by intermolecular forces, especially during collisions. In a gas, pressure broadening increases rapidly with density, and is the dominant contribution to line widths at high pressures. Normally, visible and ultraviolet lines from gaseous samples have linewidths dominated by Doppler broadening. Infrared and microwave lines have widths due primarily to pressure broadening at all but the lowest pressures.

In the remainder of this section we shall discuss some of the major aspects of spectroscopy that we have not yet described: (1) simultaneous vibration-rotation spectra; (2) the Raman effect, in which light is scattered inelastically rather than absorbed; (3) electronic spectra.

Since a real molecule may vibrate and rotate simultaneously, it can undergo transitions in which both quantum numbers change. In fact, in the ground electronic states of most diatomic molecules a pure vibrational transition is forbidden. In any such simultaneous transition  $\Delta E_{\text{vib}}$  is likely to be far greater than  $\Delta E_{\text{rot}}$  (because of the energy-level spacings), so vibration-rotation spectra are found in the same part of the spectrum as pure vibrational spectra. For  $\Sigma$  electronic states, which include most stable ground states, the selection rules are those we have already introduced:

$$\Delta v = \pm 1 \quad \text{and} \quad \Delta J = \pm 1, \quad (7.27)$$

with  $\Delta v = \pm 1$  only approximately true for anharmonic oscillators.

Figures 7.6 and 7.7 illustrate the kind of spectrum obtained when molecules undergo such transitions. Each line of the pure vibrational spectrum is replaced by a whole band of vibration-rotation lines. These lines are nearly equally spaced, as in the pure rotational spectrum; however, there is a gap in the center of the band. This gap corresponds to the pure vibrational transition with  $\Delta J = 0$ , which is forbidden for  $\Sigma$  states by the selection rule of Eq. 7.27. The position of the missing line is referred to as the *null line* or *band origin*, with wavenumber  $\tilde{\nu}_0$ . The lines of the band on each side of the origin are called the *P branch* and the *R branch*, with  $\tilde{\nu} < \tilde{\nu}_0$  and  $\tilde{\nu} > \tilde{\nu}_0$ , respectively. It is conventional to designate the upper state by a prime ( $v', J'$ , etc.) and the lower state by a double prime ( $v'', J''$ , etc.). As is shown in Fig. 7.7, the *P branch* corresponds to transitions with  $J' = J'' - 1$  ( $\Delta E < hc\tilde{\nu}_0$ ), and the *R branch* to transitions with  $J' = J'' + 1$  ( $\Delta E > hc\tilde{\nu}_0$ ). With the rotational energy in each state given by Eq. 7.21, the wavenumbers of the lines in the band are given by

$$\tilde{\nu} = \frac{E' - E''}{hc} = \tilde{\nu}_0 + B'_v J'(J'+1) - B''_v J''(J''+1), \quad (7.28)$$

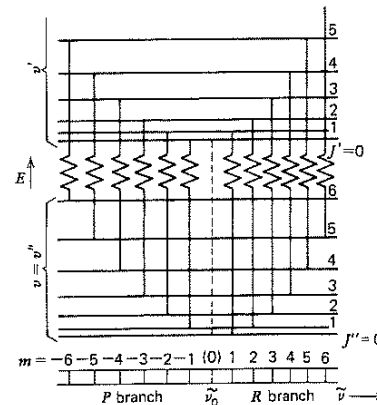


**Figure 7.7** Schematic representation of a vibration-rotation band in the infrared spectrum of a diatomic molecule in a  $\Sigma$  electronic state. Each line in the band corresponds to a transition between a lower level  $v'', J''$  and an upper level  $v', J'$ , with  $J' = J'' - 1$  in the *P* branch and  $J' = J'' + 1$  in the *R* branch. The lines are labeled with the running number  $m$ , defined in Eq. 7.29. The band origin  $\tilde{\nu}_0$  corresponds to the forbidden transition  $v'; J' = 0 \leftrightarrow v''; J'' = 0$ . The spectrum is drawn for  $B_{v'} < B_{v''}$  so that the band converges to a head (not shown) in the *R* branch.

where  $\tilde{\nu}_0 = (E''_{\text{vib}} - E'_{\text{vib}})/hc$ . The relative intensities of the lines are as usual proportional to the populations of the initial rotational states; the intensity distribution in each branch (Fig. 7.6b) resembles that in a pure rotational band (Fig. 7.4).

Equation 7.28 can be rewritten in the form

$$\tilde{\nu} = \tilde{\nu}_0 + (B'_v + B''_v)m + (B'_v - B''_v)m^2, \quad (7.29)$$

where the *running number*  $m$  equals  $-J''$  in the *P* branch and  $J'' + 1$  in the *R* branch. For a rigid rotator the spectral lines are equally spaced, but because of the quadratic term in Eq. 7.29 this cannot be true in a vibrating rotator. From Eq. 7.21 we know that  $B_v$  decreases with increasing  $v$  within a given electronic state, so  $B'_v$  must be a little smaller than  $B''_v$  in any infrared transition.<sup>15</sup> Thus the quadratic term is negative, and the spacing between successive lines must decrease with increasing  $m$ ; this effect is illustrated in Fig. 7.7 in slightly exaggerated form (since  $B'_v$  and  $B''_v$  are nearly equal). Eventually a point should be reached at which the spacing decreases to zero ( $d\tilde{\nu}/dm = 0$ ), after which  $\tilde{\nu}$  decreases with increasing  $m$ . There should thus be a sharp upper limit to the spectrum at some wavenumber  $\tilde{\nu}_b$ , which we call the *band head*. Band heads in vibration-rotation spectra always occur in the *R* branch. However,  $B'_v$  and  $B''_v$  are usually so close together that these heads appear at very high values of  $m$  (or  $J$ ), and thus are usually too weak to

<sup>15</sup> Another way to say this is that the upper state has a larger moment of inertia, since  $\langle I \rangle = \mu \langle R^2 \rangle$  increases with  $v$ .

observe in spectra taken at ordinary temperatures. We shall see that the situation is different for electronic spectra.

Our description thus far applies only to molecules in  $\Sigma$  electronic states, that is, molecules with  $\Lambda = 0$ . When  $\Lambda \neq 0$  there is a change in the selection rule, with  $\Delta J = \pm 1$  replaced by  $\Delta J = 0, \pm 1$ . (This is a consequence of the *vector* addition of the angular momenta of the photon and the molecule.) One thus observes an additional series of transitions with  $\Delta J = 0$ , known as the *Q* branch. The best-known example is in the ground state of NO, which is  $^2\Pi$ . For the *Q* branch, Eq. 7.29 is replaced by

$$\tilde{\nu}_Q = \tilde{\nu}_0 + (B'_v - B''_v)J + (B'_v - B''_v)J^2. \quad (7.30)$$

Since the spacing increases steadily in both directions, there is no band head. The coefficient  $B'_v - B''_v$  is very small, so all the observed lines of the infrared *Q* branch are very close to  $\tilde{\nu}_0$ , and under low or moderate resolution appear as a single intense line.

Up to this point we have been talking only about absorption and emission spectra, but one can also observe the spectrum of radiation *scattered* by molecules. By scattered radiation (cf. Section 2.3) we simply mean radiation that leaves the sample in a direction different from its incident direction. This involves a two-step process on the molecular level: An incident photon strikes a molecule and excites it to a highly unstable condition (in classical terms, sets up a forced, nonresonant oscillation); the molecule then attains a new stationary state by emitting a second photon, which may depart in any direction. But the two steps are virtually simultaneous, and no stationary excited state exists in the interval between them. Scattering should thus not be confused with fluorescence or phosphorescence, in which the molecule absorbs one photon, forms an excited state that lasts long enough to be characterized as a stationary state (anything from picoseconds to hours), then decays by emitting a second photon. (Very rapid fluorescence merges into scattering; it is not important to make a sharp distinction in such cases.) In either kind of process the two photons need not have the same energy; if they do not, of course, the final state of the molecule is different from the initial state, and a spectrum is observed. If the incident and scattered photons do have the same energy, one speaks of *Rayleigh scattering*, corresponding to the *elastic* scattering of particles. The effect is the same as if a single photon bounced off the molecule. If the energies are different, the process is called *Raman*<sup>16</sup> *scattering*, corresponding to inelastic scattering of particles. It is the *Raman* effect that gives rise to a spectrum.

A schematic Raman spectrum is illustrated in Fig. 7.8. To keep the spectrum simple, one ordinarily uses a monochromatic beam of incident light, that is, light of a single wavelength, usually in the visible or ultraviolet. The scattered

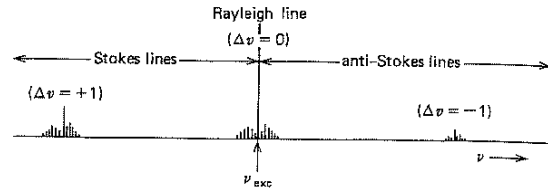


Figure 7.8 Schematic Raman spectrum of a diatomic gas. Three vibrational bands are shown, each with its rotational fine structure. The intense line at the exciting frequency  $\nu_{\text{exc}}$  is due mainly to Rayleigh scattering; in the other bands the center line is the unresolved *Q* branch.

light is customarily observed at right angles to the incident beam. Since Rayleigh scattering is by far the more likely effect,<sup>17</sup> the scattered light is dominated by a single intense line, the *Rayleigh line*, with the same wavelength as the incident light. All the other lines in the spectrum are the result of Raman scattering. If  $\nu_{\text{exc}}$  is the exciting frequency, a line of frequency  $\nu$  corresponds to a molecular transition of energy

$$\Delta E = h(\nu_{\text{exc}} - \nu). \quad (7.31)$$

Note that the frequency shift  $\nu - \nu_{\text{exc}}$  for a given transition is independent of  $\nu_{\text{exc}}$  itself, depending only on  $\Delta E$ . The shift may be to either lower or higher frequency, corresponding respectively to net absorption and net emission of energy by the molecule. The lines with  $\nu < \nu_{\text{exc}}$  are called *Stokes lines*, and those with  $\nu > \nu_{\text{exc}}$  are called *anti-Stokes lines*. As in the infrared spectrum, each vibrational transition gives rise to a closely spaced band of lines corresponding to different rotational transitions. Since at ordinary temperatures most molecules are in the vibrational ground state, the Stokes band for a given  $|\Delta\nu|$  is much more intense than the corresponding anti-Stokes band.

What kinds of transitions do we see in the Raman spectrum? Let us look again at Eq. 4.33, from which we find the transition probability. This equation involves the molecular dipole moment  $\mu$ , which we have thus far taken to be the moment in the absence of external fields; let us call the latter  $\mu_0$ . But the incident light beam has an electric field oscillating at frequency  $\nu_{\text{exc}}$ , and this must in general induce an additional dipole moment in the molecule. (The electrons follow the field more easily than the heavy nuclei, so the centers of positive and negative charge oscillate relative to one another.) The total molecular dipole moment is thus  $\mu_0 + \mu_{\text{ind}}$ , with the induced moment given by

$$\mu_{\text{ind}} = \alpha \mathbf{E} = \alpha \mathbf{E}_0 \cos 2\pi\nu_{\text{exc}}t, \quad (7.32)$$

<sup>16</sup> The phenomenon was predicted in 1923 by A. Smekal and first demonstrated by C. V. Raman and K. S. Krishnan in 1928.

<sup>17</sup> Incidentally, the probability of Rayleigh scattering is proportional to  $\lambda^{-4}$ , so that from a beam of white light far more blue than red will be scattered. This is why the sky is blue.

where  $E$  is the oscillating field and  $\alpha$  is the molecular polarizability (cf. Section 10.1). We can thus rewrite Eq. 4.33 as

$$\mu_{n'n} = \int \dots \int \psi_{n'}^* \mu_0 \psi_n d\tau + E \int \dots \int \psi_{n'}^* \alpha \psi_n d\tau. \quad (7.33)$$

(Remember that the transition probability between states  $n$  and  $n'$  is proportional to  $|\mu_{n'n}|^2$ .) Consider a vibrational-rotational transition for which we define  $\nu_{nn'} \equiv |E_{n'} - E_n|/\hbar$ . This transition can occur in either of two ways. If the first term in Eq. 7.33 is nonzero, there can be ordinary absorption or emission of radiation with frequency  $\nu_{nn'}$  in the infrared or microwave regions; but this can occur only when there is a permanent dipole moment  $\mu_0$ , and thus is not possible for homonuclear molecules. Here we are interested in the second possibility. If the second term in Eq. 7.33 is nonzero, a Raman scattering process can occur in which the scattered light has the frequency  $\nu_{exc} \pm \nu_{nn'}$ . When the incident light is in the visible or ultraviolet, we have  $\nu_{exc} >> \nu_{nn'}$ , and the scattered light is in the same region. Just as the first integral vanishes unless  $\mu_0$  changes in the course of the vibration or rotation, the second integral vanishes unless  $\alpha$  changes. But all diatomic molecules have a nonzero polarizability, which varies with both bond length and orientation to the field: Thus both homonuclear and heteronuclear molecules display Raman spectra.

Since the mechanisms are so different, we need not be surprised if different selection rules apply for Raman and ordinary infrared transitions. The selection rule for vibration is in fact the same:  $\Delta\nu = \pm 1$  for the harmonic oscillator, with weaker bands corresponding to  $\Delta\nu = \pm 2, \pm 3, \dots$  for anharmonic molecules; we also have a band with  $\Delta\nu = 0$ , corresponding to the pure rotational spectrum. But the rotational selection rule for diatomic molecules in  $\Sigma$  states is quite different from the rule for simple absorption or emission; for Raman transitions,

$$\Delta J = 0, \pm 1, \pm 2. \quad (7.34)$$

Thus, each band contains an *S* branch ( $\Delta J = +2$ ), an *O* branch ( $\Delta J = -2$ ), and a *Q* branch ( $\Delta J = 0$ ); the *Q*-branch lines are again given by Eq. 7.30 and are hard to resolve. For molecules with  $A \neq 0$  the selection rule becomes  $\Delta J = 0, \pm 1, \pm 2$ , and *P* and *R* branches are also observed.

Raman spectroscopy offers a useful complement to infrared spectroscopy for studying molecular vibrations and rotations. Raman spectra are observed for transitions that do not appear at all in the infrared, including the entire vibration-rotation spectrum of homonuclear diatomic molecules. This technique has one significant drawback, in that Raman transitions are relatively weak; their intensities are low compared with typical infrared transitions. This is to be expected, since a Raman transition involves two fairly unlikely processes rather than one. Note also that the measurement of Raman spectra is not limited to the infrared region. Any convenient exciting line can be used, since the frequency shift is independent of the exciting frequency. In

fact,  $\nu_{exc}$  is usually chosen to be in the visible or ultraviolet regions, where  $\nu_{exc} \gg \nu_{nn'}$  and the whole Raman spectrum can be found close to the exciting line. Normally, Raman spectra are far less intense than infrared spectra, because they result from a scattering process, which is second-order in the dipole moment; i.e., the intensity depends on the fourth power of matrix elements of that operator, rather than first-order, dependent on the square of such matrix elements. Intensities of Raman spectra can be enhanced either by using exciting radiation of a frequency near a resonant absorption frequency of the scatterer (*resonance Raman spectroscopy*) or by exciting the scatterers when they are on the surface of a metal, where the polarizability of the conduction electrons of the metallic substrate enhances the effect (*surface-enhanced Raman spectroscopy*).

Finally we come to electronic spectra. Since the electronic states of a molecule typically differ in energy by several electron volts, transitions between them are generally observed in the visible and ultraviolet regions. To a given electronic transition there corresponds a series of bands, one for each accessible vibrational transition; within a band there is a line for each possible rotational transition. A typical electronic spectrum is shown in Fig. 7.9.

The most prominent features of an electronic band spectrum are the band heads, the sharply defined edges on one side of the bands. We have already explained the origin of band heads in the context of vibration-rotation spectra. The most important selection rule for electronic transitions is that for the rotational quantum number  $J$ , namely

$$\Delta J = 0, \pm 1, \quad (7.35)$$

with the following exceptions:  $\Delta J = 0$  (the *Q* branch) does not occur if  $A = 0$  in both initial and final states, that is, if both are  $\Sigma$  states; and the transition  $(J' = 0) \leftrightarrow (J'' = 0)$  is always forbidden. Thus there are always *P* and *R* branches, and in most cases also a *Q* branch. The wavenumbers in these branches are again given by Eqs. 7.29 and 7.30, but the

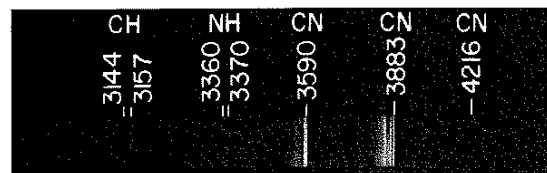


**Figure 7.9** A typical electronic absorption spectrum of a gas undergoing a rapid reaction. The spectrum shows the presence of three diatomic molecules, CH, NH, and CN, none of which is stable under ordinary conditions. The numbers are wavelengths, in angstroms, of the band heads. This spectrum was taken with what is called a "medium dispersion" prism spectrograph, exhibiting the spectral range from about 200 to 700 nm (2000 to 7000 Å) on a 10-in. photographic plate. The photograph is printed in negative so absorption lines appear white. From D. W. Cornell, R. S. Berry, and W. Lwowski, *J. Am. Chem. Soc.* **88**, 544 (1966).

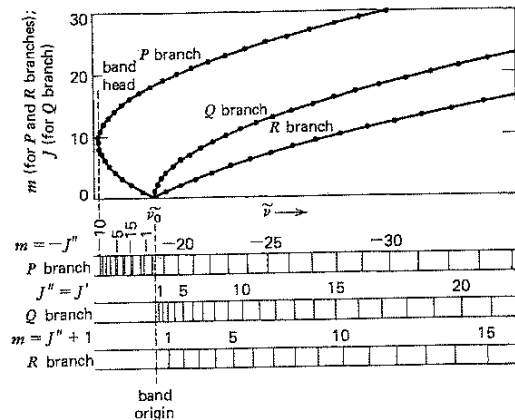
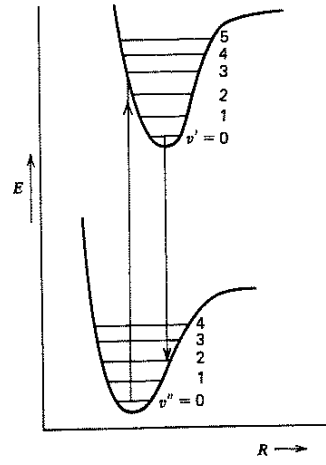


**Figure 7.10** Structure of an electronic band spectrum. The upper part of the figure is what is known as a *Fortrat diagram*, showing the parabolic curves describing the three branches according to Eqs. 7.29 and 7.30. Below are shown the corresponding spectral lines of the three branches (which would be superimposed in the actual spectrum). The spectrum illustrated has a head in the *P* branch, at about  $m = -9$ .

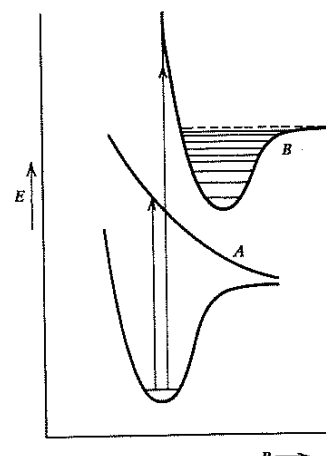
physical situation is quite different. In infrared transitions  $B'_v$  and  $B''_v$  are nearly equal, so heads appear only at high  $m$  and the *Q* branch is very narrow. In electronic spectra this is no longer the case. Since two electronic states are involved, with completely different  $E(R)$  curves and values of  $R_e$  there is no reason why  $B'_v$  and  $B''_v$  should be close to each other. Thus sharp band heads can appear at low values of  $m$ , and the *Q* branch can be as broad as the *P* and *R* branches; an example is analyzed in Fig. 7.10.

Another difference from the infrared spectrum is that either  $B'_v$  or  $B''_v$  may be the larger, depending on which state has the higher moment of inertia, so a head may appear in either the *P* or the *R* branch. Because the band heads are so well defined, they are commonly used for identification and analysis of spectra.

There is no vibrational selection rule in electronic transitions; its place is taken by the *Franck-Condon principle*. This assumes that, during an electronic transition, the nuclei tend to retain their initial positions and momenta. The concept is based on the rapidity with which the very light electrons make their transition, relative to the time and impulse required for the nuclei to change their positions and momenta. Retention of position means that the transition in a single molecule can be represented schematically by a vertical line between the potential curves of the upper and lower electronic states,  $E(R)$  and  $E''(R)$ , respectively. Retention of momentum means that the lower terminus of this "transition line" should be as far above  $E''(R)$  as the upper terminus is above  $E'(R)$ . Such lines are normally drawn in the simplest way, connecting one potential curve with the other. The vertical lines in Fig. 7.11a illustrate such transitions. Strictly, position and momentum cannot both be preserved in a transition between bound states; the most proba-



(a)



(b)

**Figure 7.11** Illustration of the Franck-Condon principle. (a) Single excited state: Any  $v' - v''$  transition is possible, but the likely are between states having maximum values of  $|\psi_{\text{vib}}|^2$  (Fig. 4.4) at nearly the same  $R$ . Here, for example, an excitation from  $v'' = 0$  is most likely to yield  $v' = 3$ , and the state  $v' = 3$  is most likely to decay to  $v'' = 2$ , as indicated by the vertical arrow. (b) Two ways to obtain a continuous spectrum: excitation to an unstable state (A), or to a stable state (B) at a level above its dissociation limit.

ble transitions should be those for which both conditions are most nearly satisfied. In addition, different vibrational states have their maximum values of  $|\psi_{\text{vib}}|^2$  at different values of  $R$ . The more nearly these values coincide for a given  $v'$ , the more likely that transition is to be observed. (Remember that the maximum of  $|\psi_{\text{vib}}|^2$  lies at  $R = v = 0$ , but near the extremes of the vibration for high  $v$  states; cf. Fig. 4.4.) Each electronic transition gives rise

set of vibrational bands, the relative intensities of which vary in accord with these principles. If the final state lies above the dissociation limit, as in Fig. 7.11b, a continuous spectrum will be observed. This is always the case when the electronic state in question is unstable, like the  $\text{H}_2 b^3\Sigma_u^+$  state we discussed in Section 6.10.

To make the concept of the Franck-Condon principle more precise, we write out the electronic counterpart of Eq. 7.12 for a diatomic molecule. The wave function for the initial state is  $\psi_{\text{nuc}}(R)\psi_{\text{elec}}(r, R)$ , and for the final state,  $\psi'_{\text{nuc}}(R)\psi'_{\text{elec}}(r, R)$ . We neglect the rotational wave functions, which are not relevant at this point, and use  $r$  to represent all electronic coordinates, as we did in Eqs. 6.2 and 6.3. The transition is electronic; for convenience, suppose that it is induced by a uniform electromagnetic field, so that the transition operator is the electronic dipole moment operator  $\mu(r)$ . Then the transition amplitude is

$$A = \int dR \int \psi_{\text{nuc}}^*(R) \psi_{\text{elec}}^*(r, R) \mu(r) \psi'_{\text{nuc}}(R) \psi'_{\text{elec}}(r, R) dr. \quad (7.36)$$

We frequently approximate the value of  $A$  by assuming that the electronic factor—the electronic transition dipole—is given by its value at  $R = R_e$ , so that the electronic factor of the transition dipole takes the form

$$\langle \mu(R) \rangle_{R_e} = \int \psi_{\text{elec}}^*(r, R_e) \mu(r) \psi'_{\text{elec}}(r, R_e) dr. \quad (7.37a)$$

This is called the Condon approximation. With this approximation, the full transition dipole is

$$\langle \mu \rangle_{\text{Condon}} = \langle \mu(R) \rangle_{R_e} \int \psi_{\text{nuc}}^*(R) \psi'_{\text{nuc}}(R) dR. \quad (7.37b)$$

Alternatively, we can call upon the mean value theorem and our knowledge that the expectation of  $\mu(r)$  is bounded to tell us that there is some mean value  $\langle \mu(r) \rangle_0$  of  $\mu(r, R)$  for which the accurate dipole moment,  $\langle \mu \rangle_{\text{acc}}$ , is

$$\langle \mu \rangle_{\text{acc}} = \langle \mu(r) \rangle_0 \int \psi_{\text{nuc}}^*(R) \psi'_{\text{nuc}}(R) dR. \quad (7.38)$$

In words, the transition amplitude can be written to be proportional to the overlap of the vibrational wave functions of the initial and final states (see Appendix 6A). If  $\psi_{\text{nuc}}(r)$  and  $\psi'_{\text{nuc}}(R)$  have amplitudes distributed in the same range of  $R$  and if they have similar wavelengths, that overlap is large. The first of these conditions corresponds to the preservation of location; the second, to the preservation of momentum. If neither is well met, the integral  $\langle \mu \rangle_{\text{acc}}$  of Eq. 7.37 is small and the transition probability, proportional to  $|\langle \mu \rangle_{\text{acc}}|^2$ , is correspondingly low.

Not all electronic transitions are allowed; here again we find selection rules. The total angular momentum  $\mathbf{J}$  has the magnitude  $[J(J+1)]^{1/2}\hbar$ , where the rotational quantum number  $J$  obeys the selection rule of Eq. 7.35. For a

diatomic molecule,  $\mathbf{J}$  is the sum of orbital and spin electronic components and the angular momentum of nuclear rotation. As in the atom (Sections 5.6 and 5.7), all these components interact with one another, but some kinds of coupling are more important than others. We shall assume that one can separately define the total electronic orbital angular momentum  $\mathbf{L}$ , with  $z$  component  $\Lambda\hbar$ , and the total electronic spin angular momentum  $\mathbf{S}$ , of magnitude  $[S(S+1)]^{1/2}\hbar$ . When spin-orbit coupling can be neglected,<sup>18</sup> one finds the selection rules

$$\Delta\Lambda = 0, \pm 1 \quad (7.39)$$

( $\Sigma \leftrightarrow \Sigma$  or  $\Sigma \leftrightarrow \Pi$  allowed, but  $\Sigma \leftrightarrow \Delta$  forbidden) and

$$\Delta S = 0 \quad (7.40)$$

( ${}^1\Sigma \leftrightarrow {}^1\Sigma$  allowed,  ${}^1\Sigma \leftrightarrow {}^3\Sigma$  forbidden). There are additional selection rules for various coupling conditions, but we shall ignore these. For homonuclear molecules one must also consider the symmetry of the wave function, since the parity of the wave function always changes in an electronic transition; we write this rule as

$$g \leftrightarrow u, \quad g \leftrightarrow g, \quad u \leftrightarrow u, \quad (7.41)$$

where “ $\leftrightarrow$ ” designates a forbidden transition. (In the orbital approximation, the same rule holds for the orbitals if only one electron takes part in the transition.) On the other hand, the wave function’s symmetry under interchange of electrons or nuclei is fundamentally associated with the indistinguishability of identical particles, and must always be conserved:

$$s \leftrightarrow s, \quad a \leftrightarrow a, \quad s \leftrightarrow a \quad (7.42)$$

( $s$  = symmetric,  $a$  = antisymmetric). This consequence of particle identity is probably the strictest of all molecular selection rules.

We have been able to give only the barest outline of molecular spectroscopy. To finish our treatment of the subject, let us mention one additional complication: the *isotope effect*. The spacing of both vibrational and rotational energy levels depends on the molecule’s reduced mass  $\mu$ , which of course varies from one isotopic species to another. The effect is quite large for hydrogen, as we illustrated in Table 7.1. It is still present in even the heaviest molecules. For example, a given vibration-rotation band of BrCl appears in the spectrum at four different (but overlapping) positions, corresponding to  ${}^{79}\text{Br}{}^{35}\text{Cl}$ ,  ${}^{81}\text{Br}{}^{35}\text{Cl}$ ,  ${}^{79}\text{Br}{}^{37}\text{Cl}$ , and

<sup>18</sup> Spin-orbit coupling does occur, of course, and as in atoms gives the spectrum a fine structure. In addition, when  $\Lambda > 0$  electronic-rotational interaction splits the otherwise degenerate energy levels with  $M_J = \pm |M_s|$  ( $\Lambda$ -type doubling). We shall say more about these effects in Section 7.9.

$^{81}\text{Br}^{37}\text{Cl}$ ; in the pure rotational spectrum there are four closely spaced lines for each transition. This is one more complexity that the spectroscopist must take into account when analyzing a spectrum. But this very complexity makes it possible to excite selectively a spectral line or band of a single isotopic species. Such selective excitation can be used as a first step for starting a photo-induced chemical reaction or ionization that allows one to separate one isotope from another, a process that is otherwise difficult and costly.

## 7.4 The Ionic Bond

We can now return to the problem of chemical bonding. In Chapter 6 we introduced the basic principles of covalent bonding, for the simple cases of one- and two-electron molecules; later in this chapter we shall extend these principles to the general problem of the electronic structure of diatomic molecules. First, however, we must examine a class of molecules constituting such an extreme case that they are best described in terms of a different (and simpler) model. These are the molecules, best typified by the diatomic alkali halides, in which we can say that there is an *ionic bond*.

The characteristic feature of such a molecule is that its properties—especially electron distribution and bonding energy—closely resemble those of two oppositely charged ions in close proximity. The NaCl molecule, for example, is quite like the ion pair  $\text{Na}^+\text{Cl}^-$ . Of course, some redistribution of electronic charge occurs in the formation of any diatomic molecule from the atoms. In a covalent bond this redistribution is rather subtle: A quite small amount of charge is shifted from antibonding to bonding regions, increasing the net bonding force enough to hold the molecule together. But in a homonuclear molecule like  $\text{H}_2$  the total amount of charge in each half of the molecule must be the same as in the separated atoms. In the alkali halides we have a charge redistribution of quite a different order. Charge roughly equivalent to one electron shifts from one atom to the other, i.e., from the region surrounding one nucleus to that surrounding the other. This is clearly illustrated by Fig. 7.12, which shows that the electron distribution in the LiF molecule is much more like the ion pair  $\text{Li}^+ + \text{F}^-$  than the neutral atoms Li + F.

Why does a charge shift of this magnitude occur? As always in bonding problems, because the resulting charge distribution gives the lowest energy for the molecule as a whole. Thus ionic bonding is most likely to occur when an electron can be easily removed from one atom and easily added to the other—"easily" in both cases refers to the energy involved. In the terminology we introduced in Section 5.5, one atom must have a low ionization potential and the other a high electron affinity. It is obvious from Figs. 5.6 and 5.7 that these conditions are best satisfied for the alkali halides. This reasoning is confirmed by detailed calculations of the molecular wave functions, such as those

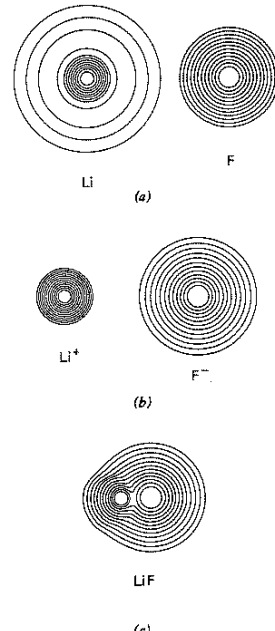


Figure 7.12 Electron distribution in the lithium-fluorine system. (a) Separated atoms, Li + F. (b) Separated ions,  $\text{Li}^+ + \text{F}^-$ . (c) The LiF molecule at the equilibrium internuclear separation,  $R_e = 1.564 \text{ \AA}$ . Diagrams taken from A. C. Wahl, *Sci. Am.* 322, No. 4, 54 (April 1970).

leading to Fig. 7.12. But calculations of this type are essentially the same as those used in covalently bonded molecules. We brought up ionic bonding at this point mainly because there is a *simpler* way to get useful results. Let us see now what it is.

The model we use could not be simpler. We assume that the molecule *is* an ion pair, and calculate the energy of interaction between two ions at close range. Why is this easier than calculating the interaction between two neutral atoms? The answer is clear when we consider the two cases at long range. There is virtually no interaction between two neutral atoms at long range;<sup>19</sup> the dominant terms in the bonding energy result from the reorganization of charge that occurs when the atoms come close together, and must thus be calculated in terms of the forces between individual electrons and nuclei. But two oppositely charged ions do interact strongly at quite long range because of our old friend, the attractive Coulomb force. In first approximation the ions are spherically symmetric charge distributions, which interact as if all their charge were concentrated at the nuclei. Thus

<sup>19</sup> The van der Waals attraction that exists between all atoms or molecules at long range (see Chapter 10, especially Section 10.1) is negligible in comparison with the energies involved in bonding.

the long-range force between the ions is the same as that between two point charges: The force is given by Eq. 1.5 and the corresponding potential energy by Eq. 2.55. Since this interaction involves the whole charge of the ions, even at  $R_e$  it is much larger than the corrections resulting from charge reorganization. One can readily confirm this assertion, since the Coulomb energy ( $e^2/4\pi\epsilon_0 R$ ) is remarkably easy to calculate. It will be seen in Table 7.3 that the Coulomb energy at  $R_e$  by itself gives a fairly good approximation to the observed bond energy (last column). (Note that to carry out this confirmation, we must know  $R_e$  from some other source.)

The existence of an  $R_e$  implies that another force, in addition to the attractive Coulomb force, contributes to the bond. As in all molecules, the equilibrium bond length  $R_e$  is the distance at which there is a balance between attraction and repulsion. The repulsion here is essentially the same as that which occurs when any two atoms or ions "come in contact," that is, when there is significant overlap between the atomic (ionic) wave functions. There is no simple expression that would enable us to calculate this repulsive force as easily as the attractive Coulomb force. A detailed calculation can of course be made in terms of individual electrons and nuclei, but that is just what we are trying to avoid. Fortunately, there is an empirical expression that gives a good description of the short-range repulsion: The potential energy is assumed to fall off exponentially with distance,

$$V_{\text{rep}}(R) = Be^{-R/\rho}, \quad (7.43)$$

where  $B$  and  $\rho$  are constants. This is the repulsive part of the *Born-Mayer potential*, originally introduced to describe the similar interaction in ionic crystals. One can at least get a qualitative idea of why the repulsive potential has this steep form. For very small  $R$  the potential is dominated by the direct internuclear repulsion, which has the relatively slowly decreasing Coulombic form ( $V \propto R^{-1}$ ); yet for  $R \geq R_e$  the repulsive part of the potential becomes extremely small. The repulsive potential must thus decrease appreciably faster than  $R^{-1}$  in the intermediate region, and the exponential is one of the simplest functions that has this behavior.<sup>20</sup> The reason for this steep decrease is the increased screening of the nuclei from one another as the amount of electronic charge between them increases with increasing  $R$ . This process is essentially complete at a distance slightly greater than  $R_e$ , as the overlap of the atomic wave functions becomes negligible.

In the ionic bond model, then, the total potential energy of a diatomic molecule must include a Coulombic ion-attraction term and a short-range repulsion term like

<sup>20</sup> An even more suitable (but less tractable) repulsive potential would be  $V_{\text{rep}}(r) = BR^{-1} e^{-R/\rho}$ , which gives the correct Coulomb behavior as  $R \rightarrow 0$ . This "screened Coulomb potential" is also known as the *Debye potential* in the context of ionic solutions, as we shall see in Chapter 26.

**Table 7.3** Test of the Ionic Bond Model for Some Alkali Halide Molecules\*

Molecule	$R_e$ (Å)	$e^2/4\pi\epsilon_0 R_e$ (eV)	Ionic Dissociation Energy, $D_e(MX \rightarrow \text{ions})(\text{eV})$	
			Calculated	Observed
LiF	1.564	9.21	7.9996	7.983
LiCl	2.021	7.14	6.513	6.648
NaCl	2.361	6.10	5.616	5.750
KF	2.171	6.63	5.993	6.036
KI	3.048	4.72	4.458	4.601
RbCl	2.7869	5.17	4.835	4.917
CsCl	2.906	4.96	4.692	4.870

\* Data taken from P. Brumer and M. Karplus, *J. Chem. Phys.* **58**, 3903 (1973) and references therein.

Eq. 7.43. Additional corrections can be added; the most important of these is an attractive term due to the *polarization* of each ion by the charge on the other. That is, the field of each ion tends to push the other ion's nucleus in one direction and its electrons in the opposite direction, creating an induced dipole on which the first ion exerts an additional attractive force. This process is analyzed in Section 10.1. The magnitude of the polarization energy for each ion is given by Eq. 10.14. Combining this with the other terms, we find a total ionic bond interaction energy of

$$E(R) = -\frac{q_1 q_2}{4\pi\epsilon_0 R} + Be^{-R/\rho} - \frac{\alpha_1 q_2^2 + \alpha_2 q_1^2}{32\pi^2 \epsilon_0^2 R^4}, \quad (7.44)$$

where  $q_i$  is the charge and  $\alpha_i$  the polarizability of the  $i$ th ion; for the alkali halides we of course have  $q(M^+) = -q(X^-) = e$ .

The validity of the ionic bond model can be tested by evaluating Eq. 7.44 at  $R = R_e$  and comparing the result with the experimental dissociation energy. But here we must be careful. Equation 7.44 gives the energy of the ionic molecule MX relative to the separated ions  $M^+ + X^-$ ; this corresponds to the "ionic dissociation energy"

$$D_e(MX \rightarrow M^+ + X^-) = E(M^+ + X^-, R = \infty) - E(MX, R = R_e). \quad (7.45)$$

However, the ground state of the system at large  $R$  corresponds to the neutral atoms in their ground states, not to the ions. This is true for any pair of atoms: Since the lowest ionization potentials ( $I$ ) are greater than the highest electron affinities ( $A$ ), it always requires energy to make a pair of separated ions from the ground-state neutral atoms. This energy of ion-pair formation is

$$E(M^+ + X^-, R = \infty) - E(M + X, R = \infty) = I(M) - A(X). \quad (7.46)$$

## 202 • More about Diatomic Molecules

The true equilibrium dissociation energy<sup>21</sup> of the MX molecule is thus that into the separated neutral atoms,

$$D_e(\text{MX} \rightarrow \text{M} + \text{X}) = D_e(\text{MX} \rightarrow \text{M}^+ + \text{X}^-) - I(\text{M}) + A(\text{X}). \quad (7.47)$$

The predictions of the ionic bond model for a number of alkali halides are compared with experiment in Table 7.3. The “ionic dissociation energies” are those defined by Eq. 7.45. The calculated values are essentially the values of  $-E(R_e)$  predicted by Eq. 7.44, with some minor corrections (van der Waals interaction, dipole–dipole interaction, etc.). The values of  $B$  and  $\rho$  are fitted to the repulsive part of the  $E(R)$  curve, and the values of the  $\alpha_i$ ’s to the observed dipole moment. It turns out that the repulsive and polarization terms are both so small near  $R_e$  that the ionic Coulomb potential alone ( $e^2/4\pi\epsilon_0 R_e$ ) gives a fairly good approximation to  $D_e$ , as we noted earlier. With the other terms included, the agreement with experiment is within a few percent. We conclude that the ionic bond model gives a satisfactory description of the alkali halide molecules. This is not surprising, since Eq. 7.44 is basically the same as the equation used to calculate the lattice energy of an MX crystal, which is well known to be a lattice of  $\text{M}^+$  and  $\text{X}^-$  ions (see Chapter 11).

For an additional test of the ionic bond model, let us consider the dipole moments of ionic molecules. If such a molecule did consist simply of two spherical nonoverlapping ions with charges  $\pm q$  a distance  $R_e$  apart, the magnitude of the dipole moment would be given by Eq. 4.29 as  $\mu = qR_e$ , or  $eR_e$  for the alkali halides. As can be seen from Table 7.4, the actual dipole moments<sup>22</sup> are appreciably less. This discrepancy is due to the polarization effect already mentioned. By attracting the electrons of a negative ion away from the nucleus and toward itself, a positive ion has the effect of reducing the dipole moment; the negative ion attracts the positive ion’s nucleus and repels its electrons. The more polarizable the ions are, the more the molecular dipole moment is reduced. In fact, this effect can be used to evaluate the  $\alpha_i$ ’s of Eq. 7.44. The polarizability of an ion is roughly proportional to its size. In most of the alkali halides the  $\text{X}^-$  ions are significantly larger and thus more polarizable than the  $\text{M}^+$  ions, so the principal effect is the distortion of the halide ion; the alkali ion is effectively very stiff.

Table 7.4 Dipole Moments of Some Ionic Molecules

Molecule	Ionic Charge, $q$	$R_e$ (Å)	$qR_e$ (D)	Measured Dipole Moment, $\mu$ (D)
LiH	$\pm e$	1.595	7.66	5.882
LiF	$\pm e$	1.564	7.51	6.325
LiCl	$\pm e$	2.018	9.69	7.126
LiBr	$\pm e$	2.170	10.42	7.265
LiI	$\pm e$	2.392	11.49	7.428
NaCl	$\pm e$	2.361	11.34	9.001
KCl	$\pm e$	2.667	12.81	10.269
RbCl	$\pm e$	2.787	13.39	10.510
CsCl	$\pm e$	2.906	13.96	10.387
HCl	$\pm e$	1.275	6.12	1.109
TlCl	$\pm e$	2.485	11.94	4.543
SrO	$\pm 2e$	1.920	18.44	8.900
BaO	$\pm 2e$	1.940	18.64	7.954

The extent of polarization is of course also affected by the charge doing the polarizing. The larger the value of  $q$ , the more the dipole moment is reduced. This is made strikingly clear by the example of SrO and BaO in Table 7.4. Naive chemical notions (based on the stability of closed-shell structures) suggest that these molecules might have the structure  $\text{M}^{2+}\text{O}^{2-}$ , but examination of the second ionization potentials (Fig. 5.6) shows the unlikelihood of this idea. In fact, the alkaline earth oxides have dipole moments close to what one would expect for pairs of singly charged ions. One can still describe these compounds with an ionic bond model, but it takes a more elaborate version than we have used for the alkali halides. The reason is that the ions involved,  $\text{Ba}^+$  and  $\text{O}^-$ , for example, have open shells and are thus far more easily distorted by polarization than closed-shell ions (cf. Pacchioni et al., Phys. Rev. B 48, 11573 [1993]).

It might seem that the ionic bond model is of limited importance, since it is directly applicable to only a small class of diatomic molecules. But the utility of the concept actually extends over a far wider range. For one thing, it can be used with little change to describe the bonding in a vast number of ionic crystals. (In fact, it works better for crystals than for single molecules, since the presence of neighbors on all sides of each ion reduces the polarization effects.) The model displays very clearly the distinction between the long-range attractive and short-range repulsive forces, whose balance is crucial for the existence of stable chemical bonds. Moreover, the ionic bond provides us with the extreme case of a chemical bond having the maximum asymmetry of charge distribution. The homonuclear covalent bond, with its perfectly symmetric charge distribution, lies at the other end of this scale, and the bonds in other heteronuclear diatomic molecules fall between these extremes. One can usefully interpret most bonds as some kind of mixture or superposition of ionic and symmetric covalent contributions.

<sup>21</sup> That is, the well depth, measured from the  $E(R)$  minimum, not from the ground vibrational state.

<sup>22</sup> Dipole moments can be measured in several ways. If an electric field is applied to a gas of polar molecules, the molecules will tend to align themselves with the field. The extent of this alignment can be related to the gas’s dielectric constant, and thus to the (measured) capacitance of the system. The electric field also splits the degenerate rotational energy levels with the same  $J$  and different  $M_J$  (Stark effect); this splitting can be observed either directly in the microwave spectrum or by measuring the deflection of molecular beams by the field.

Finally, we can use the ionic model to gain an insight into the nature of bonding that applies even to covalent molecules. Consider any two atoms that form a bond. In the long-range limit, each atom consists of one or more valence electrons outside a closed-shell core—"outside" in the sense that the core electrons have very low charge density at the radii where the valence electrons have their maxima. As the atoms move closer together, bonding effects occur as the valence electrons begin to overlap. But even near  $R_e$  there is no significant overlap between one atom's valence electrons and the other atom's core. An atomic core is essentially the same as a spherically symmetric ion. If an ionic bond model is valid for two ions in "contact" with each other, it should also apply reasonably well for the core part of the interaction in an ordinary bond. Given the distance between the cores, only the Coulombic part of the interaction should be important; in other words, the cores act much like point charges. This means that it is a fairly good approximation to neglect the atomic cores and consider only the valence electrons<sup>23</sup> in describing chemical bonding. This is of course precisely the approximation made in elementary treatments of chemistry, and now we can see why it works as well as it does.

## 7.5 Homonuclear Diatomic Molecules: Molecular Orbitals and Orbital Correlation

To study the electronic structure of covalent diatomic molecules, we must further develop the theory introduced in Chapter 6. We shall base the next part of our discussion on the molecular orbital approach, the simplest and clearest for our present purposes. Thus we assume that each electron sees only the average field of the others and can be described by a one-electron wave function. Since each orbital can "contain" only two electrons (with opposite spin), one must in general use several orbitals to describe a molecule.

Suppose that one finds a suitable set of molecular orbitals; what does one do with them? The most important thing to know is how the energies and shapes of the orbitals vary as some characteristic parameter of the molecule is changed. For a diatomic molecule the key parameter is the internuclear distance  $R$ . Given the sequence of orbital energies, one can develop an Aufbau principle like that used for atoms and derive the equilibrium electronic configuration of the molecule. The orbital energies as functions of  $R$  are most simply displayed in a correlation diagram, like the one we drew for  $H_2^+$  in Section 6.5. We shall see that these and other properties of orbitals vary systematically in series of molecules.

<sup>23</sup> In a transition metal atom the "valence electrons" must include the partly filled inner  $d$  or  $f$  subshells, which are quite close to the atom's "surface."

The first tool we need for the description of molecular orbitals is a systematic way of classifying them. Just as atomic orbitals are given the names of the analogous states of the one-electron H atom, molecular orbitals are named after the states of the one-electron  $H_2^+$  molecule. We have already introduced most of the terminology needed, but we shall review it here. Both the orbitals and the states of the molecule as a whole are classified in terms of the wave function's symmetry properties.

We have introduced two kinds of symmetry thus far, the *permutational* symmetry associated with the indistinguishability of elementary particles, and the *spatial* symmetry associated with the indistinguishability of coordinate systems. It is spatial symmetry that concerns us here; we classify molecules according to the invariance of their physical description under specific kinds of coordinate changes—rotation, reflection, and inversion. We must keep in mind that a change in a molecule's coordinate frame is equivalent to an equal but opposite change in the molecule itself; translating the origin of coordinates a distance  $+x_0$  along the  $x$  axis with the molecule fixed is equivalent to translating the molecule a distance  $-x_0$  in a fixed coordinate system. For convenience we describe spatial transformations in terms of moving the molecule rather than the coordinates, but the two are equivalent. Each of us can think of symmetry and invariance in whichever way seems clearer. Now let us list the kinds of symmetry properties that apply to diatomic molecules.

1. The most important symmetry property, at least for the molecular energy, describes the behavior of the electronic wave function under rotation about the internuclear axis. This is given by the quantum number  $\lambda$  ( $\Lambda$  for the many-electron wave function), which specifies the angular momentum about the internuclear axis:  $L_z = \pm \lambda \hbar$ . The corresponding part of the wave function is  $e^{\pm i\lambda\phi}$ , where  $\phi$  is the angle of rotation about the  $z$  axis (Fig. 6.1). Any rotation through an angle  $\omega$  simply changes the wave function to  $e^{\pm i\lambda(\phi + \omega)}$ , introducing a constant phase factor  $e^{\pm i\lambda\omega}$  but leaving the angular momentum unchanged. This corresponds to the fact that all values of  $\phi$  are physically indistinguishable. States with  $L_z = +\lambda \hbar$  and  $L_z = -\lambda \hbar$  (for  $\Lambda > 0$ ) are doubly degenerate. We identify states with  $L_z = +\lambda \hbar$ ;  $\lambda, \Lambda = 0, 1, 2, 3, \dots$  by the already familiar designations  $\sigma, \pi, \delta, \varphi, \dots$  (orbitals),  $\Sigma, \Pi, \Delta, \Phi, \dots$  (molecules).
2. The molecule is also physically unchanged by reflection in a plane containing the  $z$  axis, the axis of the bond. The electronic wave function must either remain unchanged or reverse its sign; the two cases are designated by the superscripts  $+$  and  $-$ , respectively. For  $\Lambda > 0$ , one of the degenerate molecular states with  $L_z = \pm \lambda \hbar$  is  $+$ , the other  $-$ , and the superscript is usually omitted;  $\Sigma$  states must be either  $\Sigma^+$  or  $\Sigma^-$ , but all those we discussed in Chapter 6 are  $\Sigma^+$ .

- Symmetry properties (1) and (2) apply to all diatomic (or other linear) molecules. In a homonuclear molecule the two ends are indistinguishable, imposing an additional symmetry condition:
- The electronic wave function must either remain unchanged (even parity) or reverse its sign (odd parity) when the molecule is inverted through its center of symmetry,  $\psi(-x, -y, -z) = \pm\psi(x, y, z)$ . As described in Section 6.5, we designate even and odd states by the subscripts *g* and *u*, respectively.

We have spoken here only of the electronic wave function (assuming the Born–Oppenheimer approximation), but there are also symmetry conditions on the total molecular wave function. The most important of these is its symmetry or antisymmetry (denoted by *s* or *a*) under interchange of identical nuclei, which divides the rotational levels into two groups. We shall postpone analysis of this subject to Chapter 21, which treats the relation between symmetry and the distribution of molecules over energy levels.

Now we ask how the orbitals vary as a function of internuclear distance. The limiting cases are simple enough: as  $R \rightarrow \infty$  the molecule behaves like two separated atoms; as  $R \rightarrow 0$  it collapses into a simple united atom. We generally know the states, orbitals, and orbital energies of both the separated-atom and united-atom limits. Given the Born–Oppenheimer approximation, we know that the total electronic energy of a molecule varies smoothly with  $R$ . If the orbital approximation holds for all  $R$ , we can say the same about the orbital energies, which we designate as  $\epsilon_i(R)$ . Thus we can join the united-atom and separated-atom orbital energies by a set of smooth  $\epsilon_i(R)$  curves, making up what we have already defined as a correlation diagram. In the one-electron diagram for  $H_2^+$  (Fig. 6.9) many of the energy levels are degenerate. A more typical example is the  $N_2$  molecule (Fig. 7.13), whose united-atom limit is the silicon atom. It is often unnecessary in such a diagram to give the energies quantitatively for intermediate values of  $R$ . Frequently the ordering of connecting lines as functions of  $R$ , with the limiting energies, is sufficient for analysis of physical phenomena.

How, then, does one know where to draw the connecting lines between the separated-atom and united-atom limits? The rules are quite straightforward, all taking the form of conservation laws:

- Angular momentum about the internuclear axis (defined by the quantum number  $\lambda$ ) is conserved, so that a  $\pi$  orbital, for example, remains a  $\pi$  orbital for all values of  $R$ . Since  $\lambda\hbar$  gives the absolute value of  $L_z$ , in the two limits  $\lambda$  goes over into  $|m_l|$ , the absolute value of the atomic quantum number  $m_l$ . In the united-atom limit, for each subshell with quantum numbers  $n, l$  there are  $2l+1$  degenerate atomic orbitals, whose angular momentum components along a given axis have the values  $L_z = m_l\hbar$  ( $m_l = -l, -l+1, \dots, l-1, l$ ); we of course take the

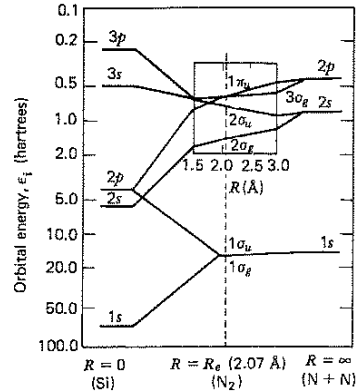


**Figure 7.13** Correlation diagram for orbitals of  $N_2$ . The orbital energy curves in the inset rectangle are those calculated by P. E. Cade, K. D. Sales, and A. C. Wahl, *J. Chem. Phys.* 44, 1973 (1966); elsewhere the correlation curves are straight lines connecting the atomic and molecular orbital energies.

$z$  axis to be the same as the internuclear axis for  $R > 0$ . As soon as  $R$  does have a value greater than zero, these degenerate orbitals become physically distinguishable and have distinct energies, except that each pair with  $m_l = \pm |m_l|$  remains degenerate. Thus the  $2l+1$  molecular orbitals have only  $l$  distinct energy levels, with values of  $\lambda (= |m_l|)$  ranging from 0 to  $l$ . For example, the  $3d$  subshell of the united atom has five degenerate orbitals ( $l = 2, m_l = -2, \dots, 2$ ) which in the molecule become a single  $3d\sigma$  orbital ( $\lambda = 0$ ), a degenerate pair of  $3d\pi$  orbitals ( $\lambda = 1$ ), and another degenerate pair of  $3d\delta$  orbitals ( $\lambda = 2$ ).

- In homonuclear molecules, the parity of each orbital is also conserved. Consider the separated-atom limit. Each atomic subshell yields the same orbitals as in the united atom, and each of these orbitals has its exact counterpart on the other atom. By exactly the same reasoning as in our analysis of  $H_2^+$  (Section 6.3), the symmetry of a homonuclear molecule requires that as  $R \rightarrow \infty$  all its orbitals take on the form of a sum or difference of two atomic orbitals. Thus for each atomic orbital  $\varphi$ , there are two molecular orbitals,  $(\varphi_A) \pm (\varphi_B)$ , which as  $R \rightarrow \infty$  have the same energy; the sum is obviously of even parity (*g*) and the difference of odd parity (*u*). As  $R$  decreases the LCAO approximation no longer holds exactly and the two orbitals become nondegenerate, but the parity remains the same. Corresponding to our example above, the  $3d$  subshells of identical separated atoms yield 10 molecular orbitals:  $\sigma_g$   $3d$ ,  $\sigma_u$   $3d$ , and a degenerate pair each of  $\pi_g$   $3d$ ,  $\pi_u$   $3d$ ,  $\delta_g$   $3d$ ,  $\delta_u$   $3d$ . In the united-atom limit the parity of the orbitals is easily derived from the form of the spherical harmonics (Table 3.1): All orbitals with even  $l$  are *g*, since they are polynomials of even degree in  $\sin \theta$  and  $\cos \theta$ ; similarly, all orbitals with

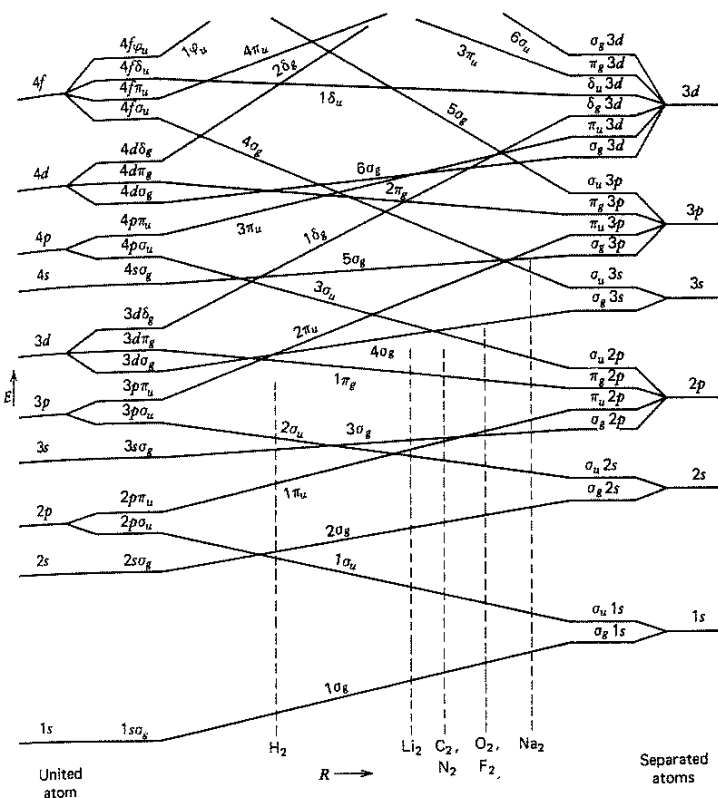


**Figure 7.14** Orbital correlation diagram for homonuclear diatomic molecules. Each orbital is labeled by the three systems described in Section 6.5. The energy scale is schematic, but adjusted so that the sequence of orbital energies in several molecules can be shown by vertical dashed lines (corresponding roughly to  $R = R_e$ ). The orbitals whose lines slant upward from left to right are bonding; those whose lines slant downward are antibonding.

odd  $l$  are  $u$ . Thus our five united-atom  $3d$  orbitals, for example, are all  $g$  (having  $l = 2$ ).

Now we can define all the molecular orbitals near the united-atom and separated-atom limits, with notations of the form  $1s\sigma_g$  and  $\sigma_g1s$ , respectively, as illustrated at the left and right sides of Fig. 7.14. We still need to know how to correlate these limits. Given that  $\lambda$  and parity are conserved, we must correlate only orbitals of the same symmetry type  $\sigma_g$  with  $\sigma_g$ ,  $\pi_u$  with  $\pi_u$  and so on. But there are many orbitals (an infinite number, in fact) of each type. To decide which correlates with which, we need a third and final rule:

- Orbitals are connected in order of increasing energy. In the two limits, the order of orbital energies is that of the isolated atoms (cf. Fig. 5.2). Two connecting lines may cross if they refer to orbitals that differ in  $\lambda$  or parity, but must *not* cross if they refer to orbitals of the same type. This is the *noncrossing rule*, which we introduced in Section 6.5. It has its origin in the fundamental but unproven assumption that there are no *accidental* degeneracies in nature: There is always some perturbation that keeps two states of a system from having exactly the same energy, unless some fundamental symmetry underlies the degeneracy. The spherical symmetry of an atom is responsible

for the  $(2l + 1)$ -fold degeneracy of states with quantum number  $l$ , and the axial symmetry of a diatomic molecule for the twofold degeneracy of states with  $\lambda > 0$ ; in the fine structure, even these degeneracies are removed. Among the commonest perturbations that can cause crossings to be avoided is the kinetic energy of the nuclei affecting the electronic energy. Expressed in quantum mechanical terms, this is precisely the breakdown of the Born–Oppenheimer approximation. Its magnitude and effect appears when we compute the matrix elements of the *nuclear* kinetic energy operator  $H_{\text{nuc}}$  acting on the electronic wave functions  $\psi_{\text{elec}}(r, R)$ , precisely the contributions explicitly neglected in the discussion of footnote 2 of Chapter 6. The effects of perturbations of this kind are typically important only when two potential curves are very close. Appendix 7A discusses the way this can be analyzed and presents an introduction to perturbation theory.

Given the noncrossing rule, the construction of the correlation diagram is simple. We connect the lowest  $\sigma_g$  orbital on one side with the lowest  $\sigma_g$  orbital on the other, giving the  $1\sigma_g$  molecular orbital, which is always the lowest-energy orbital. Similarly, we connect the second-lowest  $\sigma_g$  orbitals to give the  $2\sigma_g$  molecular orbital, and so forth. The same

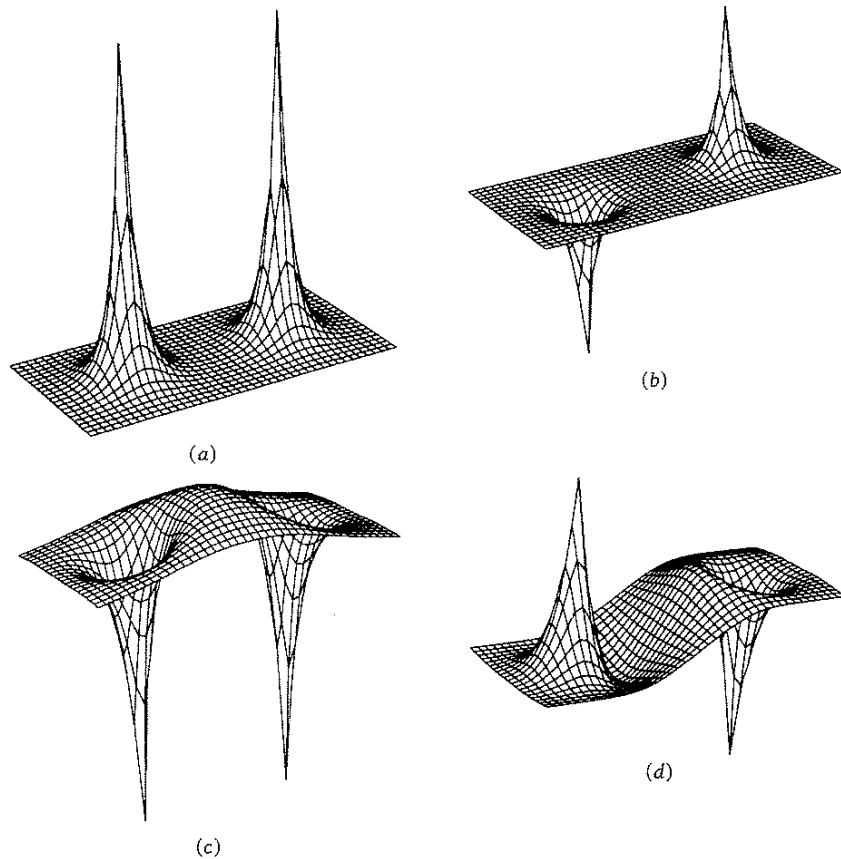


**Figure 7.15** Amplitudes of the lowest orbitals of the  $\text{Li}_2$  molecule. The graphs are all drawn for an  $\text{Li}-\text{Li}$  distance of  $2.67 \text{ \AA}$  or  $5.047$  bohrs, the equilibrium distance. The representation gives a projection of a three-dimensional plot with the vertical scale linear in  $(\text{electron density})^{1/2}$ . The first three orbitals, shown as (a), (b), and (c), are the  $1\sigma_g$  ( $1s_A + 1s_B$ , nearly), the  $1\sigma_u$  ( $1s_A - 1s_B$ , nearly), and the  $2\sigma_g$  (roughly  $2s_A + 2s_B$ ) and are normally occupied. The  $2\sigma_u$  orbital, (d), is normally empty. Calculations were carried out by Mary Dolan and plotted by Mary Dolan and David Campbell.

process is carried out for each of the other symmetry types. We thus obtain the diagram of Fig. 7.14. The energy scale of Fig. 7.14 is schematic only, and not intended to represent the true spacing of energy levels.

The quantum number  $\lambda$ , equivalent to  $|m_l|$ , is a good quantum number within the orbital approximation for all values of  $R$ , and corresponds to the one conserved component of angular momentum. By contrast, the quantum numbers  $n$  and  $l$  for a given orbital are often different in the united-atom and separated-atom limits. The angular momentum quantum number  $l$  simply loses its meaning in the molecule because the total angular momentum of an individual electron is not conserved when the electron moves in a nonspherical potential. We could say that the quantum number  $n$  retains some validity, as an index to the number of nodes ( $n - 1$ ) in the orbital wave function at a given  $R$ ; but this number varies with  $R$ , and is not ordinarily used to identify orbitals. An orbital for which  $n$  is higher in the united atom than in the separated atoms is said to be *promoted*. The energies of promoted orbitals are generally also higher in the united-atom limit, because their promotion more than compensates for the larger nuclear charge of the united atom. Correspondingly, the

energies of nonpromoted orbitals are always lower in the united-atom limit. The reason for calling attention to the distinction is this. Electrons in nonpromoted orbitals tend to stabilize, and those in promoted orbitals to destabilize the formation of a bond. In other words, promoted orbitals are usually antibonding, and nonpromoted orbitals are generally bonding.

Finally, we should say something about the shapes of the molecular orbitals. These are basically the same as the orbitals in  $\text{H}_2^+$ , several of which were shown in Fig. 6.8. Figures 7.15 and 7.16 show the amplitudes of several orbitals for  $\text{Li}_2$  and for  $\text{N}_2$  and  $\text{CO}$ . The nodal surfaces of orbitals are of particular interest because they are closely related to the symmetry of the orbital. For example, an orbital with  $\lambda \neq 0$  has  $\lambda$  nodal planes containing the internuclear axis, which remain nodal planes for all values of  $R$ . All  $\sigma_u$ ,  $\pi_g$ ,  $\delta_u$ ,  $\varphi_g$ , . . . orbitals have an additional nodal plane through the center of symmetry, perpendicular to the bond axis. The shapes of other nodal surfaces, such as those radial nodes that are spheres in free atoms, vary with  $R$ , usually in a complicated manner. Two nodal surfaces of the separated atoms are likely to merge into one at small  $R$ , as in the  $2\sigma_g$  orbital (Fig. 6.8).

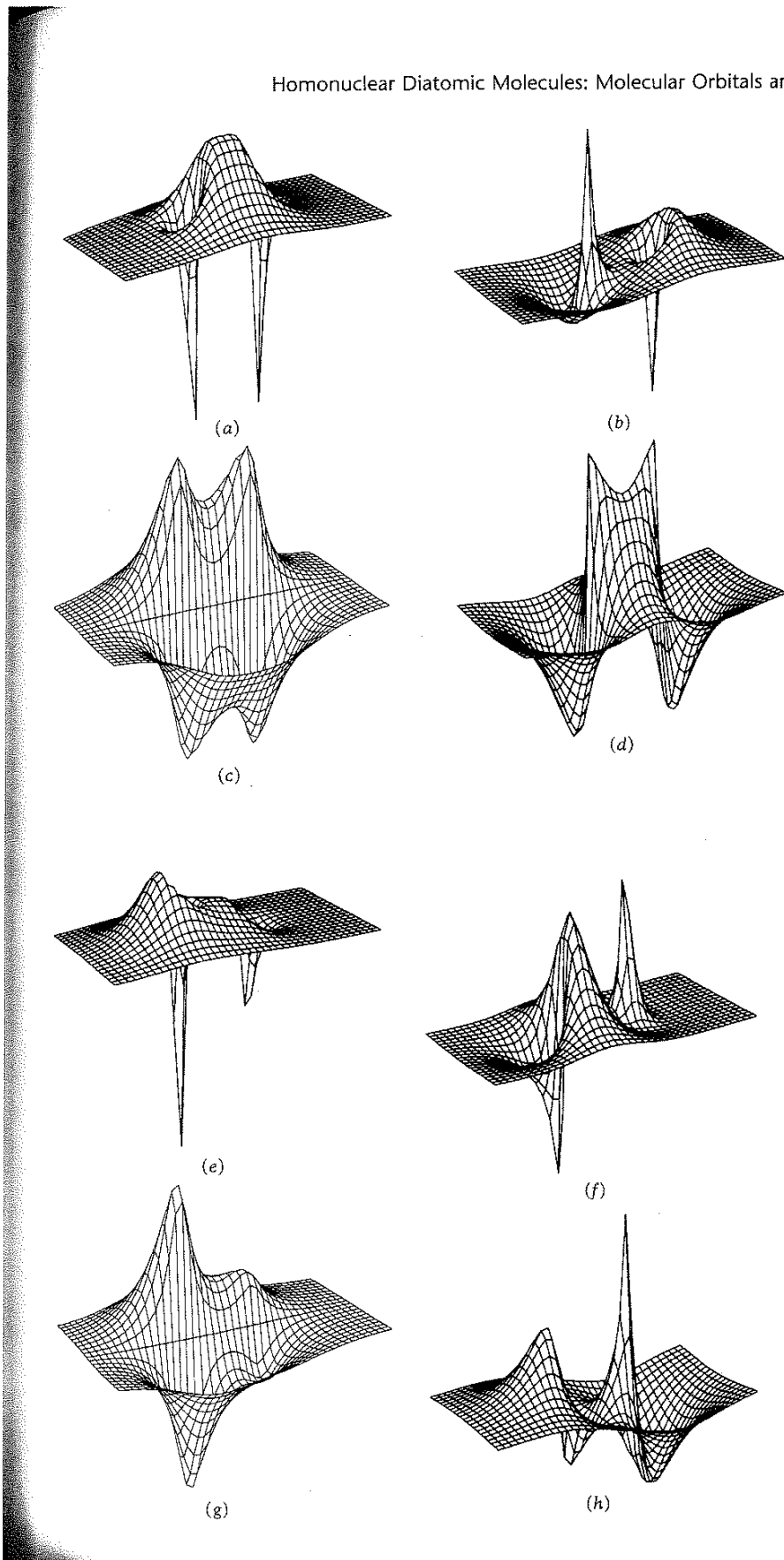


**Figure 7.16** Amplitudes of the normally occupied orbitals of  $N_2$  and CO that correlate with 2s and 2p orbitals of the separated atoms. The N—N bond distance is 1.10 Å or 2.08 bohrs; the C—O bond distance is 1.13 Å or 2.14 bohrs. All amplitudes are plotted with a vertical scale linear in  $\psi$  itself. (a)  $N_2, 2\sigma_g$  (largely  $2s_A + 2s_B$ ). (b)  $N_2, 2\sigma_u$  (largely  $2s_A - 2s_B$ ). (c)  $N_2, 1\pi_g$  (largely  $2p\pi_A + 2p\pi_B$ ). (d)  $N_2, 3\sigma_g$  (roughly  $2p\sigma_A - 2p\sigma_B$  if both atoms are drawn with right-handed coordinate systems). (e), (f), (g), (h) are the corresponding orbitals for CO. Calculations were carried out by Mary Dolan and plotted by Mary Dolan and David Campbell.

## 7.6 Homonuclear Diatomic Molecules: Aufbau Principle and Structure of First-Row Molecules

To the extent that the molecular orbital model is valid, we can describe the electronic structure of a diatomic molecule in terms of an Aufbau principle. Just as in atoms, we assign the electrons to orbitals in order of increasing energy until all the electrons are accounted for. But it is clear from Fig. 7.14 that the order of orbital energies varies with  $R$ . The sequence for a given molecule must be determined empirically, using spectroscopic and chemical evidence. We have drawn Fig. 7.14 so that the orbital sequences for a number of molecules (at  $R_e$ ) can be indicated by vertical lines: One simply reads up each dashed line to find the orbitals in order of increasing energy. The representation is still only schematic and tells us nothing about the relative spacing of the energy levels, but note the agreement with the more quantitative Fig. 7.13.

The Pauli exclusion principle still applies: Each orbital can hold only two electrons, which must be assigned opposite spins. Remember that the lines in Fig. 7.14 represent not individual orbitals but orbital energy levels. Each  $\sigma$  level represents a single orbital, holding two electrons, but each  $\pi$ ,  $\delta$ , . . . level represents two degenerate orbitals (with  $L_z = \pm\lambda$ ) and can thus hold four electrons. Applying this rule, we obtain the ground-state configurations listed in Table 7.5 for the homonuclear diatomic molecules through the first row of the periodic table.

The fact that we can write a configuration for a molecule does not mean that such a molecule really exists as a stable, observable entity. For example, the Aufbau principle implies that the ground state of  $\text{He}_2$  should clearly be  $(1\sigma_g)^2(1\sigma_u)^2$ ; yet there is no stable  $\text{He}_2$  molecule corresponding to this configuration.<sup>24</sup> We must thus look into the conditions governing the stability of a molecule.

The key point here is that some orbitals are bonding, others antibonding. The principles developed in the last chapter indicate that if  $R > R_e$ , the bonding orbitals normally have a higher electron density between the nuclei than in the separated atoms, whereas the antibonding orbitals have a lower electron density between the nuclei than in the separated atoms. It is clear that all the orbitals with nodal planes midway between the nuclei (cf. Fig. 6.8) must be antibonding. Thus all  $\sigma_u$ ,  $\pi_g$ ,  $\delta_u$ , . . . orbitals are antibonding. These are molecular orbitals in which there is destructive interference between the atomic orbitals, and may be referred to as “minus” orbitals. The “plus” orbitals with constructive interference ( $\sigma_g$ ,  $\pi_u$ ,  $\delta_g$ , . . .) are ordinarily bonding. Note that the “plus” and “minus” orbitals can be classified into pairs, with each orbital of the separated atoms producing one of each type,  $\phi_A \pm \phi_B$  in the simple LCAO approxima-

tion. This pairing is precise and unambiguous in homonuclear molecules, but loses some of its clarity in molecules composed of two very different atoms. The electronic energies of bonding and antibonding orbitals generally increase and decrease, respectively, with increasing  $R$ ; the energy levels in Fig. 7.14 have been drawn to reflect this. (In fact,  $\text{He}_2$  does exist, bound by exceedingly weak forces, by far the weakest among all known molecules. These are van der Waals forces, not covalent forces.)

Let us apply this information to the ground states of the simplest few molecules. The  $\text{H}_2^+$  molecule-ion has one electron in the bonding  $1\sigma_g$  orbital, and a dissociation energy ( $D_e$ ) of 2.79 eV. The  $\text{H}_2$  molecule has the configuration  $(1\sigma_g)^2$  with both electrons in the bonding orbital; the dissociation energy,  $D_e = 4.75$  eV, is nearly twice that for  $\text{H}_2^+$ . But the excited state  $(1\sigma_g)(1\sigma_u)$  (i.e.,  $b^3\Sigma_u^+$ , cf. Fig. 6.11), with one bonding and one antibonding electron, is unstable. There exists a  $\text{He}_2^+$  molecule-ion, which is stable in the sense that its  $E(R)$  curve has a true minimum, at  $R_e = 1.08 \text{ \AA}$ . The dissociation energy of  $\text{He}_2^+$ , the difference between  $E(R_e)$  and the energy of  $\text{He}(1s^2) + \text{He}^+(1s)$ , is about 2.5 eV, close to that of  $\text{H}_2^+$ . The configuration should be  $(1\sigma_g)^2(1\sigma_u)$ , which, like  $\text{H}_2^+$ , has one more bonding than antibonding electron. And  $\text{He}_2$ ,  $(1\sigma_g)^2(1\sigma_u)^2$ , with two bonding and two antibonding electrons, only barely exists as a stable molecule.

We can draw a fairly obvious generalization from these data: The bonding power of an electron in a bonding (“plus”) orbital is roughly equal to the antibonding power of an electron in the complementary antibonding (“minus”) orbital. In fact, the antibonding effect is usually slightly greater. There are a number of plausible ways to account for this imbalance. Perhaps the most physically explicit explanation is that electron-electron repulsion tends to limit the amount of charge in the strongly bonding region. Thus any “molecule” in which equal numbers of bonding and antibonding orbitals are filled has no net bonding force, and does not exhibit a chemical bond. We predict that  $\text{Be}_2$  and  $\text{Ne}_2$  as well as  $\text{He}_2$  should not exist as stable molecules; the same conclusion holds for any species in which the separated atoms have only filled orbitals (such as  $\text{Ar}_2$ ,  $\text{Kr}_2$ ,  $\text{Xe}_2$ ). This is the molecular orbital explanation for the “inertness” of closed-shell atoms.

We conclude that the strength of the bonding in a homonuclear diatomic molecule should be roughly proportional to the *bond order*, defined as the number of bonding pairs of electrons minus the number of antibonding pairs. Bond orders of 1, 2, and 3 correspond to what are conventionally called single, double, and triple bonds. Table 7.5 includes the bond orders and dissociation energies of the first-row molecules, which can be seen to support our hypothesis.

In general, when a molecule is best described in the separated-atom scheme, the molecular orbitals deriving from the same subshell of the separated atoms tend to be very close in energy. This is the case for  $R \geq R_e$  in first-row molecules, and is especially noticeable when one compares

<sup>24</sup> But there are many stable excited states, the lowest of which is  $(1\sigma_g)^2(1\sigma_u)(2\sigma_g)$ .

Table 7.5 Ground States of the Homonuclear Diatomic Molecules from H<sub>2</sub> to Ne<sub>2</sub><sup>\*</sup>

Molecule	Electron Configuration <sup>a</sup>	Term Symbol	Bond Order	D <sub>e</sub> (eV)	R <sub>e</sub> (Å)
H <sub>2</sub>	(1σ <sub>g</sub> ) <sup>2</sup>	1Σ <sub>g</sub> <sup>+</sup>	1	4.7478	0.7412
He <sub>2</sub>	(1σ <sub>g</sub> ) <sup>2</sup> (1σ <sub>u</sub> ) <sup>2</sup>	1Σ <sub>g</sub> <sup>+</sup>	0	<10 <sup>-5</sup>	>50
Li <sub>2</sub>	KK(2σ <sub>g</sub> ) <sup>2</sup>	1Σ <sub>g</sub> <sup>+</sup>	1	1.14 ± 0.3	2.6725
Be <sub>2</sub>	KK(2σ <sub>g</sub> ) <sup>2</sup> (2σ <sub>u</sub> ) <sup>2</sup>	1Σ <sub>g</sub> <sup>+</sup>	0	—	—
B <sub>2</sub>	KK(2σ <sub>g</sub> ) <sup>2</sup> (2σ <sub>u</sub> ) <sup>2</sup> (1π <sub>u</sub> ) <sup>2</sup>	3Σ <sub>g</sub> <sup>-</sup>	1	3.0 ± 0.2	1.590
C <sub>2</sub>	KK(2σ <sub>g</sub> ) <sup>2</sup> (2σ <sub>u</sub> ) <sup>2</sup> (1π <sub>u</sub> ) <sup>4</sup>	1Σ <sub>g</sub> <sup>+</sup>	2	6.24 ± 0.22	1.2425
N <sub>2</sub>	KK(2σ <sub>g</sub> ) <sup>2</sup> (2σ <sub>u</sub> ) <sup>2</sup> (3σ <sub>g</sub> ) <sup>2</sup> (1π <sub>u</sub> ) <sup>4</sup> (1π <sub>g</sub> ) <sup>2</sup>	1Σ <sub>g</sub> <sup>+</sup>	3	9.7559 ± 0.0017	1.094
O <sub>2</sub>	KK(2σ <sub>g</sub> ) <sup>2</sup> (2σ <sub>u</sub> ) <sup>2</sup> (3σ <sub>g</sub> ) <sup>2</sup> (1π <sub>u</sub> ) <sup>4</sup> (1π <sub>g</sub> ) <sup>2</sup>	3Σ <sub>g</sub> <sup>-</sup>	2	5.116 ± 0.004	1.2075
F <sub>2</sub>	KK(2σ <sub>g</sub> ) <sup>2</sup> (2σ <sub>u</sub> ) <sup>2</sup> (3σ <sub>g</sub> ) <sup>2</sup> (1π <sub>u</sub> ) <sup>4</sup> (1π <sub>g</sub> ) <sup>4</sup>	1Σ <sub>g</sub> <sup>+</sup>	1	1.604 ± 0.1	1.409
Ne <sub>2</sub>	KK(2σ <sub>g</sub> ) <sup>2</sup> (2σ <sub>u</sub> ) <sup>2</sup> (3σ <sub>g</sub> ) <sup>2</sup> (1π <sub>u</sub> ) <sup>4</sup> (1π <sub>g</sub> ) <sup>2</sup> (3σ <sub>u</sub> ) <sup>2</sup>	1Σ <sub>g</sub> <sup>+</sup>	0	—	—

\* Taken from B. de B. Darwent, *Bond Dissociation Energies in Simple Molecules*, NSRDS-NBS 31, U.S. Dept. of Commerce (U.S. Govt. Printing Office, Washington, D.C., 1970).

<sup>a</sup> The designation KK refers to the filled inner-shell configuration (1σ<sub>g</sub>)<sup>2</sup>(1σ<sub>u</sub>)<sup>2</sup>, corresponding to filled K ( $n = 1$ ) shells in the separated atoms.

the 1π<sub>u</sub>(π<sub>u</sub>2p) and 3σ<sub>g</sub>(σ<sub>g</sub>2p) orbitals. In the ground states of B<sub>2</sub> and C<sub>2</sub> only the 1π<sub>u</sub> orbitals are occupied, which implies that in these species 1π<sub>u</sub> has lower energy than 3σ<sub>g</sub>. The experimental evidence<sup>25</sup> indicates that this is also true for N<sub>2</sub> where both levels are first occupied in the ground state, but that the 3σ<sub>g</sub> electrons are more tightly bound in O<sub>2</sub> and F<sub>2</sub>. This behavior is represented by the crossover of the 1π<sub>u</sub> and 3σ<sub>g</sub> lines between N<sub>2</sub> and O<sub>2</sub> in Fig. 7.14. The evidence from which these conclusions are drawn is primarily that of photoelectron spectroscopy.<sup>26</sup> It follows from Koopman's Theorem (Section 5.4) that the energy of an orbital should equal the energy required to ionize an electron from it.

Let us survey how the physical and chemical properties of the molecules in Table 7.5 reflect their configurations. Hydrogen has been sufficiently covered in the last chapter. As already noted, He<sub>2</sub>, Be<sub>2</sub>, and Ne<sub>2</sub> do not exist as stable molecules in their ground states; at ordinary temperatures helium and neon are monatomic gases, whereas beryllium is a metal that vaporizes (b.p. 2970°C) to a monatomic gas.<sup>27</sup> But we shall now consider each of the other stable species individually.

Lithium is also a metal at ordinary temperatures. Its vapor is primarily monatomic, containing only a few percent of Li<sub>2</sub> molecules. This can be attributed to the relative weakness of the Li–Li bond. Similar behavior is found for the other alkali metals; the bonds become longer and weaker in successively heavier molecules in the series. The bonds are

weak for the same reason that the alkali atoms are large (Section 5.5). The valence (ns) electrons are loosely bound and diffuse in the atoms, and even in the molecules the electron density between the nuclei is low. In contrast to H<sub>2</sub><sup>+</sup> and H<sub>2</sub><sup>+</sup>, the one-electron bonds in the Li<sub>2</sub><sup>+</sup>, Na<sub>2</sub><sup>+</sup>, . . . ions are stronger than the bonds in the corresponding neutral molecules. Apparently the electron–electron repulsion (including that between valence and core electrons) outweighs the bonding effect of the second valence electron.

Not as much is known about the vapor of boron, which remains a black semiconducting solid to well over 2000°C. However, spectroscopy has shown that the B<sub>2</sub> molecule is a reasonably stable species at high temperatures. The bond is of a “normal” length, and correspondingly much stronger than the bond in Li<sub>2</sub>.

As for carbon, C<sub>2</sub> molecules are well known in flames, shock waves, arcs, or indeed any hot system containing an excess of carbon. But the study of carbon vapor is complicated by the presence of larger polymers. Up to around 5000°C the vapor is mainly C<sub>3</sub>, with significant amounts of C<sub>4</sub>, C<sub>5</sub>, . . . , after C<sub>2</sub>, particularly the odd-numbered members; it is not easy to get a large concentration of C<sub>2</sub>. This situation reflects the ease with which carbon forms chains or networks of bonds, as in the solid forms of diamond and graphite and the enormous variety of organic compounds. One reason for this behavior is revealed by the energy spectrum of C<sub>2</sub> (Table 7.6): The energies of the 1π<sub>u</sub> and 3σ<sub>g</sub> orbitals are so close together that C<sub>2</sub> always contains a significant number of molecules in the lowest excited configuration, KK(2σ<sub>g</sub>)<sup>2</sup>(2σ<sub>u</sub>)<sup>2</sup>(1π<sub>u</sub>)<sup>3</sup>(3σ<sub>g</sub>).<sup>28</sup> The

<sup>25</sup> The calculation shown in Fig. 7.13 predicts that 3σ<sub>g</sub> should be lower than 1π<sub>u</sub> in N<sub>2</sub>, but by a very small amount; the experimental energies are in the reverse order.

<sup>26</sup> In this technique a sample is ionized by irradiation with photons of known energy, usually in the vacuum ultraviolet or x-ray regions, and the energies of the emitted electrons are measured; subtraction gives the ionization energy for each electron. See Section 7.10.

<sup>27</sup> However, there are stable Mg<sub>2</sub>, Ca<sub>2</sub>, . . . molecules, indicating that the simple MO theory is not adequate to describe these molecules.

<sup>28</sup> It is much easier to observe transitions to or from this excited state than transitions involving the closed-shell ground state. As a result, for many years the . . . (1π<sub>u</sub>)<sup>3</sup>(3σ<sub>g</sub>) configuration was thought to be the true ground state. The correct analysis of the spectrum and the ordering of states was only made in 1963 by Ballik and Ramsay.

## 210 • More about Diatomic Molecules

**Table 7.6** Some Low-Lying Excited States of First-Row Homonuclear Diatomic Molecules

Molecule	State	Configuration	Energy above Ground State (eV)	
Li <sub>2</sub>	A <sup>1</sup> Σ <sub>u</sub> <sup>+</sup>	KK(2σ <sub>g</sub> )(2σ <sub>u</sub> )	1.744	
	B <sup>1</sup> Π <sub>u</sub>	KK(2σ <sub>g</sub> )(1π <sub>u</sub> )	2.534	
	C <sup>1</sup> Π <sub>u</sub>	KK(2σ <sub>g</sub> )(2π <sub>u</sub> ) or KK(1π <sub>u</sub> ) <sup>2</sup>	3.788	
	D <sup>1</sup> Π <sub>u</sub>	?	≤4.233	
B <sub>2</sub>	A <sup>3</sup> Σ <sub>u</sub> <sup>-</sup>	KK(2σ <sub>g</sub> ) <sup>2</sup> (2σ <sub>u</sub> ) <sup>2</sup> (3σ <sub>g</sub> )(3σ <sub>u</sub> )	3.791	
C <sub>2</sub>	a <sup>3</sup> Π <sub>u</sub>	KK(2σ <sub>g</sub> ) <sup>2</sup> (2σ <sub>u</sub> ) <sup>2</sup> (1π <sub>u</sub> ) <sup>3</sup> (3σ <sub>g</sub> )	0.089	
	B <sup>3</sup> Σ <sub>g</sub> <sup>+</sup>	KK(2σ <sub>g</sub> ) <sup>2</sup> (2σ <sub>u</sub> ) <sup>2</sup> (1π <sub>u</sub> ) <sup>2</sup> (3σ <sub>g</sub> ) <sup>2</sup>	0.789	
	A <sup>1</sup> Π <sub>u</sub>	KK(2σ <sub>g</sub> ) <sup>2</sup> (2σ <sub>u</sub> ) <sup>2</sup> (1π <sub>u</sub> ) <sup>2</sup> (3σ <sub>g</sub> )	1.040	
	c <sup>3</sup> Σ <sub>u</sub> <sup>+</sup>	KK(2σ <sub>g</sub> ) <sup>2</sup> (2σ <sub>u</sub> )(1π <sub>u</sub> ) <sup>4</sup> (3σ <sub>g</sub> )	1.651	
	d <sup>3</sup> Π <sub>g</sub>	KK(2σ <sub>g</sub> ) <sup>2</sup> (2σ <sub>u</sub> )(1π <sub>u</sub> ) <sup>3</sup> (3σ <sub>g</sub> ) <sup>2</sup>	2.482	
	C <sup>1</sup> Π <sub>g</sub>	KK(2σ <sub>g</sub> ) <sup>2</sup> (2σ <sub>u</sub> )(1π <sub>u</sub> ) <sup>3</sup> (3σ <sub>g</sub> ) <sup>2</sup>	4.248	
	C <sup>1</sup> Π <sub>g</sub>	KK(2σ <sub>g</sub> ) <sup>2</sup> (2σ <sub>u</sub> ) <sup>2</sup> (1π <sub>u</sub> ) <sup>2</sup> (3σ <sub>g</sub> )(1π <sub>g</sub> )	4.643	
	e <sup>3</sup> Π <sub>g</sub>	KK(2σ <sub>g</sub> ) <sup>2</sup> (2σ <sub>u</sub> ) <sup>2</sup> (1π <sub>u</sub> ) <sup>2</sup> (3σ <sub>g</sub> )(1π <sub>g</sub> )	5.058	
N <sub>2</sub>	A <sup>3</sup> Σ <sub>u</sub> <sup>+</sup>	KK(2σ <sub>g</sub> ) <sup>2</sup> (2σ <sub>u</sub> ) <sup>2</sup> (1π <sub>u</sub> ) <sup>2</sup> (3σ <sub>g</sub> ) <sup>2</sup> (1π <sub>u</sub> )	6.169	
(cf. Fig. 7.5)	B <sup>3</sup> Π <sub>g</sub>	KK(2σ <sub>g</sub> ) <sup>2</sup> (2σ <sub>u</sub> ) <sup>2</sup> (1π <sub>u</sub> ) <sup>4</sup> (3σ <sub>g</sub> )(1π <sub>g</sub> )	7.353	
	W <sup>3</sup> Δ <sub>u</sub>	KK(2σ <sub>g</sub> ) <sup>2</sup> (2σ <sub>u</sub> ) <sup>2</sup> (1π <sub>u</sub> ) <sup>3</sup> (3σ <sub>g</sub> ) <sup>2</sup> (1π <sub>g</sub> )	7.356	
	B <sup>3</sup> Σ <sub>u</sub> <sup>-</sup>	KK(2σ <sub>g</sub> ) <sup>2</sup> (2σ <sub>u</sub> ) <sup>2</sup> (1π <sub>u</sub> ) <sup>3</sup> (3σ <sub>g</sub> ) <sup>2</sup> (1π <sub>g</sub> )	8.165	
	O <sub>2</sub>	a <sup>1</sup> Δ <sub>g</sub>	KK(2σ <sub>g</sub> ) <sup>2</sup> (2σ <sub>u</sub> ) <sup>2</sup> (3σ <sub>g</sub> ) <sup>2</sup> (1π <sub>u</sub> ) <sup>4</sup> (1π <sub>g</sub> ) <sup>2</sup>	0.977
	b <sup>3</sup> Σ <sub>g</sub> <sup>+</sup>	KK(2σ <sub>g</sub> ) <sup>2</sup> (2σ <sub>u</sub> ) <sup>2</sup> (3σ <sub>g</sub> ) <sup>2</sup> (1π <sub>u</sub> ) <sup>4</sup> (1π <sub>g</sub> ) <sup>2</sup>	1.627	
	c <sup>1</sup> Σ <sub>u</sub> <sup>-</sup>	KK(2σ <sub>g</sub> ) <sup>2</sup> (2σ <sub>u</sub> ) <sup>2</sup> (3σ <sub>g</sub> ) <sup>2</sup> (1π <sub>u</sub> ) <sup>4</sup> (1π <sub>g</sub> ) <sup>2</sup>	4.050	
	C <sup>3</sup> Δ <sub>u</sub>	KK(2σ <sub>g</sub> ) <sup>2</sup> (2σ <sub>u</sub> ) <sup>2</sup> (3σ <sub>g</sub> ) <sup>2</sup> (1π <sub>u</sub> ) <sup>4</sup> (1π <sub>g</sub> ) <sup>2</sup>	4.255	
F <sub>2</sub>	A <sup>3</sup> Σ <sub>u</sub> <sup>+</sup>	KK(2σ <sub>g</sub> ) <sup>2</sup> (2σ <sub>u</sub> ) <sup>2</sup> (3σ <sub>g</sub> ) <sup>2</sup> (1π <sub>u</sub> ) <sup>3</sup> (1π <sub>g</sub> ) <sup>3</sup>	4.340	
	B <sup>3</sup> Σ <sub>u</sub> <sup>-</sup>	KK(2σ <sub>g</sub> ) <sup>2</sup> (2σ <sub>u</sub> ) <sup>2</sup> (3σ <sub>g</sub> ) <sup>2</sup> (1π <sub>u</sub> ) <sup>3</sup> (1π <sub>g</sub> ) <sup>3</sup>	6.120	
F <sub>2</sub>	<sup>3</sup> Π <sub>u</sub>	KK(2σ <sub>g</sub> ) <sup>2</sup> (2σ <sub>u</sub> ) <sup>2</sup> (3σ <sub>g</sub> ) <sup>2</sup> (1π <sub>u</sub> ) <sup>4</sup> (1π <sub>g</sub> ) <sup>3</sup> (3σ <sub>u</sub> )	~ 1–1.5 (not observed)	
	A <sup>1</sup> Π <sub>u</sub>	KK(2σ <sub>g</sub> ) <sup>2</sup> (2σ <sub>u</sub> ) <sup>2</sup> (3σ <sub>g</sub> ) <sup>2</sup> (1π <sub>u</sub> ) <sup>4</sup> (1π <sub>g</sub> ) <sup>3</sup> (3σ <sub>u</sub> )	repulsive	
	B <sup>1</sup> Π <sub>g</sub>	KK(2σ <sub>g</sub> ) <sup>2</sup> (2σ <sub>u</sub> ) <sup>2</sup> (3σ <sub>g</sub> ) <sup>2</sup> (1π <sub>u</sub> ) <sup>3</sup> (1π <sub>g</sub> ) <sup>4</sup> (3σ <sub>u</sub> )	?	

unpaired electrons can readily form bonds with other C atoms, gaining more than enough energy to compensate for the excitation. (Carbon poses a very special situation: Under some conditions, e.g., in an electric arc and ca. 100 torr of He, carbon forms the soccer-ball-like molecule C<sub>60</sub>, a shell of 60 carbon atoms, called “buckminsterfullerene” and larger members of the series of “cage compounds” which are generically called “fullerenes.” The C<sub>60</sub> molecule is a remarkably stable species found in 1984 and made in sufficient quantity for a definitive determination of its structure in 1991. Its structure is precisely that of a standard soccer ball, with carbon atoms at the vertices of all the polyhedral faces. Besides their conventional chemistry, the fullerenes can hold atoms of other substances—e.g., He, Ar, or some metal atoms, within their cages.)

This illustrates the general principle that low-lying excited states facilitate bond formation. We introduced this idea (in a negative sense) in Section 5.5 to account for the “inertness” of the rare gas atoms, but it also applies to molecules. The molecules Li<sub>2</sub>, B<sub>2</sub>, and C<sub>2</sub> all have fairly low

excited states (Table 7.6), and can thus exist only in the vapor phase; the solid forms of these elements (and of most other elements) have structures in which each atom is bonded to many nearest neighbors. In contrast, the first excited state of N<sub>2</sub> is very high (cf. Fig. 7.5), and nitrogen exists as discrete diatomic molecules even in the solid phase, which is thus called a *molecular crystal*. The ground state of N<sub>2</sub> is effectively a closed-shell structure, with all the occupied orbitals filled, and the physical properties of nitrogen are in many ways similar to those of an inert gas. In particular, N<sub>2</sub> exists as a gas to well below room temperature.

The properties of oxygen are unusual in several respects. The ground state of O<sub>2</sub> has the configuration . . . (1π<sub>g</sub>)<sup>2</sup>. Since there are two degenerate 1π<sub>g</sub> orbitals, the 1π<sub>g</sub> electrons can go in either the same or different orbitals, leading to singlet and triplet states, respectively. In analogy to Hund’s rule for atoms, and for the same reasons, the triplet state is of lower energy. Thus the ground state of O<sub>2</sub> has S = 1 and is paramagnetic; the explanation of this phenome-

non was one of the early triumphs of molecular orbital theory.<sup>29</sup> Additional confirmation is provided by the ions derived from O<sub>2</sub>, in which the bond length (and thus strength) varies in accordance with the MO bond order:

Species	Ground-State Configuration	Bond Order	R <sub>e</sub> (Å)	D <sub>0</sub> (eV)
O <sub>2</sub> <sup>+</sup>	... (3σ <sub>g</sub> ) <sup>2</sup> (1π <sub>u</sub> ) <sup>4</sup> (1π <sub>g</sub> )	2 1/2	1.117	6.662
O <sub>2</sub>	... (3σ <sub>g</sub> ) <sup>2</sup> (1π <sub>u</sub> ) <sup>4</sup> (1π <sub>g</sub> ) <sup>2</sup>	2	1.208	5.116
O <sub>2</sub> <sup>-</sup>	... (3σ <sub>g</sub> ) <sup>2</sup> (1π <sub>u</sub> ) <sup>4</sup> (1π <sub>g</sub> ) <sup>3</sup>	1 1/2	1.33	4.07
O <sub>2</sub> <sup>2-</sup>	... (3σ <sub>g</sub> ) <sup>2</sup> (1π <sub>u</sub> ) <sup>4</sup> (1π <sub>g</sub> ) <sup>4</sup>	1	1.49 (in solid Na <sub>2</sub> O <sub>2</sub> , etc.)	

But in O<sub>2</sub> the ground state itself has unpaired electrons. How is it that additional bonds do not form<sup>30</sup> as in carbon? The answer may be that the electrons in question are in the antibonding 1π<sub>g</sub> orbitals; the next available bonding orbital is the much higher 4σ<sub>g</sub>. Yet S<sub>2</sub>, with a similar orbital structure, readily polymerizes to ring molecules such as S<sub>8</sub> and S<sub>6</sub>. Whatever the reason, the O<sub>2</sub> molecule is the stable form of oxygen at all temperatures below those at which the molecules dissociate. Like nitrogen, oxygen is a room-temperature gas and a low-temperature molecular crystal.

Finally, the F<sub>2</sub> molecule is similar to N<sub>2</sub> in that it has a closed-shell ground state and relatively inaccessible excited states. Fluorine shows the same "inert" behavior as nitrogen and oxygen—inert with regard to physical properties only, since F<sub>2</sub>, like O<sub>2</sub>, is highly reactive chemically. The energy of the first excited state is probably quite low, but transitions from the ground state are strongly forbidden.

Thus far we have discussed only electron configurations and the qualitative inferences one can draw from them. Of course the configurations are only the starting point for molecular orbital calculations. We need not go into the details of these calculations here; the methods are those we outlined in Chapter 6. One sets up a trial wave function in some way and computes the energy as a function of R by Eq. 5.11. The trial function ordinarily contains adjustable parameters which are varied to minimize the energy. Within the orbital approximation, the molecular wave function has the form of the antisymmetrized Hartree-Fock product (Eq. 6.63), in which the φ's are molecular orbitals. The simplest trial MOs are LCAO functions of the type already discussed, for example,

$$\phi(2\sigma_g) = \phi(\sigma_g 2s) = C[\phi_A(2s) + \phi_B(2s)], \quad (7.48)$$

but such simplistic forms give unsuitably inaccurate results for anything more complicated than H<sub>2</sub>. The next step is to go beyond the correlation diagram and use mixtures of atomic orbitals of appropriate symmetry to generate "better" atomic orbitals, as in

$$\begin{aligned} \phi(2\sigma_g) &= C_1\phi(\sigma_g 2s) \\ &\quad + C_2\phi(\sigma_g 1s) + C_3\phi(\sigma_g 2p) + \dots \end{aligned} \quad (7.49)$$

This process is called *hybridization* and will be discussed in greater detail in the next chapter. However the trial MOs are set up, the energy is then minimized by the self-consistent-field method. As in atomic calculations, the speed of convergence depends largely on what functions are chosen to represent the atomic orbitals. The best SCF MO calculations now give essentially accurate Hartree-Fock results for first-row molecules, and are being extended to larger molecules as larger computers are introduced. The Hartree-Fock solution, we recall, is the best possible solution *within the one-electron-orbital approximation*; it is adequate for many purposes. The correlation energy, the difference between the true energy and the Hartree-Fock energy, can be calculated by configuration interaction or similar techniques (Section 6.9). For simple molecules, the best calculations lead to predictions of spectral line positions within about 10–20 cm<sup>-1</sup> of the observed lines. This is accurate enough to be very useful for identification, but considerably less accurate than the measurement of spectral lines.

The energy is not the only molecular property that can be computed. We can gain insights from examining the electron distributions in homonuclear diatomic molecules. In Figs. 6.7, 7.15, and 7.16, we looked at orbital amplitudes. Now we turn to total densities. Figure 7.17 shows typical "three-dimensional" pictures of total densities for three molecules. Figure 7.18 shows electron-density contour maps for a larger set. All were obtained from SCF calculations. Electron densities are given in Fig. 7.18 for both individual orbitals and the molecule as a whole. In the H<sub>2</sub> molecule all but the innermost few contours are nearly circular, that is, the outer portions of the electron distribution resemble that in the spherical He atom; even between the nuclei the electron density is only slightly below that at the two nuclear peaks. In contrast, the weakly bound Li<sub>2</sub> molecule is quite like two separate atoms, with a very deep valley between the two peaks. For the other first-row molecules, the stronger the bond, the more nearly the total electron density resembles that in a single atom. The "saddle" between the nuclei is still quite low in B<sub>2</sub>, reaches about half the peak height in N<sub>2</sub>, and has fallen again by the time we reach F<sub>2</sub>. However, the outer reaches of the electron distribution shrink steadily with increasing Z, the same trend one finds for atomic sizes across a period. As for the orbitals, note that all the inner-shell (1σ<sub>g</sub> and 1σ<sub>u</sub>) orbitals of the first-row molecules do not differ significantly from the core densities in two separate atoms. Although the calculations leading to Fig. 7.18 neglect electron correlation, one could hardly tell the difference on the scale of these figures.

<sup>29</sup> The simple valence bond theory would predict one of the structures :O=O:, which is not paramagnetic, or :O—O:, which is too weakly bonded. The MO interpretation straightforwardly accounts for both the paramagnetism and the bond order, :O—O:.

<sup>30</sup> Oxygen does form the O<sub>3</sub> (ozone) molecule, but no further polymerization has been observed. Indeed, O<sub>3</sub> is quite unstable relative to O<sub>2</sub>; the reaction 2O<sub>3</sub> → 3O<sub>2</sub> occurs readily if a suitable catalyst is present.

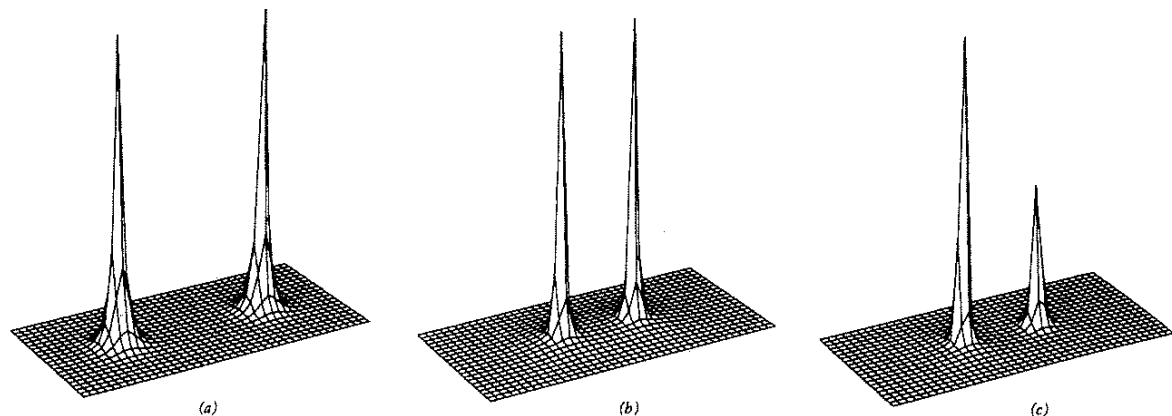


**Figure 7.17** Total electron densities for (a)  $\text{Li}_2$ ; (b)  $\text{N}_2$ ; (c)  $\text{CO}$ . Each molecule is taken at its equilibrium internuclear distance. Calculations were carried out by Mary Dolan and plotted by Mary Dolan and David Campbell.

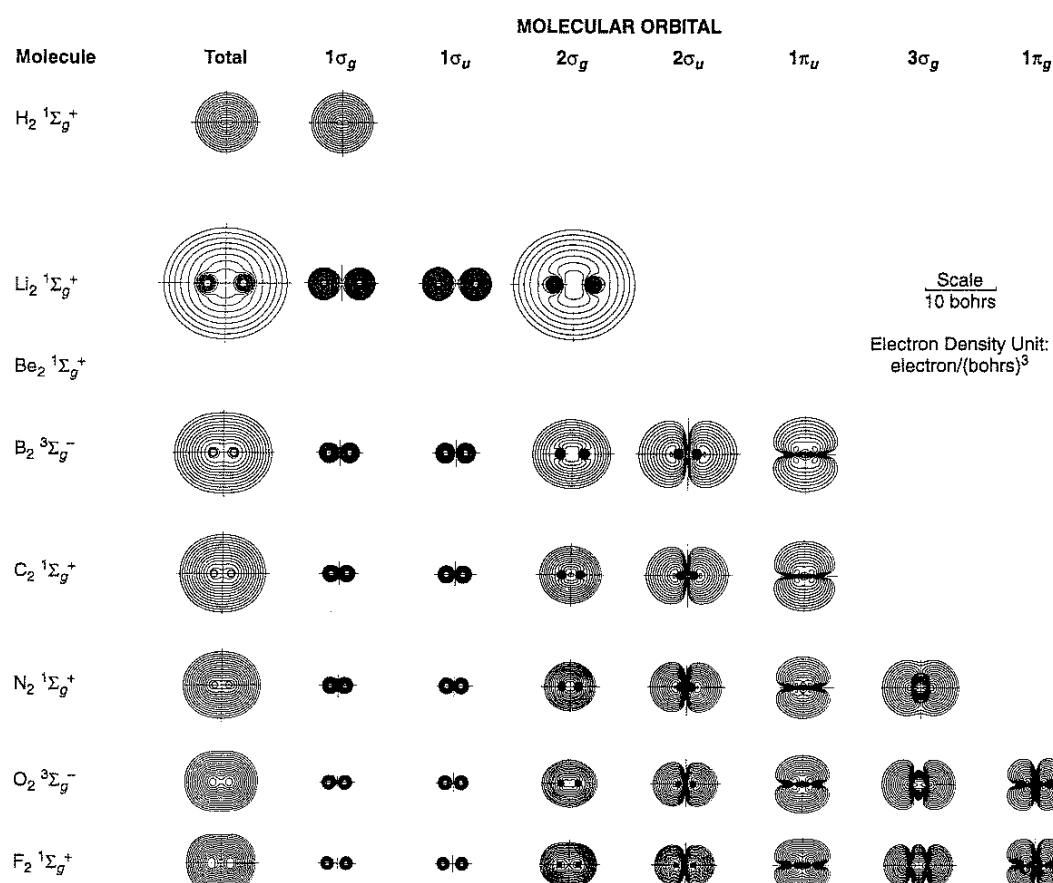


**Figure 7.18** Contour maps of electron densities of orbitals and of total electron densities for the seven lightest stable homonuclear molecules. From A. C. Wahl, *Sci. Am.* 322, No. 4, 54 (April 1970).

## 7.7 Introduction to Heteronuclear Diatomic Molecules: Electronegativity

A heteronuclear molecule has no end-to-end symmetry. Thus symmetry condition 3 of Section 7.5 is not applicable: Neither the orbitals nor the molecular wave function can be described as  $g$  or  $u$ . Otherwise our previous nomenclature can be retained. In the orbital approximation, the molecular orbitals tend to localize predominantly around one nucleus or the other; the ionic molecules of Section 7.4 are an

extreme case of this. Only when the molecule is very close to the united-atom limit do the normally occupied orbitals have comparable amplitudes around both nuclei. This asymmetric charge distribution carries over to the molecule as a whole, and heteronuclear molecules are therefore polar, that is, have nonzero dipole moments.

As in homonuclear molecules, we can use a correlation diagram to represent the sequence of orbital energies. Figure 7.19 $a$  is a general correlation diagram for heteronuclear diatomic molecules. Since the two atoms are different, they

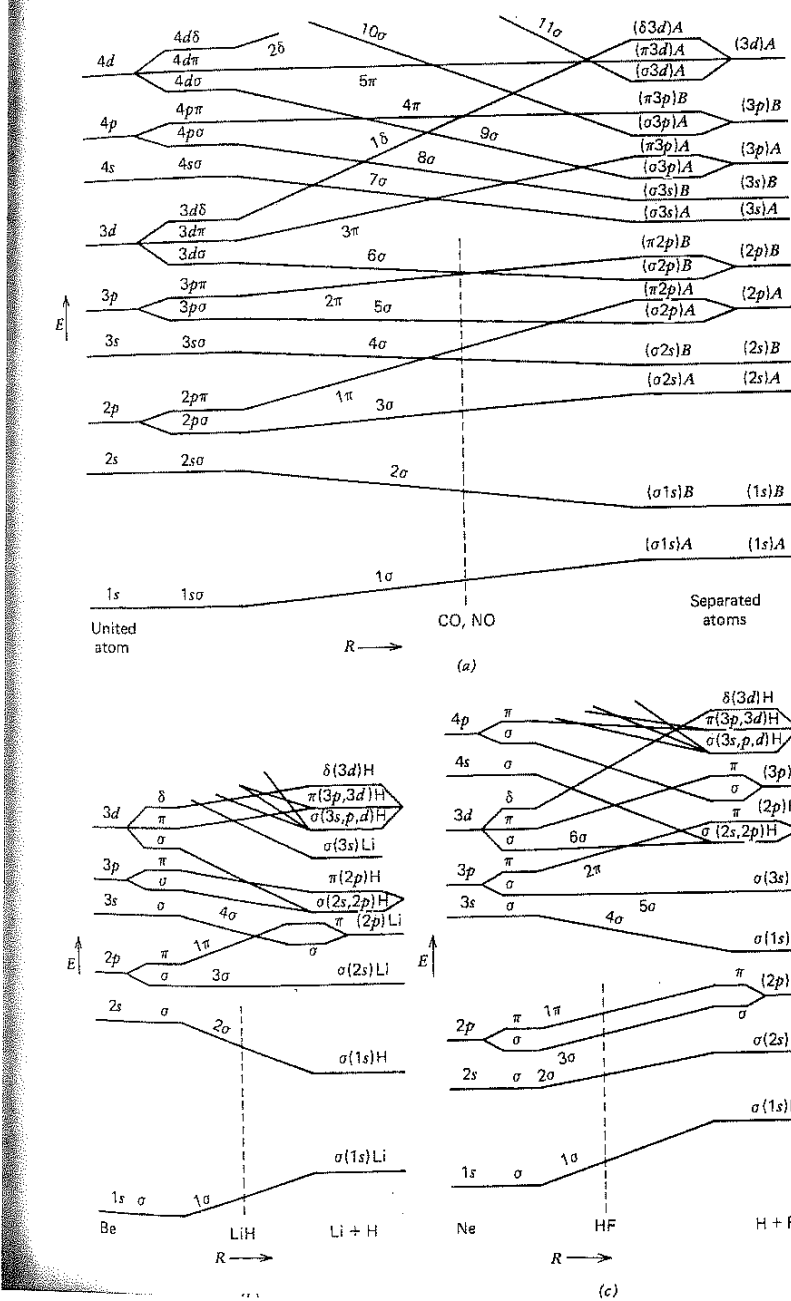


**Figure 7.19** Correlation diagrams for heteronuclear diatomic molecules: (a) for atoms of nearly equal size; (b) for  $\text{LiH}$ ; (c) for  $\text{HF}$ . (In the latter two diagrams the degenerate  $\text{H}$  levels are grouped as in Fig. 6.9.)

## 214 • More about Diatomic Molecules

have different energy levels in the separated-atom limit. Our assumption is that in this limit each molecular orbital correlates only with an atomic orbital of one or the other atom (the atom around which its amplitude is greatest). As we shall see, this is an oversimplification. The resulting correlation diagram is somewhat simpler than that for homonuclear molecules, primarily because there are no orbital parities that must be matched. However, it contains an additional element of arbitrariness, in that the relationship between A and B separated-atom levels varies with the nature of these atoms: The higher an atom's nuclear charge Z, the lower are that atom's energy levels of a given  $n$  and  $l$ . The effect is especially pronounced when one of the atoms is hydrogen. In Figs. 7.19b and 7.19c we illustrate this with correlation diagrams for LiH and HF; the other first-row diatomic hydrides are intermediate between these two.

What is the nature of the orbitals in heteronuclear molecules? In the LCAO approximation they consist of sums or differences of atomic orbitals in unequal amounts. Thus one might write a given molecular orbital  $\phi_n$  as

$$\phi_n = \alpha(R)(\phi_i)_A + \beta(R)(\phi_i)_B, \quad (7.50)$$

where  $(\phi_i)_A$  and  $(\phi_i)_B$  are atomic orbitals of atoms A and B. The coefficients  $\alpha(R)$  and  $\beta(R)$ , like those in Eqs. 6.76 and 6.79, are constants for any given value of  $R$ . The correlation diagrams imply that either  $\alpha(R)$  or  $\beta(R)$  vanishes in the separated-atom limit; at  $R_e$  one coefficient is usually much greater than the other.<sup>31</sup> Results such as this are obtained by the usual SCF techniques, and can be improved by using hybridized atomic orbitals, as in Eq. 7.49. One can again obtain orbital and whole-molecule electron densities: Compare the "charge densities"—strictly, total probability densities—shown in Fig. 7.20 for the first-row diatomic hydrides with Fig. 7.18 for homonuclear molecules. Although one cannot yet determine the electron distribution experimentally with comparable precision, these results are generally in agreement with chemical intuition and the measured properties of molecules.

In Section 5.5 we said that "electronegativity" describes an atom's power to attract electrons. In Fig. 7.20 we see a clear illustration of what this means. In a heteronuclear molecule the electrons that form the chemical bond—that is, those in the highest occupied bonding orbital—are found primarily near the more electronegative atom.<sup>32</sup> Among the first-row hydrides, calculations like those leading to

<sup>31</sup> In particular, inner-shell MOs are almost pure atomic orbitals: For example, in all the first-row hydrides (HA) the  $1\sigma$  orbital is found to be over 99%  $(1s)_A$ . This further confirms our conclusion in Section 7.4 that atomic cores take little part in bonding.

<sup>32</sup> The lowest normally empty orbital—such as  $3\sigma$  in LiH or  $4\sigma$  in HF—is commonly centered around the electropositive atom. Such an orbital is normally antibonding: Since it is usually a promoted orbital, the separated-atom electrons must be forced "uphill" to occupy it. If overlap is neglected and the bonding orbital is approximated by  $\alpha\phi_A + \beta\phi_B$ , orthogonality requires that the corresponding antibonding orbital be  $\beta\phi_A - \alpha\phi_B$ .

Fig. 7.20 show clearly that hydrogen is intermediate in electronegativity between metals and nonmetals. In HF the  $3\sigma$  bonding orbital is mainly centered around the F atom, whereas in LiH the  $2\sigma$  orbital is almost entirely around the H atom. In fact, the alkali metals are so much more electropositive than hydrogen that all the alkali hydrides can be regarded as ionic molecules ( $M^+H^-$ ), just like the alkali halides; in the solid state these compounds consist of separate  $M^+$  and  $H^-(1s^2)$  ions. Similar behavior is found for  $CaH_2$  and the heavier alkaline earth hydrides. We shall see that the empirical electronegativity scales agree with these conclusions.

The simplest electronegativity scale is that proposed by R. S. Mulliken. It is based on the idea that an atom's ability to hold its outermost electrons is proportional to its ionization potential ( $I$ ), whereas its ability to attract additional electrons is proportional to its electron affinity ( $A$ ). The Mulliken electronegativity is thus defined by the average of the two quantities,

$$x^M = K^M \left( \frac{I+A}{2} \right), \quad (7.51)$$

where  $K^M = (3.15 \text{ eV})^{-1}$ . The numerical factor is chosen to give a convenient scale, one in which the highest electronegativity (that of F) is about 4.0. The chief drawback of the Mulliken scale is that it uses isolated-atom properties, whereas "electronegativity" is meant to describe the behavior of an atom *in a molecule*. Other scales have thus been devised using molecular properties; we shall describe only one of these.

Linus Pauling suggested that the bond in a heteronuclear molecule could be regarded as the sum of two contributions: a covalent part (which is the only contribution in a homonuclear molecule) and an ionic part. In Pauling's valence bond interpretation, the bond in the molecule AB is a hybrid of the structures A—B and  $A^+B^-$ , if A is the more electropositive atom. On purely empirical grounds, the covalent contribution to the bond energy is taken to be the geometric mean of the covalent A—A and B—B bond energies. By subtraction the ionic contribution is

$$\Delta = D_e(A-B) - [D_e(A-A)D_e(B-B)]^{1/2}, \quad (7.52)$$

where the  $D_e$  to be used here is the measured or inferred single-bond energy.<sup>33</sup> The apparent electronegativity difference between atoms A and B is found to correlate well with the square root of  $\Delta$ , so the Pauling electronegativity is defined by the equation

$$(x^P)_B - (x^P)_A = K^P \Delta^{1/2}, \quad (7.53)$$

<sup>33</sup> This is not necessarily the dissociation energy of the diatomic molecule. For example,  $N_2$  has  $D_e = 9.8 \text{ eV}$  but contains a triple bond; the N—N single-bond energy of  $1.65 \text{ eV}$  is obtained from measurements on molecules such as  $H_2N-NH_2$ . See Chapter 14 for a discussion of bond-energy calculations.

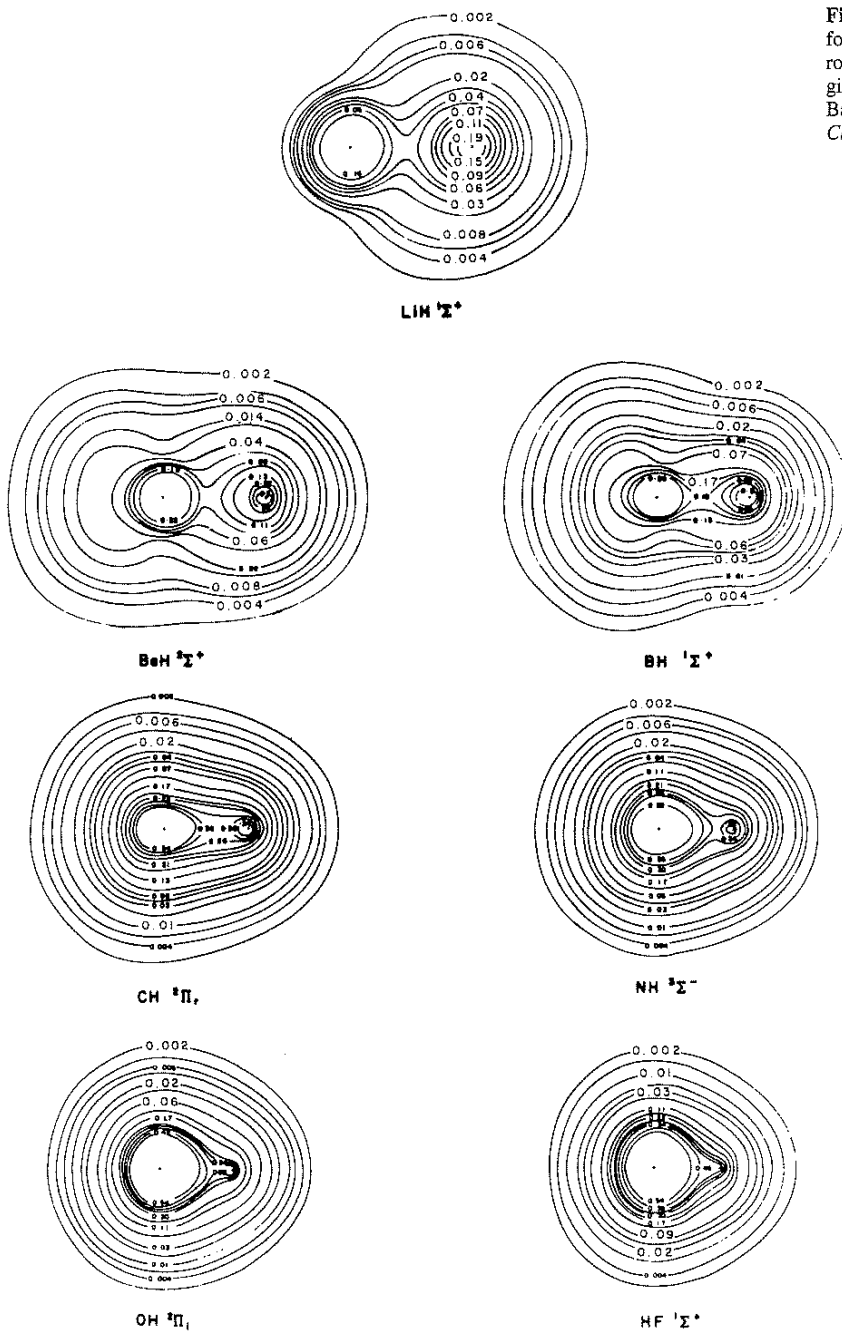


**Figure 7.20** Electron-density contours for total probability densities of the first-row diatomic hydride molecules. Energies are given in hartrees. From R. F. W. Bader, I. Keaveny, and P. E. Cade, *J. Chem. Phys.* **47**, 3381 (1967).

with  $K^P = (1 \text{ eV})^{-1/2} = (96.5 \text{ kJ/mol})^{-1/2}$ ; the scale is anchored by again setting  $(x^P)_F \approx 4.0$ .

The numerical factors of the Pauling and Mulliken scales were deliberately chosen to bring the two scales into conformity with each other. The two do indeed agree quite closely, as can be seen from the values in Table 7.7 for first-row elements:

**Table 7.7** Mulliken and Pauling Electronegativities for First-Row Atoms

	Li	Be	B	C	N	O	F
$x^M$	0.94	1.46	2.01	2.63	2.33	3.17	3.91
$x^P$	0.98	1.57	2.04	2.55	3.04	3.44	3.98

The Pauling electronegativities listed in Table 7.7 are actually based on the Coulomb force felt by an electron at the atom's covalent radius, and are probably the best available comprehensive set. It can be seen that the values confirm our qualitative conclusions above.

## 7.8 Bonding in LiH; Crossing and Noncrossing Potential Curves

Let us take a closer look at lithium hydride, the simplest stable heteronuclear molecule. At ordinary temperatures this species is a white crystalline solid (m.p. 680°C), but individual LiH molecules exist in the gas phase. The separated-atom limit is  $\text{Li}(1s^2 2s) + \text{H}(1s)$ ; the united-atom limit is  $\text{Be}(1s^2 2s^2)$ . Examining Fig. 7.19b, we see that the lowest orbital, the  $1\sigma$ , correlates naturally with the  $1s$  orbitals of both Li and Be; this orbital is thus closely centered around the Li nucleus for all values of  $R$ . The next orbital, the  $2\sigma$ , is much higher on the energy scale (about 60 eV at  $R_e$ ). In the separated-atom limit, the  $\text{H}(1s)$  orbital has a binding energy (ionization potential) of 13.6 eV, whereas the  $\text{Li}(2s)$  orbital has a binding energy of only 5.36 eV (cf. Fig. 7.21). Because of this large energy difference, the  $2\sigma$  orbital even near  $R_e$  is primarily like  $\text{H}(1s)$ ; that is, by far the largest coefficient<sup>34</sup> in Eq. 7.50 is that of  $(\varphi_{1s})_{\text{H}}$ . The  $3\sigma$  orbital, on the other hand, is mainly like  $\text{Li}(2s)$ . The LiH molecule has four electrons; applying the Aufbau principle, we conclude that the ground-state configuration near  $R_e$  should be  $1\sigma^2 2\sigma^2$ , corresponding to a  ${}^1\Sigma$  state. Since the valence ( $2\sigma$ ) electrons are centered near the H nucleus, the molecule should be largely ionic, with the effective structure  $\text{Li}^+ \text{H}^-$ . Spectroscopic and dipole-moment measurements confirm these conclusions.

As usual, however, the simple MO method breaks down at large  $R$ . Suppose that we take the molecule at  $R_e$  and slowly move the nuclei away from each other. If the electrons remained in the same orbitals (as represented by the correlation diagram), the separated-atom limit would be the ionic  $\text{Li}^+(1s^2) + \text{H}^-(1s^2)$ . But we know that any two neutral atoms A and B have a lower total energy than the corre-

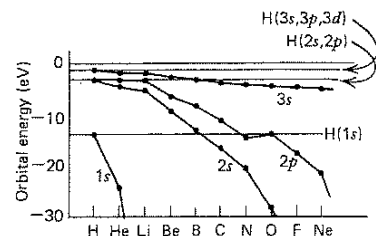


**Figure 7.21** Orbital energies of first-row atoms. The energy plotted is that required to remove an electron from the orbital in question, as obtained from spectroscopic data.

sponding ions  $\text{A}^+$  and  $\text{B}^-$ . Eq. 7.46 gives the energy of ion-pair formation as

$$Q(\text{A}^+\text{B}^-) \equiv E(\text{A}^+ + \text{B}^-) - E(\text{A} + \text{B}) = I(\text{A}) - A(\text{B}), \quad (7.54)$$

which is always positive. For LiH we have  $I(\text{Li}) = 5.36$  eV,  $A(\text{H}) = 0.75$  eV,  $Q(\text{Li}^+\text{H}^-) = 4.61$  eV. The problem here is rather akin to that we found for  $\text{H}_2$  in Section 6.6. There (and for any other homonuclear molecule) a single-configuration MO method predicts a 50%-ionic limit; here (and for any other heteronuclear molecule with an even number of electrons) it predicts a 100%-ionic limit. Within the MO framework, the paradox can again be resolved by the use of configuration interaction. Such a description of the LiH molecule would be given by the wave function

$$X(R)\psi(1\sigma^2 2\sigma^2) + Y(R)\psi(1\sigma^2 2\sigma 3\sigma),$$

in which we must have  $X(R) \gg Y(R)$  for  $R \leq R_e$ ,  $Y(R) \gg X(R)$  as  $R \rightarrow \infty$ , so that at long range we have the configuration  $1\sigma^2 2\sigma 3\sigma \rightarrow \text{Li}(1s^2 2s) + \text{H}(1s)$ .

Accurate multiconfiguration calculations have been carried out for LiH and other diatomic hydrides, cf. Meyer and Rosmus, *J. Chem. Phys.* **63**, 2356 (1975) and for first-row species such as  $\text{N}_2$ , cf. Andersson et al., *J. Chem. Phys.* **96**, 1218 (1992),  $\text{O}_2$ , cf. Vahtras et al., *J. Chem. Phys.* **96**, 2118 (1992), and  $\text{CO}$ , cf. Docken and Liu, *J. Chem. Phys.* **66**, 4309 (1977). However results of the same accuracy have not yet been reported for many other heteronuclear molecules. It is thus useful to know the limits of the single-configuration model. Fortunately, we can get a good idea of these limits from a very simple and crude calculation of the potential energy. Consider the two long-range states,  $\text{Li} + \text{H}$  and  $\text{Li}^+ + \text{H}^-$ ; what happens in each case if we decrease  $R$  slowly, neglecting configuration interaction? In the ionic case the model of Section 7.4 should be applicable, with the interaction energy given by Eq. 7.44. This energy is dominated by the Coulomb term,  $-e^2/4\pi\epsilon_0 R$ . Even at  $R_e$  this term gives a fairly good approximation to  $D_e$  (cf. Table 7.3), and at a somewhat larger distance, large enough to neglect overlap of the electron clouds, it should be the only significant term. Let us then assume that  $E_{\text{ionic}}(R) = -e^2/4\pi\epsilon_0 R$  for large  $R$ . To the same order of approximation, the two neutral atoms

<sup>34</sup> Here are the results of a SCF-MO calculation on LiH, using hybridized atomic orbitals on the Li atom. The numbers tabulated are the coefficients  $C_{ni}$  in the expression  $\varphi_n = \sum_i c_{ni}\varphi_i$ , where  $\varphi_n$  is a molecular orbital and the  $\varphi_i$  are atomic orbitals.

	$\varphi_i$			
$\varphi_n$	$\text{Li}(1s)$	$\text{Li}(2s)$	$\text{Li}(2\sigma)$	$\text{H}(1s)$
$1\sigma$	0.997	0.016	-0.005	0.006
$2\sigma$	0.131	-0.323	-0.231	-0.685
$3\sigma$	0.134	-0.805	0.599	0.148

Better calculations have been performed, using many more atomic orbitals, but the basic pattern remains the same.

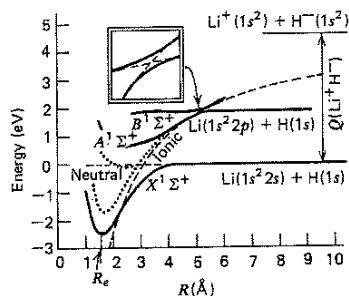


Figure 7.22 Potential energy curves for LiH: - - - simple model described in text,

$$E_{\text{ionic}}(R) = E(\text{Li}^+ + \text{H}^-) - e^2/4\pi\epsilon_0 R,$$

$$E_{\text{neutral}}(R) = E(\text{Li} + \text{H});$$

single-configuration MO calculation for the configurations  $1\sigma^2 2\sigma^2$  (ionic) and  $1\sigma^2 2\sigma 3\sigma$  (neutral); —— experimental curves for the two lowest states ( $X^1\Sigma^+$  and  $A^1\Sigma^+$ ), and the approximate location of the next state ( $B^1\Sigma^+$ ). The inset illustrates how one can join segments of single-configuration curves (- - -) to obtain curves that do not violate the noncrossing rule (—).

should have no significant interaction energy at large  $R$ . In Fig. 7.22 we have plotted these approximate potential-energy curves, which can be seen to cross at about  $2R_e$ . A single-configuration MO calculation gives essentially the same result, demonstrating the validity of this extremely crude model.

What is the significance of these results? Both single-configuration states must have the symmetry  $^1\Sigma^+$ . (There is also a  $^3\Sigma^+$  state derived from the neutral atoms, but as in  $\text{H}_2$  it should be entirely repulsive.) But the noncrossing rule is applicable to molecular states as well as individual orbitals: Two nondegenerate states of the same symmetry cannot have exactly the same energy, so their potential-energy curves cannot cross. Thus a single-configuration calculation must break down at the point where it predicts such a crossing, though it may be reasonably accurate elsewhere. One can obtain reasonably good results by joining the curve segments away from the crossing, as shown in the inset to Fig. 7.22. Curves obtained in such a way would be qualitatively similar to the actual curves for the two lowest states of LiH, shown by the solid lines in Fig. 7.22.<sup>35</sup> Similar effects occur in any of the “ionic molecules” of Section 7.4: Although the ground state is predominantly ionic near  $R_e$ , it goes over to a pair of neutral atoms at long range.

When we introduced the noncrossing rule, we mentioned that it is only approximately true; let us see why. To determine a potential-energy curve we must assume the nuclei to be at rest for each value of  $R$  (the Born–Oppenheimer approximation). The energy of a real system is thus given exactly by the  $E(R)$  curve only in the limit of infinitely slow nuclear motion, that is, in an *adiabatic* process (to use the

term we introduced in Section 6.5). In an adiabatic process the noncrossing rule can be shown to hold rigorously. But no real molecule is an adiabatic system. Since vibration is always present,  $R$  is always changing at a nonzero rate. How does this affect the noncrossing rule? In most cases where the rule applies, the two potential curves involved approach very close to each other (cf. the  $A^1\Sigma^+ - B^1\Sigma^+$  “intersection” in Fig. 7.22). Let us say that they are within  $\Delta E$  of each other over a range  $\Delta R$ . Now the uncertainty principle enters the picture: If the uncertainty in a molecule’s energy is greater than the separation between two such curves, there is a good chance of the molecule’s crossing from one curve to the other, that is, entering the transition region  $\Delta R$  in one electronic state and leaving it in another. According to Eq. 3.87, the noncrossing rule should apply only when  $\Delta t \geq \hbar/\Delta E$ , where  $\Delta t$  is the time the molecule spends within the transition region; this is called the *Massey adiabatic criterion*. If the relative speed of the two atoms is  $v = |dR/dt|$ , we have  $\Delta t = \Delta R/v$ , and the criterion becomes  $v \geq \Delta E \Delta R/\hbar$ . The speed  $v$ , of course, increases with increasing vibrational excitation. For a given crossing, the adiabatic criterion is usually satisfied for low vibrational states but not for higher states. In terms of the Born–Oppenheimer approximation, the separability of nuclear (vibrational) and electronic motions breaks down when the vibrational energy is sufficiently great.

Transitions of the type just described can also occur between states of different symmetry classes, whose potential curves *can* cross one another. The usual conservation laws and selection rules of course apply in such transitions. Processes of either kind give rise to a number of interesting phenomena, some of which are illustrated in Fig. 7.23. In ordinary dissociation (Fig. 7.23a) a molecule is excited into a repulsive state and the atoms immediately fly apart; the process takes about as long as a single vibrational period. *Predissociation* (Fig. 7.23b) is a slower process, in which the molecule is excited to a bound state  $A$ , remains there at least long enough to execute a few vibrations, then undergoes a transition to a repulsive state  $B$  which crosses<sup>36</sup> the bound state, and dissociates. *Autoionization* or *preionization* (Fig. 7.23c), which we discussed at the end of Section 6.10, is a similar transition from a bound neutral state to a state of molecule-ion plus free electron. Finally, in *phosphorescence* (Fig. 7.23d) the transition is to a lower-energy stable excited state from which decay to the ground state is forbidden (usually because it is a triplet-singlet transition, violating the rule  $\Delta S = 0$ ). Since “forbidden” is not an absolute term, the decay does occur with emission of light, but over a long period after the initial excitation.<sup>37</sup>

<sup>35</sup> Similar crossings (only one of which is shown) occur every time the “ionic” curve intersects the energy of an excited  $^1\Sigma^+$  state of  $\text{Li} + \text{H}$ .

<sup>36</sup> The figure has been drawn for two states that actually cross. If they have the same symmetry, then the lower state instead has a maximum at the “intersection,” and dissociation occurs by ordinary tunneling through this potential barrier.

<sup>37</sup> Phosphorescence should not be confused with *fluorescence*, which is the emission of light by nonforbidden transitions, most commonly singlet-singlet, and thus occurs mainly within nanoseconds (or at most microseconds) after excitation.

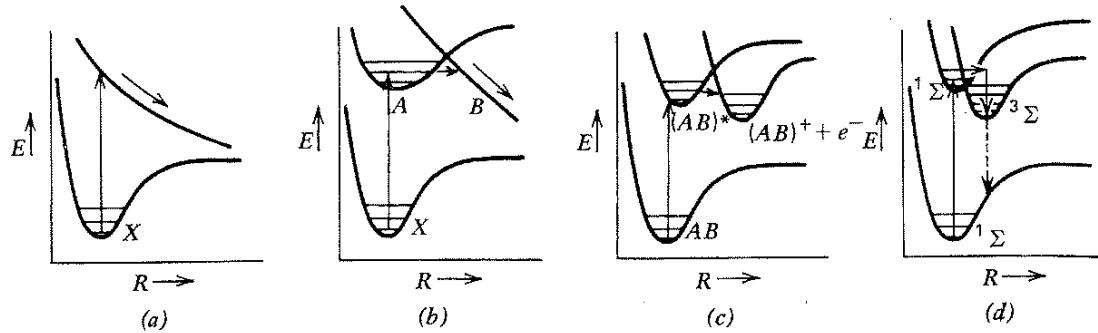


**Figure 7.23** Excited-state transitions. (a) shows ordinary dissociation, whereas the other figures show processes involving crossing potential curves: (b) predissociation; (c) autoionization; (d) phosphorescence. See discussion in the text.

## 7.9 Other First-Row Diatomic Hydrides

Except for LiH and HF, all the first-row diatomic hydrides are highly reactive species observed mainly in high-temperature systems. They are common reaction intermediates: CH can be detected in nearly all hydrocarbon flames, and OH (hydroxyl) in all flames containing oxygen and hydrogen in any form. They can also be detected by radio astronomy in interstellar space, where molecules are usually too far apart to react. The first molecule of any kind so detected was OH, in 1963. Since most of space is very cold, virtually all the molecules there must be in their ground electronic states. The states thus observed are indeed the ground states predicted by *a priori* calculations. The member of this series most commonly encountered in the laboratory is of course HF, the only one that exists as stable diatomic molecules at room temperature: HF is a colorless liquid boiling at 19.4°C.

By combining the information in Figs. 7.19 and 7.21, it is not difficult to deduce the ground-state MO configurations of the other first-row hydrides as we have done for LiH. These configurations are given in Table 7.8, along with other data on the molecules. Over this series the energy sequence of the occupied orbitals does not change, but the atomic orbitals with which they correlate do. For example, in LiH and BeH the  $2\sigma$  orbital correlates with and thus largely resembles the H(1s) orbital. Since H(1s) and B(2s) have nearly the same energy, the  $2\sigma$  orbital in BH is a roughly equal mixture of the two, and in CH and beyond the  $2\sigma$  orbital is predominantly the heavy-atom 2s, which lies below the H(1s). Similar analyses can be made for the other orbitals. Although the  $3\sigma$  and  $1\pi$  orbitals (from CH on) are degenerate in both limits, the  $3\sigma$  in each case is found to have a lower energy at  $R_e$  and thus is occupied first.

What is the bonding nature of these orbitals? Remember that a bonding orbital is expected to have a higher electron density in the bonding region than one finds in the separated atoms. The  $1\sigma$  orbital in all these molecules is virtually identical to the heavy-atom 1s, and like most inner-core

orbitals is essentially nonbonding. The  $1\pi$  orbital is also nonbonding, since it consists of only the heavy-atom 2p with no significant contribution from hydrogen. (The lowest p orbital of hydrogen is at a much higher energy.) The  $2\sigma$  orbital is clearly bonding in LiH, but takes less and less part in the bonding as it becomes more like the heavy-atom 2s; in HF it can also be considered nonbonding. But the slack is taken up by the  $3\sigma$  orbital, which, from CH onward is the main constituent of the bond. In simple chemical terms, one can think of the combination  $2\sigma^23\sigma^2$  as adding to a single bond and a nonbonding lone pair, as in the Lewis formulas for :B:H or H :F:, but the bond is really made up of contributions from both orbitals.

The strength of the bonding, as indicated by the value of  $D_e$ , increases fairly steadily from LiH to HF. Even more clear-cut is the upward trend in the vibrational frequency  $\bar{\nu}_e$ . This cannot be due to the relation  $\bar{\nu}_e \propto \mu^{-1/2}$ , since the reduced mass  $\mu$  varies very little over this series ( $\mu_{\text{LiH}} = 0.88 \text{ } m_{\text{H}}$ ;  $\mu_{\text{HF}} = 0.96 \text{ } m_{\text{H}}$ ). But  $\bar{\nu}_e$  does correlate well with the decrease in the bond length  $R_e$ , which is of course due to the decreasing size of the heavy atoms (Section 5.5). An increase in  $\bar{\nu}_e$  corresponds to a more sharply curved potential minimum, and we conclude that both the depth and the curvature of the potential wells tend to increase as  $R_e$  decreases.<sup>38</sup> The long-range attractive forces have much the same form between any two atoms, depending mainly on the electronegativity difference, but the short-range repulsive forces depend strongly on the atomic "sizes." Thus the position of the potential minimum in the hydrides must be sensitive mainly to the repulsive forces. This is in fact generally true, and is what makes the concept of a "covalent radius" meaningful.

Now let us look at the dipole moments. It can be seen that the magnitude of  $\mu$  decreases sharply from LiH, then increases slightly toward HF. Presumably this is due to a

<sup>38</sup> This agrees with the empirical Badger's rule (see footnote 9 on page 190).

Table 7.8 Ground States of First-Row Diatomic Hydrides

Molecule	Electron Configuration	Term Symbol	$D_e$ (eV)	$R_e$ (Å)	$\bar{\nu}_e$ (cm <sup>-1</sup> )	$ \mu $ (D)
LiH	$1\sigma^2 2\sigma^2$	${}^1\Sigma^+$	2.515	1.5954	1406	5.88
BeH	$1\sigma^2 2\sigma^2 3\sigma$	${}^2\Sigma^+$	$2.4 \pm 0.3$	1.297	2058	(0.3 calc.)
BH	$1\sigma^2 2\sigma^2 3\sigma^2$	${}^1\Sigma^+$	3.54	1.236	2367	1.27
CH	$1\sigma^2 2\sigma^2 3\sigma^2 1\pi$	${}^2\Pi$	3.65	1.124	2859	1.46
NH	$1\sigma^2 2\sigma^2 3\sigma^2 1\pi^2$	${}^3\Sigma^-$	3.40	1.045	3126	(1.0–1.9 calc.)
OH	$1\sigma^2 2\sigma^2 3\sigma^2 1\pi^3$	${}^1\Pi$	4.621	0.9706	3735	1.66
HF	$1\sigma^2 2\sigma^2 3\sigma^2 1\pi^4$	${}^1\Sigma^+$	6.11	0.9168	4139	1.82

change in polarity, as the heavy atom changes from being more electropositive to more electronegative. However, there are no direct measurements of the direction of  $\mu$  in these molecules. Apart from LiH, how can we tell whether a given molecule is primarily  $H^+X^-$  or  $X^+H^-$ ? A good idea of this can be obtained from the long-range limit. If we set the energy of two separated atoms  $A + B$  as zero, then the energy of the ion pair  $A^+ + B^-$  is simply the  $Q(A^+B^-)$  of Eq. 7.54, that is,  $I(A) - A(B)$ . If we calculate  $Q(H^+X^-)$  and  $Q(X^+H^-)$ , the smaller of these quantities must correspond to the lowest ionic state at  $R = \infty$ , which is probably the principal ionic contribution to the ground state at  $R = R_e$ . For example, in CH we have  $Q(C^+H^-) = I(C) - A(H) = 11.26 \text{ eV} - 0.75 \text{ eV} = 10.51 \text{ eV}$ ,  $Q(H^+C^-) = I(H) - A(C) = 13.60 \text{ eV} - 1.25 \text{ eV} = 12.35 \text{ eV}$ ; thus  $C^+ + H^-$  has an energy 1.84 eV lower than  $H^+ + C^-$ , and the CH molecule should be primarily  $C^+H^-$ . For the series of first-row hydrides such calculations give:

X	Li	Be	B	C	N	O	F
$Q(X^+H^-)$ (eV)	4.61	8.57	7.55	10.51	13.78	12.86	16.67
$Q(H^+X^-)$ (eV)	12.98	13.22	13.42	12.35	13.8	12.13	10.15

Thus, the heavy atom should be the positive end of the molecule in LiH, BeH, BH, and CH, the negative end in OH and HF, whereas the NH molecule should be very nearly nonpolar. These results are plausible, and are supported by the electron-distribution calculations of Fig. 7.20.

So far we have spoken only of the ground states of the diatomic hydrides. Although we shall make no detailed study of the excited states, it is worthwhile to survey the relationship between molecular states and those of the separated atoms. This can be done systematically by extending the vector model of Section 5.6 from atoms to molecules. The method is applicable to both heteronuclear and homonuclear molecules, though complicated in the latter case by degeneracies.

As an example, let us consider the manifold of states of the CH molecule derived from the ground states of the separated atoms. As we showed in Section 5.6, these ground states are  $C(^3P)$  ( $L = 1, S = 1$ ) and  $H(^2S)$  ( $L = 0, S = \frac{1}{2}$ ). The spin and orbital angular momenta of the atoms add as vec-

tors to give those of the molecule. The reasoning is the same as we applied to obtain the values of  $J$  in connection with Eq. 5.30. Since  $S$  is quantized in integral steps, its possible values for a diatomic molecule are

$$S = S_A + S_B, S_A + S_B - 1, \dots, |S_A - S_B|, \quad (7.55)$$

where  $S_A$  and  $S_B$  are the atomic values. In this case we can have  $S = \frac{3}{2}$  or  $S = \frac{1}{2}$ , that is, quartet or doublet states. As for the orbital angular momentum, we are concerned only with its component along the internuclear axis. The quantum number  $\Lambda$  is given by

$$\Lambda = |(M_L)_A + (M_L)_B|, \quad (7.56)$$

where each  $M_L$  can have any of its possible values  $L, L-1, \dots, -L$ . In CH we have  $(M_L)_C = 1, 0, -1$ , and  $(M_L)_H = 0$ , giving the possible values  $\Lambda = 0$  ( $\Sigma$  states) or  $\Lambda = 1$  (degenerate  $\Pi$  states). Since the spin and orbital angular momenta add independently, we should have all told from  $C(^3P) + H(^2S)$  the states  ${}^2\Pi$ ,  ${}^2\Sigma$ ,  ${}^4\Pi$ , and  ${}^4\Sigma$ , in order of increasing energy. The order is that predicted by Hund's rules, with  $\Lambda$  replacing  $L$ . The state  ${}^2\Pi$  is in fact the ground state of CH, and  ${}^2\Sigma$  is the lowest observed excited state; the other two states are as yet unobserved. Similar analyses can be made for any other pair of separated-atom states.

It is generally true, as it is for CH, that some of the states generated from a given separated-atom limit remain unobserved. The reason for this is that many of the states have no stable minima in their  $E(R)$  curves. Such states have no characteristic band spectra by which they can be identified, but only continuum radiation. Indeed, their potential curves are sometimes so strongly repulsive that molecules with  $R$  near the ground-state  $R_e$  are not encountered at all. To see how such repulsive states come about, let us consider the  ${}^4\Pi$  state of CH. This state has  $S = \frac{3}{2}$ , and thus must have at least three singly occupied orbitals; to have  $\Lambda = 1$ , there must be an odd number of electrons in  $\pi$  orbitals. The lowest-energy configuration meeting these specifications is  $1\sigma^2 2\sigma^2 3\sigma 1\pi^4 \sigma$ , where one electron is promoted from the  $3\sigma$  to the  $4\sigma$  orbital, which is so strongly antibonding that it overcomes the remaining bonding forces. (In the  ${}^2\Sigma$  state, with configuration  $1\sigma^2 2\sigma^2 3\sigma 1\pi^2$ , electron to the nonbonding  $1\pi$

orbital is enough to reduce the binding energy to only 0.4 eV.) Despite the repulsive nature of the  $^4\Pi$  state, it must become the lowest-energy state at some small value of  $R$ , since it correlates with the united-atom ground state, N( $^4S$ ), which also has three singly occupied orbitals. As  $R \rightarrow 0$  we have  $1\sigma \rightarrow 1s$ ,  $2\sigma \rightarrow 2s$ ,  $3\sigma \rightarrow 2p\sigma$ ;  $1\pi \rightarrow 2p\pi$ .

We mentioned previously that the diatomic hydrides have been observed by radio astronomy. But just what kind of transitions can these molecules have in the radiofrequency region of the spectrum? For OH, for example, even the pure rotational spectrum is well into the infrared region, with  $B_e = 18.9 \text{ cm}^{-1}$ . First of all, the energy levels of molecules show fine-structure splitting, which, as in atoms (Section 5.7), is due primarily to spin-orbit interaction. When the spin and orbital angular momenta are strongly coupled, analogous to  $LS$  coupling in atoms, the component of total angular momentum along the internuclear axis is  $\Omega\hbar$ , where

$$\Omega = |\Lambda + \Sigma| \quad (\Sigma = S, S-1, \dots, -S). \quad (7.57)$$

The quantum numbers  $\Lambda$ ,  $\Sigma$ ,  $\Omega$  correspond to the atomic  $M_L$ ,  $M_S$ ,  $M_J$ , respectively. By "strongly coupled" we mean that the orbiting electrons produce a magnetic field that tends to align the spin magnetic moment with the axis. There are other types of coupling, but we need consider only this one. The ground-state term of the OH molecule is  $^2\Pi(S = \frac{1}{2}, \Lambda = 1)$ , with the possible values  $\Sigma = \frac{1}{2}, -\frac{1}{2}$  and  $\Omega = \frac{3}{2}, \frac{1}{2}$ . Thus there are two states, designated as  $^2\Pi_{3/2}$  (the ground state) and  $^2\Pi_{1/2}$ . But the energy difference between these states is 0.017 eV (corresponding to  $140 \text{ cm}^{-1}$ ), which is even greater than the rotational spacing.<sup>39</sup> One thus observes two distinct though overlapping rotational bands in laboratory spectra, so we must seek further for a radiofrequency transition. Besides the coupling between spin and orbital electronic angular momenta, there is a much weaker interaction between electronic and *rotational* angular momenta. This interaction destroys the degeneracy between the two states differing only in the orientation of  $\mathbf{L}$  (with  $L_z = \pm\Lambda\hbar$ ; cf. Section 6.5), and is thus known as  $\Lambda$ -type doubling.<sup>40</sup> The splitting is proportional to  $J(J+1)$ , where  $J$  is the rotational quantum number. For the  $J = 1$  state of OH ( $^2\Pi_{3/2}$ ) it equals  $7.8 \times 10^{-6} \text{ eV}$  or  $0.063 \text{ cm}^{-1}$ , which is indeed in the radiofrequency region. Thus we see how successively weaker interactions can give us finer and finer probes of molecular structure.

The final topic we shall discuss in this section takes us out of the realm of pure intramolecular forces; this is the *hydrogen bond*, a phenomenon of which HF provides the

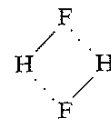
simplest illustration. The subject is introduced here, rather than in Chapter 10, because it is so characteristic of HF. A number of compounds in which hydrogen is bonded to very electronegative elements (mainly F, O, and N) show strong attractive forces between molecules. For example, although one expects boiling points in a family of compounds to increase with molecular weight as in the inert gases, HF, H<sub>2</sub>O, and NH<sub>3</sub> go counter to this trend:

NH <sub>3</sub>	-33.4	H <sub>2</sub> O	0.0	HF	19.5	Ne	-245.9
PH <sub>3</sub>	-133	H <sub>2</sub> S	-60.7	HCl	-84.9	Ar	-185.7
AsH <sub>3</sub>	-55	H <sub>2</sub> Se	-41.5	HBr	-67.0	Kr	-152.3
SbH <sub>3</sub>	-17.1	H <sub>2</sub> Te	-2.2	HI	-35.4	Xe	-107.1

(boiling points in °C). The heats of vaporization vary in the same way; those for HF, H<sub>2</sub>O, and NH<sub>3</sub> are higher than expected by 20–40 kJ/mol (0.2–0.4 eV/molecule). This is about one order of magnitude weaker than a normal covalent bond, but still much stronger than ordinary intermolecular attractions (see Chapter 10); for example, the potential well for two Ar atoms is about 0.01 eV deep. Data from spectroscopy, neutron diffraction, and other sources clearly show that in these substances the hydrogen atoms are normally located between two electronegative atoms, but closer to one than the other. This is usually indicated by a formula such as H—F · · · H—F, with the "long bond" shown by dots.

How does a hydrogen atom between two electronegative atoms have a bonding effect? We know that in an HF molecule the bond is strongly polar, so that there is an excess of negative charge on the F atom and an excess of positive charge on the H atom. As in our model for ionic bonds, one can to a good approximation treat each atom as a point charge but with a charge less than  $e$ . Just as negative charge in the region between two positive nuclei tends to draw them together (see Section 6.1), so a positively charged H atom between two negatively charged F atoms exerts a bonding force—but a much weaker one, because the charges are only partial and the distances greater. In an MO treatment, one might consider the ordinarily nonbonding  $2\sigma$  orbital of one HF molecule to include an H(1s) component from the other molecule. The hydrogen bond tends to pull the H atom away from its nearest-neighbor fluorine, with the net effect of weakening the restoring force in the H—F oscillator (in which the H does nearly all the moving). This effect lowers  $\bar{v}_e$  from  $4138 \text{ cm}^{-1}$  in free HF to about  $3400 \text{ cm}^{-1}$  in (HF)<sub>2</sub> showing that the environment of the H atom is rather drastically changed by hydrogen bonding.

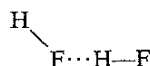
The simplest example of a "molecule" showing hydrogen bonding is the dimer (HF)<sub>2</sub> which exists in the gas at relatively low temperatures. Two possible structures come to mind, neither of which corresponds to the true structure. One might expect either the linear H—F · · · H—F, or the ring



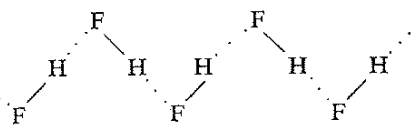
<sup>39</sup> The average temperature of interstellar space is probably about 3 K, corresponding to an average molecular energy of only  $4 \times 10^{-4} \text{ eV}$  ( $3 \text{ cm}^{-1}$ ); thus, virtually all OH molecules in space should be in the  $^2\Pi_{3/2}$  state if they are in thermal equilibrium.

<sup>40</sup> When  $\Lambda = 0$ , that is, in  $\Sigma$  states, there can still be an interaction between spin and rotational angular momenta. But  $^1\Sigma$  states (like atomic  $^1S$  states) have no fine structure except that due to nuclear spin.

with two hydrogen bonds. In reality, the HF dimer appears to have the bent structure



The location of the central H is very close to the F—F axis. More highly polymerized forms also exist, and liquid and solid HF are basically made up of long zigzag chains:



In the next chapter we shall see why the chains are bent rather than linear. If equimolar amounts of HF and KF are crystallized together, one obtains a well-defined crystalline species  $\text{KHF}_2$ , made of  $\text{K}^+$  and  $\text{FHF}^-$  ions; in the  $\text{FHF}^-$  ion the hydrogen atom is found to be exactly midway between the two F atoms. This carries the hydrogen bond to its ultimate form, with the H atom associated with no particular molecule.<sup>41</sup>

One would expect all these molecules to have ground-state electron configurations equivalent to that of  $\text{C}_2$ , that is,  $1\sigma^2 2\sigma^2 3\sigma^2 4\sigma^2 1\pi^4$ . The ground states of  $\text{C}_2$ ,  $\text{BeO}$ , and  $\text{LiF}$  are all  ${}^1\Sigma$ , corresponding to this configuration. Although the lowest known state of BN is  ${}^3\Pi$ , corresponding to what was long thought to be the ground state of  $\text{C}_2$  (see footnote 28 on page 209), the low-lying  ${}^1\Sigma$  state has not yet been observed, and the ground state may yet prove to be this  ${}^1\Sigma$  state. Within the series, the orbitals change character regularly as the difference between the nuclear charges grows. The  $1\sigma$  and  $2\sigma$  orbitals, which we approximate by  $1s_A \pm 1s_B$  in  $\text{C}_2$ , become the  $1s$  orbitals of the high-Z and low-Z atom, respectively: They do not mix significantly with the  $n = 2$  orbitals, since even in LiF the Li( $1s$ ) orbital has appreciably lower energy than the F( $2s$ ). The  $3\sigma$  orbital changes from  $2s_A + 2s_B$  in  $\text{C}_2$  to the high-Z (N, O, or F)  $2s$ , and the  $1\pi$  from  $2p_A + 2p_B$  to the  $2\pi p$  orbital on the high-Z atom. But the  $4\sigma$  orbital, which correlates with the atomic  $2s$  in  $\text{C}_2$ , becomes more and more like the  $\sigma 2p$  of the high-Z atom as one goes to LiF. (Cf. the atomic orbital energies in Fig. 7.21.)

Some of the properties of molecules in this and other series are listed in Table 7.9. From  $\text{C}_2$  to LiF the bond lengths increase and the vibrational frequencies decrease, but the dissociation energy varies in a more complicated

## 7.10 Isoelectronic and Other Series

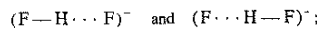
To interpret the differences among molecules, we must find or invent concepts that characterize the important changes from one molecule to another. Which concepts we choose will depend on the molecules under consideration. Thus far the key factor in our analysis of diatomic molecules has been the number of electrons, added one by one to a relatively stable set of orbitals. In heteronuclear molecules we needed the additional concept of orbital polarity, leading to the distinction between ionic and covalent bonding. To study the polarity effect in relative isolation, let us now consider some sets of molecules with the same total number of electrons—what we call *isoelectronic* series of molecules.

Among the simplest and most informative of such series is that isoelectronic with  $\text{C}_2$ , including BN, BeO, and LiF, in order of increasing polarity. All are known as diatomic molecules in the vapor phase, with properties varying from  $\text{C}_2$ , which is homonuclear and thus covalently bound, to LiF, a very ionic molecule which we described in Section 7.4. It is worth noting that a similar transition from covalent to ionic bonding is found in the solid forms of these species, from the covalent structures of carbon (diamond and graphite) to the ionic lattice of  $\text{Li}^+\text{F}^-$ .

Table 7.9 Properties of Some Series of Diatomic Molecules

Ground State	$D_0$ (eV)	$R_e$ (Å)	$\bar{\nu}_e$ (cm $^{-1}$ )	$ \mu $ (D)
<i>Isoelectronic Series</i>				
$\text{C}_2$ ${}^1\Sigma_g^+$	6.24	1.2425	1855	0
BN ${}^3\Pi$ (?)	3.99	1.281	1515	(1.4 calc.)
BeO ${}^1\Sigma^+$	4.60	1.331	1487	(7.3 calc.)
LiF ${}^1\Sigma^+$	5.94	1.564	910	6.33
$\text{N}_2$ ${}^1\Sigma_g^+$	9.760	1.094	2358	0
CO ${}^1\Sigma^+$	11.09	1.128	2170	0.112
BF ${}^1\Sigma^+$	7.85	1.262	1401	0.5 ± 0.2
<i>Families of the Periodic Table</i>				
HF ${}^1\Sigma^+$	5.86	0.917	4139	1.826
HCl ${}^1\Sigma^+$	4.446	1.275	2991	1.109
HBr ${}^1\Sigma^+$	3.755	1.414	2649	0.828
HI ${}^1\Sigma^+$	3.053	1.609	2308	0.448
Li <sub>2</sub> ${}^1\Sigma_g^+$	1.12	2.672	351.4	0
Na <sub>2</sub> ${}^1\Sigma_g^+$	0.75	3.079	159.2	0
K <sub>2</sub> ${}^1\Sigma_g^+$	0.51	3.923	92.6	0
Rb <sub>2</sub> ${}^1\Sigma_g^+$	0.47	4.20	57.3	0
Cs <sub>2</sub> ${}^1\Sigma_g^+$	0.45	4.58	42.0	0
F <sub>2</sub> ${}^1\Sigma_g^+$	1.604	1.409	919.0	0
Cl <sub>2</sub> ${}^1\Sigma_g^+$	2.484	1.988	559.7	0
Br <sub>2</sub> ${}^1\Sigma_g^+$	1.971	2.281	323.3	0
I <sub>2</sub> ${}^1\Sigma_g^+$	1.544	2.667	214.5	0

<sup>41</sup> The valence bond theory treats  $\text{FHF}^-$  as a hybrid of the structures



in MO theory one must use "three-center orbitals," with contributions from all three atoms.

manner. This is the result of a balance between two opposing trends: The covalent bonding power weakens as the bond grows longer and the orbitals become more nonbonding, but the ionic contribution to the bond increases as the charge distribution becomes more polarized. The dipole moment of course increases with the electronegativity difference between the two atoms.

Another interesting set of isoelectronic molecules consists of N<sub>2</sub>, CO, and BF. Both N<sub>2</sub> and CO exist as stable diatomic gases at room temperature, and even consist of diatomic molecules in the solid state; BF, however, is unstable.<sup>42</sup> The properties listed in Table 7.9 show the same conflicting trends as in the previous series. All three compounds have  ${}^1\Sigma$  ground states, corresponding to the configuration  $1\sigma^2 2\sigma^2 3\sigma^2 4\sigma^2 1\pi^4 5\sigma^2$ . In CO, calculations show that the  $1\sigma$  and  $2\sigma$  orbitals are essentially atomic  $1s$  orbitals, the  $3\sigma$  and  $5\sigma$  orbitals are largely concentrated on O and C, respectively, whereas the  $4\sigma$  and doubly degenerate  $1s$  orbitals furnish the bulk of the bonding. This corresponds approximately to the Lewis formula :C≡O:. That the dissociation energy of CO is higher than that of N<sub>2</sub> can be attributed to a small amount of ionic character added to what is still essentially a triple bond. In BF, ionic bonding is presumably important, but not enough to make ionic B<sup>+</sup>F<sup>-</sup> crystals stable.

There are a number of striking similarities in the physical properties of N<sub>2</sub> and CO. (Their chemical properties are of course rather different, but even there the two exhibit comparable inertness toward some reagents—notably *not* toward hemoglobin!) The gas densities, boiling points, viscosities, and thermal conductivities of the two species are almost the same. This similarity is due in part to their near-identical molecular weights, but the intermolecular forces also reflect the similar internal structure of the two molecules. The latter is particularly apparent if one looks at the orbital binding energies, which have been measured by photoelectron spectroscopy (values in eV):

	$1\sigma$	$2\sigma$	$3\sigma$	$4\sigma$	$1\pi$	$5\sigma$
N <sub>2</sub>	409.9	409.9	37.3	18.6	16.8	15.5
CO	542.1	295.9	38.3	20.1	17.2	14.5

Except for the atomic-core  $1\sigma$  and  $2\sigma$  orbitals, the two sets of energies are almost identical; the energies obtained by molecular orbital calculations are somewhat different, but show the same pattern. Results of this sort clearly justify our treating the members of an isoelectronic species as closely related.

We must say something more here about photoelectron spectroscopy, a conceptually simple and powerful method for determining molecular energy levels. The nature of the photoelectric effect has been described in Section 2.2; here we apply it to free molecules. Specifically, suppose that

radiation of frequency  $\nu$  (energy  $h\nu$ ) strikes a molecule and releases an electron with binding energy  $\epsilon$ . If we neglect the small recoil effects, the binding energy should be given by

$$\epsilon = h\nu - T, \quad (7.58)$$

where  $T$  is the kinetic energy of the released electron. By measuring or selecting  $\nu$  and then measuring  $T$  as in the Franck–Hertz experiment, for example, one can determine  $\epsilon$ , which by Koopmans' theorem should equal the electron's orbital energy in the molecule. The energy  $h\nu$  must of course be greater than  $\epsilon$ . One most commonly uses radiation in the vacuum ultraviolet to release the valence electrons, and x-rays for the core electrons. Typically one irradiates a sample, gaseous or solid, with monochromatic radiation such as that of the He  $2p \rightarrow 1s$  transition at 584 Å, and measures the kinetic energies of the photoelectrons. Ultraviolet radiation is associated with states whose natural lifetimes are of order  $10^{-9}$  s and so, according to the uncertainty principle, can provide energy resolution at best with  $\Delta E = \hbar/\Delta t$  or about  $4 \times 10^{-6}$  eV ( $0.03 \text{ cm}^{-1}$ ), somewhat better than the energy of the electrons can be determined. With x-rays, the energy resolution is typically 1–5 eV, due in large part to the short lifetimes of the excited states from which they are emitted. Hence x-ray photoelectron spectroscopy can locate the approximate energy of shells, but one must use ultraviolet radiation to probe the separations of valence orbitals. With ultraviolet photoelectron spectroscopy it is quite straightforward to distinguish different vibrational levels, especially of the final ion, and even rotational levels of very light molecules have been resolved.

Thus far we have not carried our analysis beyond the first row of the periodic table. According to the principles outlined in Section 5.5 we expect the elements below the first row to exhibit bonding behavior similar to that of the first element in each family (alkali metals, halogens, etc.). And in fact, each family does bond in generally similar ways. But what systematic changes may we expect to find as we go down a family of diatomic molecules (varying one or both atoms)? The properties of several such series are given in Table 7.9. One can readily name others (the alkali halides, interhalogen compounds such as ClF, interalkali compounds such as NaK, the analogs of N<sub>2</sub> and O<sub>2</sub>, etc.), but essentially the same trends are found in all cases.

These trends largely reflect the effects of atomic size, which of course increases slowly as one goes down each column of the periodic table. In a similarly bonded series of molecules, the bonds must become longer and thus weaken with increasing atomic size. An additional effect is found in heteronuclear molecules: Since the nuclei become better shielded as more electrons are added, the ionization potentials, electron affinities, and thus electronegativities also decrease with atomic size. Depending on the nature of the series, these changes will either increase or decrease the ionic contribution to the bonding. There is one other effect of atomic size: The core electrons are by no means com-

<sup>42</sup> Even CO has a tendency to disproportionate,  $2\text{CO} \rightarrow \text{C} + \text{CO}_2$ , but the reaction is very slow at room temperature.

pletely shielded or nonbonding, and do take some part in bond formation; as we noted earlier, in many transition metals the inner-shell *d* electrons are almost as important as the valence electrons in bonding.

The trends in Table 7.9 are for the most part clear and consistent, with the exception of the anomalously low dissociation energy of F<sub>2</sub>. This recalls the fact that the electron affinity of F is less than that of Cl. The low dissociation energy of F<sub>2</sub> has puzzled scientists for many years. The explanation, as with the electron affinity, seems to be that the inner core electrons (1s and, to some degree, 2s) form a relatively more important fraction of the total electron cloud

in fluorine than in larger halogen atoms, so that the repulsive contribution to the F—F bond is more important than in other halogen–halogen bonds.

The macroscopic properties of molecular families often also show clear-cut trends—for example, the boiling points tabulated in the last section. However, these depend on intermolecular forces, which have more to do with the overall size of a molecule than with the nature of its bonding except where hydrogen bonding or other electrostatic effects are significant. We shall consider intermolecular forces in Chapter 10, and macroscopic behavior in Part II. For now, though, let us proceed to molecules with more than two atoms.

## APPENDIX 7A

# Perturbation Theory

The effects of small perturbations lend themselves to a set of related mathematical tools that, together, comprise *perturbation theory*. Here we outline the basic ideas of perturbation theory, just in its simplest forms, which we shall see are equivalent to its lowest orders. In the context of quantum mechanics, we suppose that there is a parameter  $\kappa$  that measures the strength of the perturbation of interest, so that we can write the Hamiltonian  $H$  as the sum of a part  $H_0$  we know and understand well, and a complicated but small part  $\kappa H_1$ , which constitutes the perturbation. We define  $H_1$  to make  $\kappa < 1$  so that the effects of the perturbation can be expressed by expansions in powers of  $\kappa$ ; which means that both the energy and the wave functions can be so expanded:

$$E = E_0 + \kappa E_1 + \kappa^2 E_2 + \dots \quad (7A.1)$$

and

$$\psi = \psi_0 + \kappa \psi_1 + \kappa^2 \psi_2 + \dots \quad (7A.2)$$

The problem is one of finding  $E_1$ ,  $E_2$ ,  $\dots$ ,  $\psi_1$ ,  $\psi_2$ ,  $\dots$  and so forth, from a Schrödinger equation whose Hamiltonian is  $H = H_0 + \kappa H_1$  and whose eigenvalues and corresponding eigenfunctions are those of Eqs. 7A.1 and 7A.2. The simple equation  $H\psi = E\psi$  becomes

$$\begin{aligned} (H_0 + \kappa H_1)(\psi_0 + \kappa \psi_1 + \kappa^2 \psi_2 + \dots) \\ = (E_0 + \kappa E_1 + \kappa^2 E_2 + \dots)(\psi_0 + \kappa \psi_1 + \kappa^2 \psi_2 + \dots); \end{aligned} \quad (7A.3)$$

a cumbersome equation indeed. However, we use a trick of mathematical reasoning here to simplify: If the parameter is truly arbitrary and may take any value in a range, say between 0 and 1, then we must be able to carry out the multiplications indicated in Eq. 7A.3, collect the terms on each side corresponding to specific powers of  $\kappa$ , and then write separate equalities for each power of  $\kappa$ . If we do this, we obtain a hierarchy of equations that begins with these:

$$H_0\psi_0 = E_0\psi_0, \quad (7A.4)$$

$$H_1\psi_0 + H_0\psi_1 = E_1\psi_0 + E_0\psi_1, \quad (7A.5)$$

$$H_2\psi_0 + H_1\psi_1 + H_0\psi_2 = E_2\psi_0 + E_1\psi_1 + E_0\psi_2, \quad (7A.6)$$

$\vdots$

and we shall not need to go further here. (As we have defined the perturbation here,  $H_2$  vanishes.) The first equa-

tion here is just the Schrödinger equation for the system in the absence of the perturbation, in effect what we assume we know to be true. The next step is evaluating the expectation value of the first-order perturbation,  $\langle E_1 \rangle$  (the change linear in  $\kappa$ ) because the change in energy of the system due to the perturbation is, to a first approximation, just  $\kappa \langle E_1 \rangle$ . To find  $\langle E_1 \rangle$ , we need only multiply on the left by and integrate over all the coordinates in the wave functions:

$$\begin{aligned} \langle E_1 \rangle &= \int \psi_0^* E_1 \psi_0 d\tau \\ &= \int \psi_0^* (H_1 \psi_0 + H_0 \psi_1 - E_0 \psi_1) d\tau, \end{aligned} \quad (7A.7)$$

which we can simplify now by invoking the requirements that  $H_0$  is Hermitian and therefore acts on its eigenfunction  $\psi_0^*$  simply to multiply it by the real number  $E_0$  and that the functions  $\psi_0$ ,  $\psi_1$ ,  $\psi_2$ ,  $\dots$  are all orthogonal and normalized. This means that the second and third terms on the right side of Eq. 7A.7 vanish, and we have simply that the first-order perturbation of the energy is the expectation value of the perturbing part of the Hamiltonian,

$$\langle E_1 \rangle = \int \psi_0^* H_1 \psi_0 d\tau. \quad (7A.8)$$

This expression tells us that the perturbation causes a first-order change in the energy if and only if the integral of Eq. 7A.8 is nonvanishing. If  $H_1$  represents the action of a uniform electric field on an atom then  $\langle E_1 \rangle$  vanishes because the energy of interaction contained in has the form of the scalar product of the electric field  $\mathbf{E}$  and the atomic dipole moment  $\mu$ :  $H_1 \propto \mathbf{E} \cdot \mu$ , and only  $\mu$  contains the coordinates appearing in the wave function. But no atom has a dipole moment, so there is no first-order perturbation of an atom's energy by a uniform electric field; i.e.,  $\langle E_1 \rangle = \mathbf{E} \cdot \int \psi_0^* \mu \psi_0 d\tau$  vanishes because the integral vanishes. There are many important perturbations of the energy that do not vanish in first order, but, like this example, many do. Note that to find the first-order perturbation of the energy, we only need to know the wave function  $\psi_0$  of the original, unperturbed problem and not any of the corrections to the wave function.

While the first-order contribution vanishes in the above example, its second-order contribution,  $\langle E_2 \rangle$ , does not. Next we evaluate  $\langle E_2 \rangle$  and along the way find the first-order correction to the wave function. We can start this by returning

to the equation for the first-order corrections, Eq. 7A.6, and rearranging it just a bit:

$$\begin{aligned} H_1\psi_0 - E_1\psi_0 &= -(H_0\psi_1 - E_0\psi_1), \text{ or} \\ (H_1 - E_1)\psi_0 &= -(H_0 - E_0)\psi_1, \end{aligned} \quad (7A.9)$$

the first step to finding  $\psi_1$ . Next, we suppose that we would like to know and express  $\psi_1$  in terms of the eigenfunctions of  $H_0$ , which we presumably know or can find. That means we will write  $\psi_1$  as a series expansion of the form

$$\psi_1 = \sum_{k=1} c_k \varphi_k, \quad (7A.10)$$

in which each of the functions  $\varphi_k$  satisfies a Schrödinger equation for the zero-th order Hamiltonian,

$$H_0\varphi_k = E_0^{(k)}\varphi_k. \quad (7A.11)$$

Note that this means that  $\psi_0 = \varphi_0$ . Our task is then to find expressions for the unknown coefficients  $c_k$ . If we substitute the expansion of Eq. 7A.10 into Eq. 7A.9, multiply that expression by any specific  $\varphi_j^*$ , and integrate over the variables of the wave function and then use both Eq. 7A.11 and the orthogonality condition on the  $\varphi_k$ 's, we obtain an explicit, calculable expression for the contribution of that particular  $\varphi_j$  to the first-order perturbation function,

$$c_j = -\frac{\int \varphi_j^* H_1 \varphi_0 d\tau}{E_0^{(j)} - E_0}. \quad (7A.12)$$

This expression tells us two things: first, the numerator shows that the more  $H_1$  transforms the unperturbed function  $\varphi_0$  into  $\varphi_j$ , the more important is the contribution of  $\varphi_j$  to the perturbed wave function; second, the denominator shows that the more the eigenvalues corresponding to  $\varphi_0$  and  $\varphi_j$  differ, the less  $\varphi_j$  contributes to the perturbed wave function.

Next we turn to the second-order equation and rearrange it, recognizing that  $H_2$  vanishes:

$$-E_2\psi_0 + (H_1 - E_1)\psi_1 + (H_0 - E_0)\psi_2 = 0, \quad (7A.13)$$

which we then multiply by  $\psi_0^*$  and integrate to find  $\langle E_2 \rangle$  or just  $E_2$ , since they are the same here. The first term gives us just  $E_2$ , and the third term vanishes. This leaves us with

$$E_2 = -\int \psi_0^* H_1 \psi_1, \quad (7A.14)$$

which becomes useful when we substitute Eqs. 7A.10 and 7A.12. With just a bit of rearranging, we find the second-order correction to the energy,

$$E_2 = \sum_k \frac{\left| \int \varphi_k^* H_1 \varphi_0 d\tau \right|^2}{E_0^{(k)} - E_0}. \quad (7A.15)$$

This expression has content similar to Eq. 7A.12, in that the more the perturbation transforms the unperturbed state into a particular excited state, the greater is that state's contribution, in this instance, to the perturbed energy, and the more distant the unperturbed and excited states are in energy, the less the excited state affects the unperturbed state.

We close with a remark about the one situation in which Eqs. 7A.12 and 7A.15 cannot be used. This is the bothersome case in which the unperturbed state is degenerate with another state with which it mixes under the action of the perturbation. If this happens, the two (or more) "offending" states, call them  $\psi_0^A$  and  $\psi_0^B$ , must be given special treatment; we consider only the example of two degenerate functions with a common eigenvalue of  $H_0$ , namely  $E_0$ . We can write the first-order wave functions as linear combinations of  $\psi_0^A$  and  $\psi_0^B$ ,

$$\begin{aligned} \psi_I &= a\psi_0^A + b\psi_0^B, \\ \psi_{II} &= a'\psi_0^A + b'\psi_0^B \end{aligned} \quad (7A.16)$$

and require that  $a^2 + b^2 = a'^2 + b'^2 = 1$  (and that  $\int \psi_I^* \psi_{II} d\tau = 0$ , if we wish to include it), that is, that the two functions we seek must be normalized and orthogonal. This gives us two simultaneous linear equations for the two independent parameters of (only one, if we include all the conditions) which have a solution if and only if the determinant of the coefficients of the unknowns is zero. The equation stating this is

$$\begin{vmatrix} \int \psi_0^A * H \psi_0^A d\tau - E & \int \psi_0^A * H \psi_0^B d\tau \\ \int \psi_0^B * H \psi_0^A d\tau & \int \psi_0^B * H \psi_0^B d\tau - E \end{vmatrix} = 0, \quad (7A.17)$$

in which we can compute all the integrals and need only to find the eigenvalues  $E$ , which are the solutions of the quadratic equation which Eq. 7A.17 represents. We can make this equation look simpler by writing the four integrals in a shorthand notation,  $\int \psi_0^A * H \psi_0^A d\tau \equiv H_{AA}$ ,  $\int \psi_0^B * H \psi_0^B d\tau \equiv H_{BB}$ , etc.,

$$\begin{vmatrix} H_{AA} - E & H_{AB} \\ H_{BA} & H_{BB} - E \end{vmatrix} = 0 \quad (7A.18)$$

or

$$(H_{AA} - E)(H_{BB} - E) - H_{BA}H_{AB} = 0 \quad (7A.19)$$

which has the solution

$$\begin{aligned} E &= \frac{1}{2}(H_{AA} - H_{BB}) \\ &\pm \frac{1}{2}\sqrt{(H_{AA} + H_{BB})^2 - (4H_{BA}H_{AB})}, \end{aligned} \quad (7A.20)$$

an equation giving the energies of the two states that are degenerate in zero-th order but not in second order. One of the most important examples of this situation is the way the energies of two electronic states (with the same symmetry) of a diatomic molecule “split” when their Born–Oppenheimer potential curves cross. The dominant perturbation in this case is most probably the action of the nuclear kinetic energy on the electronic wave functions, as discussed in Section 7.5. The full Hamiltonian is meant to be included in Eq. 7A.17, but the part that contributes to the off-diagonal elements,  $H_{AB}$  and  $H_{BA}$ , is the nuclear kinetic energy operator, with  $\psi_0^A$  and  $\psi_0^B$  as two electronic states determined within the Born–Oppenheimer approximation.

## ● FURTHER READING

- Bernath, P. F., *Spectra of Atoms and Molecules* (Oxford, New York, 1995).
- Gaydon, A. G., *Dissociation Energies and Spectra of Diatomic Molecules*, 3rd Ed. (Chapman and Hall, London, 1968).
- Herzberg, G., *Molecular Spectra and Molecular Structure, Volume I. Spectra of Diatomic Molecules*, 2nd Ed. (Van Nostrand-Reinhold, Princeton, N.J., 1950).
- Hurley, A. C., *Introduction to the Electron Theory of Small Molecules* (Academic Press, London, 1976).
- Karplus, M., and Porter, R. N., *Atoms and Molecules* (W. A. Benjamin, Inc., Menlo Park, Calif., 1970), Chapters 5, 6, and 7.
- Kauzmann, W., *Quantum Chemistry* (Academic Press, Inc., New York, 1957), Chapters 11C–G and 12.
- Kondratyev, V., *The Structure of Atoms and Molecules* (P. Noordhoff N. V., Groningen, The Netherlands, 1964), Chapters 7–10.
- Morrison, M. A., Estle, T. L., and Lane, N. F., *Quantum States of Atoms, Molecules and Solids* (Prentice-Hall, Inc., Englewood Cliffs, N.J., 1976), Chapters 12, 14–17.
- Mulliken, R. S., and Ermier, W. C., *Diatomic Molecules, Results of ab initio Calculations* (Academic Press, New York, 1977), esp. Chapters IV, V, and VI.
- Slater, J. C., *Quantum Theory of Molecules and Solids, Volume I* (McGraw-Hill Book Co., Inc., New York, 1963), esp. Chapters 5, 6, and 7.
- Streitweiser, A., and Owens, P. H., *Orbital and Electron Density Diagrams. An Application of Computer Graphics* (The Macmillan Company, New York, 1973).
- Yarkony, D. R., Ed., *Modern Electronic Structure Theory, Parts I and II* (World Scientific, Singapore, 1995).

## ● PROBLEMS

- Because the vibrational spacings of diatomic molecules generally diminish with increasing energy, it is possible to extrapolate the vibrational spacing, as a function of vibrational energy, to zero, and thereby obtain a moderately accurate estimate of the dissociation energy of the molecule. Such graphs are known as Birge–Sponer plots, after R. Birge and H. Sponer. Using values of  $\tilde{v}_e x_e$  and  $\tilde{v}_e y_e$  from Table 7.2, construct such plots for Na<sub>2</sub>, CH, and HCl, then evaluate  $D_e$  and  $D_0$ , the dissociation energies from the bottom of the potential and

from the ground vibrational state. Compare these values of  $D_0$  with those given in Table 7.2.

- Find the outer classical turning points and thus the classical zero-point amplitudes of vibration for H<sub>2</sub>, LiH, and HCl, from the data in Table 7.2. (Refer to Problems 21 and 22 in Chapter 4 if you need help finding the classical turning point.)
- Using Table 7.2, determine the vibrational quantum numbers at which the actual vibration energy level spacings of F<sub>2</sub> and Cl<sub>2</sub> deviate 1% and 10% from the harmonic spacings based on  $\tilde{v}_e$  alone.
- The dipole moment of HCl is 1.109 D (Table 7.4), its equilibrium bond length is 1.27 Å, and its vibration frequency is approximately 2991 cm<sup>-1</sup> (Table 7.2). Suppose that a spatially uniform laser beam of 1 W, with precisely this frequency and a cross section of 0.01 cm<sup>2</sup>, is incident on a sample of HCl vapor. What is the maximum instantaneous stretching force exerted by this field on an HCl molecule with  $R = R_e$ ? Based on the force constant of Table 7.2 and the assumption that the dipole moment  $\mu$  increases directly with  $R$  very near  $R_e$ , compute the effective restoring force of the chemical bond on the nuclei at their classical outer turning point in the ground vibrational state. Compare the restoring force of the bond with the stretching force of the electric field.
- Compute the average moment of inertia for the ground vibrational-electronic state of O<sub>2</sub>, assuming that this molecule is a harmonic oscillator, so that the lowest vibrational function of Table 4.2 can be used for the probability amplitude. Compare this moment of inertia with the value implied by the  $B_e$  of 1.4456 cm<sup>-1</sup> in Table 7.2.
- Most common diatomic molecules have lowest vibrational spacings that are much larger than their lowest rotational spacings, yet vibrational spacings diminish and rotational spacings increase with increasing quantum number. At what vibrational and rotational quantum numbers do these spacings become roughly equal for H<sub>2</sub>, N<sub>2</sub>, and HBr? What are the total energies of the molecules at these levels? Compare these total energies with the corresponding dissociation energies.
- Calculate the frequencies of the vibration–rotation transitions of OH from data in Table 7.2, for the transitions  $v = 0 \rightarrow 1$  and  $v = 1 \rightarrow 2$ , for  $\Delta J = -1, 0$ , and +1 for  $J$  from 0 to 10. Plot the transitions on an energy scale that displays the entire set of lines and still allows one to resolve them. What spectral resolution would be required to distinguish the lines, if one requires resolution of at least half the spacing of the most closely spaced lines?

8. As the rotational energy of a molecule increases, the centrifugal force on the nuclei adds a repulsive term to the effective potential as given in Eq. 7.19. Find the value of  $J$  for which the centrifugal potential brings the lowest point of the rotationless curve up to  $D_0$ , that is, find the first rotational state for which  $E_{\text{rot}} + V(R) > 0$  everywhere, for  $\text{H}_2$ ,  $\text{Na}_2$ , and  $\text{I}_2$ .
9. Compute a rotational analog of Problem 4. That is, assume that an assembly of  $\text{HCl}$  molecules is in a laser beam whose power density is  $1 \text{ W/cm}^2$  and whose frequency is precisely resonant with the first rotational transition of  $\text{HCl}$ . Given that its dipole moment is  $1.109 \text{ D}$ , compute the total force on the nuclei and the torque (force times lever arm from the center of mass) when the force is a maximum.
10. From the rotational line frequencies given below, compute the bond length of the diatomic molecule  $\text{NaCl}$  in its ground and first excited vibrational state. [Data are from A. Honig, M. Mandel, M. L. Stich, and C. H. Townes, *Phys. Rev.* **96**, 629 (1954).] All transitions are  $J = 1$  to  $J = 2$ .

	$v = 0 \text{ (MHz)}$	$v = 1 \text{ (MHz)}$
$\text{Na}^{35}\text{Cl}$	$26051.1 \pm 0.75$	$25857.6 \pm 0.75$
$\text{Na}^{37}\text{Cl}$	$25493.9 \pm 0.75$	$25307.5 \pm 0.75$

How much effect do the uncertainties in the spectral line frequencies have on the inferred bond lengths?

11. The rotational spectrum of a polar diatomic molecule is observed in the microwave region of the electromagnetic spectrum. In the case of  $\text{RbBr}$ , in the vibrational state  $v = 0$ , the  $J = 8 \rightarrow 9$  transition is observed at:

Molecule	(MHz)
$^{85}\text{Rb}^{79}\text{Br}$	25 596.03
$^{87}\text{Rb}^{79}\text{Br}$	25 312.99
$^{85}\text{Rb}^{81}\text{Br}$	25 268.84

Assume that  $\text{RbBr}$  behaves as a rigid rotator and calculate the internuclear separations in the various isotopic molecules. The atomic masses are  $^{79}\text{Br} = 78.94365 \text{ amu}$ ,  $^{81}\text{Br} = 80.93232 \text{ amu}$ ,  $^{85}\text{Rb} = 84.93920 \text{ amu}$ ,  $^{87}\text{Rb} = 86.93709 \text{ amu}$ . Are you surprised by your results? How do you interpret them?

12. The bond lengths of  $\text{Na}_2$  are  $3.0782 \text{ \AA}$  and  $3.63 \text{ \AA}$  in the ground and first excited electronic states, respectively. Based on this difference, compute the separation in  $\text{cm}^{-1}$  between the band origin ( $J' = 0$  to  $J'' = 0$ ) and the band head (where the rotational lines turn around and start returning on themselves) for a transition between these states.

13. One speaks of rotational bands in electronic spectra as being "degraded toward the red" or "degraded toward the blue" depending on whether the rotational line spacings eventually increase toward longer or shorter wavelengths. Such "degradation" is usually immediately apparent to the eye. Show that one can tell immediately whether  $R_e$  is greater in the ground or excited state depending on the direction of the degradation or shading.
14. Doppler broadening is very important in many regions of the spectrum and in a variety of situations, including spectroscopy of stars and the interstellar medium. The Doppler shift is the result of wave crests and peaks reaching the observer faster or slower than they would if the source of radiation and the observer were at rest relative to each other. Show that the shift in wavelength  $\Delta\lambda$  of radiation sent by a source moving with velocity  $v$  relative to the observer is given approximately by
- $$\Delta\lambda = \frac{\lambda v}{c}.$$
- Calculate the Doppler shift for radiation of  $1000 \text{ MHz}$  and  $1000 \text{ cm}^{-1}$  if  $v = 10^{-5} \text{ cm/s}$ .
15. Compare the bonding in  $\text{Cl}_2$  and  $\text{Cl}_2^+$ . How does it differ? Would you expect  $\text{Cl}_2^-$  to exist as a stable species? Why?
16. Show the forms of the nodal surfaces for the  $\sigma$ ,  $\pi$ , and  $\delta$  orbitals constructed as sums and differences of  $3d$  orbitals in the homonuclear diatomic molecule  $\text{Si}_2$ .
17. The dissociation energy of  $\text{F}_2$  is  $1.60 \text{ eV}$ , whereas those of  $\text{Cl}_2$  and  $\text{Br}_2$  are  $2.48 \text{ eV}$  and  $1.97 \text{ eV}$ , respectively. Give at least one interpretation of this apparent anomaly.
18. The molecules  $\text{N}_2$  and  $\text{C}_2\text{H}_2$  are isoelectronic. From considerations based on the electronic structure of  $\text{N}_2$ , predict the geometry (i.e., bent or linear) of  $\text{C}_2\text{H}_2$ , and discuss its electronic structure in terms of the types of orbitals occupied, nature of the orbitals, and so on.
19. Write the electron configurations for the ground states of  $\text{Mg}_2$ ,  $\text{Fe}_2$ ,  $\text{MgH}$ , and  $\text{HCl}$ . Which of these would you expect to be stable on the basis of the electron configuration alone?
20. Predict the dissociation energy, equilibrium internuclear distance, and vibration frequency  $\tilde{\nu}_e$  by extrapolation from the data in Table 7.9, for each of the following:
- $\text{At}_2$
  - $\text{DAt}$
  - $\text{Fr}_2$

## 228 • More about Diatomic Molecules

- 21.** Rationalize the empirical facts that the ionization potential of H<sub>2</sub> is greater than that of atomic H, whereas that of O<sub>2</sub> is less than that of atomic O.
- 22.** Rationalize the exponential form of the repulsive contribution to the energy of an ionic molecule, Eq. 7.43. Recall that the united-atom limit has a finite energy, achieved when the two nuclei coalesce. Hint: Consider the effect of the Pauli principle. Explain why a form  $B e^{-R/R}$  might be even more plausible.

- 23.** Consider the reaction, in a gas-phase collision,



Suppose that the initial velocity of the K atom is  $5 \times 10^4$  cm/s, and that of the HI molecule is negligibly small. Suppose that the rotational energy of HI is negligibly small. Further, suppose that the K would have approached to within 5 Å of the center of mass of the HI if no reaction occurred. Finally, assume that the velocity of the H atom leaving after the reaction is negligibly small. The energy of the KI bond is 3.34 eV and that of the HI bond is 3.06 eV. The internuclear separation in KI is 3.048 Å, and the vibrational frequency is 173 cm<sup>-1</sup>. What do the conditions for conservation of energy, linear momentum, and angular momentum imply about the vibrational and rotational state of the product molecule KI? Estimate the rotational quantum number  $J$  and the vibrational quantum number  $\nu$  that characterize the product KI. (Hint: Look back at Rutherford scattering to see how the angular momentum of a particle moving toward another molecule is related to its velocity and the impact parameter; cf. Appendix 2A.)

- 24.** The hydrogen halides have continuous electronic absorption spectra, the onsets being about 2500 Å for HCl, 2650 Å for HBr, and 3270 Å for HI.
- How do you interpret these observations? Draw likely potential energy curves for the states in question in HI.
  - If the difference in energy between the  ${}^2P_{1/2}$  and  ${}^2P_{3/2}$  states of the I atom is 1 eV, must the onsets of production of these two dissociated iodine atoms from HI also be separated by 1 eV?
  - What is the likely consequence of irradiating HI with light of wavelength 2537 Å? 1849 Å?
- 25.** The occurrence of predissociation is often inferred from spectra by the sudden appearance of wide, diffuse lines where at lower energies the lines are narrow and sharp. Explain why this is an indication of predissociation or

autoionization. How would you distinguish predissociation from autoionization experimentally?

- 26.** Compare the dissociation energies, bond lengths, and vibrational frequencies of a number of diatomic molecules, for example, from Table 7.2. Examine these for correlations among bond length, dissociation energy, and vibration frequency. What correlations do you find? (Other sources of data should also be consulted.)
- 27.** Use (a) the HF-SCF, (b) the CISD, and (c) the MP<sub>2</sub> methods along with a 6-31G(d) basis set (which adds a set of *d*-type polarization functions to nonhydrogen atoms) to compute values of  $D_e$  and b  $R_e$  for the ground electronic states of the homonuclear diatomic molecules N<sub>2</sub> and F<sub>2</sub>. Compare the calculated values with the experimental values found in Table 7.5.
- 28.** Using the computed value of  $R_e$  (from Problem 7.27) and Eq. 7.21, calculate the rotational constant,  $B_p$ , for the N<sub>2</sub> and F<sub>2</sub> molecules. Compare the calculated values with the experimental values found in Table 7.2.
- 29.** Use the same electronic structure methods and basis set utilized in Problem 7.27 to compute the fundamental harmonic vibrational frequency of N<sub>2</sub> and F<sub>2</sub> in their ground electronic states. Using the fundamental harmonic vibrational frequency and the value of  $D_e$  calculated in Problem 7.27, compute a theoretical estimate of the values of  $D_0$  for the two homonuclear diatomics. Compare with the experimental values found in Table 7.2.
- 30.** Use (a) the HF-SCF, (b) the CISD, and (c) the MP<sub>2</sub> (second-order Møller-Plesset perturbation theory) methods along with a 6-31G(*d,p*) basis set (which adds a set of *d*-type polarization functions to nonhydrogen atoms and a set of *p*-type polarization functions to hydrogen) for the heteronuclear diatomic molecules HF and LiF in their ground electronic states, computing  $D_e$ ,  $R_e$ , the fundamental harmonic vibrational frequency, and  $D_0$ . Additionally, compute the dipole moments of HF and LiF. Compare the calculated results with values given in Tables 7.2, 7.4, and 7.8.
- 31.** The third excited electronic state of F<sub>2</sub> has a symmetry  ${}^1\Pi_g$ . Use the CISD method along with a 6-31G(*d*) basis set to compute values of  $D_e$  and  $R_e$  for F<sub>2</sub> in this excited electronic state. Estimate the energy difference between the ground electronic state and the third excited electronic state of F<sub>2</sub> by using the results from Problem 7.27. Compare with the experimental difference.